STIMULUS-DRIVEN SPECTRAL AND TEMPORAL ANALYSIS OF ECG, EEG AND EMG SIGNALS

A thesis submitted toward partial fulfillment of the requirements for the degree of

Master of Engineering

In

Biomedical Engineering

Submitted by

SANJOY KUMAR DAS

EXAMINATION ROLL NO.: M4BMD23010

CLASS ROLL NO.: 002130201009

REGISTRATION NO.: 160469 of 2021-2022

Under the supervision of

Prof. (Dr.) Monisha Chakraborty

Professor

School of Bioscience and Engineering

Jadavpur University

Course affiliated to

Faculty of Engineering and Technology

Jadavpur University

Kolkata-700032

India

2023

M.E. (Biomedical Engineering) course affiliated to

Faculty of Engineering and Technology

Jadavpur University

Kolkata-700032

CERTIFICATE OF RECOMMENDATION

This is to certify that the thesis entitled **"Stimulus-Driven Spectral and Temporal Analysis of ECG, EEG and EMG Signals"** is a bonafide work carried out by **SANJOY KUMAR DAS** under my supervision and guidance for partial fulfillment of the requirement for Post Graduate Degree of Master of Engineering (Biomedical Engineering) in School of Bioscience and Engineering during the academic session 2021-2023.

_____

THESIS ADVISOR
Prof. (Dr.) Monisha Chakraborty
Professor
School of Bioscience and Engineering
Jadavpur University
Kolkata-700032

_____

DIRECTOR
School of Bioscience and Engineering
Jadavpur University
Kolkata-700032

_____

DEAN
Faculty Council of Interdisciplinary Studies, Law and Management
Jadavpur University
Kolkata-700032

M.E. (Biomedical Engineering) course affiliated to

Faculty of Engineering and Technology

Jadavpur University

Kolkata-700032

CERTIFICATE OF APPROVAL**

The foregoing thesis is hereby approved as a creditable study of an Engineering subject carried out and presented in a manner satisfactory to warrant its acceptance as a prerequisite to the degree for which it has been submitted. It is understood that by this approval the undersigned do not necessarily endorse or approve any statement made opinion expressed or conclusion drawn therein but approve the thesis only for the purpose for which it has been submitted.

_____ _____

Prof. (Dr.) Monisha Chakraborty
(Thesis Advisor)
Professor
School of Bioscience and Engineering
Jadavpur University
Kolkata-700032

Signature of Examiner

****Only in case the thesis is approved.

DECLARATION OF ORIGINALITY AND COMPLIANCE OF ACADEMIC ETHICS

I hereby declare that this thesis contains a literature survey and original research work by the undersigned candidate, as part of his **Master of Engineering** in **Biomedical Engineering** studies during the academic session 2021-2023.

All information in this document has been obtained and presented in accordance with academic rules and ethical conduct.

I also declare that, as required by these rules and conduct. I have fully cited and referred all material and results that are not original to this work.

NAME: **SANJOY KUMAR DAS**

CLASS ROLL NO.: **002130201009**

EXAMINATION ROLL NO.: **M4BMD23010**

REGISTRATION NO.: **160469 of 2021-2022**

THESIS TITLE: **Stimulus-Driven Spectral and Temporal Analysis of ECG, EEG and EMG Signals**

SIGNATURE: **DATE:**

ACKNOWLEDGEMENT

I would like to take this opportunity to express my heartiest gratitude to my respected thesis advisor, Prof. (Dr.) Monisha Chakraborty, Professor, School of Bioscience and Engineering, Jadavpur University for giving me an opportunity to work under her guidance as well as for establishing chances for me to engage in an exciting area of research. She has always been a steady source of encouragement, and her belief in my ability has always inspired me to work more. Without her guidance, encouragement, cooperation, and support, I would not have been able to complete this thesis.

I would like to express my sincere gratitude to our respected Director, School of Bioscience and Engineering, Jadavpur University for your unwavering support throughout the journey of my thesis.

I am grateful to Dr. Piyali Basak, Associate Professor, School of Bioscience and Engineering, Jadavpur University for her constant support throughout the tenure of my master degree program at the School of Bioscience and Engineering, Jadavpur University

I would also like to extend a special thank you to my respected senior, Nilotpal Das, a Ph.D. scholar and CSIR Senior Research Fellow (SRF) in the Biomedical Instrumentation Laboratory in the School of Bio-Science and Engineering department at Jadavpur University. His invaluable suggestions, unconditional support, friendly help, and motivation have transformed the laboratory into a unique and enriching learning environment.

I would like to convey my gratitude and love to all of my batch mates, without whom life would be a very boring place. They were always there to lift my spirits.

I would also like to thank all my seniors, nonteaching staff and juniors for their thoughtful cooperation.

Last, but not least, I want to express my heartfelt gratitude and my love for my family who have been the constant support and strength for me to go on with my higher education.

Date: **Sanjoy Kumar Das**

Dedicated to my Late Grandparents, Mangal Chandra Das and Durga Das, and my Father Late Laxman Chandra Das and Mother Hayrani Das

PREFACE

The human body is a complicated and carefully organized system made up of numerous interrelated subsystems. These systems collaborate to ensure the body's functionality, equilibrium, and reaction to external stimuli. Biosignals are inherent signals produced by the human body that provide useful information about physiological and pathological situations. Monitoring and analysis of biosignals provide a window into many physiological processes, guiding diagnosis, treatment, and medical research. Understanding the interactions between human body systems and the biological signals they generate is essential to understanding the mysteries of health and disease. Through the following whole study, the thesis will try to contribute to this field of research. The evaluation of signal constituents at various frequencies is known as spectral analysis, which makes it possible to discover rhythmic patterns. The temporal analysis, on the other hand, focuses on how signals evolve over time, capturing the orderly progression of events in physiological responses. This study aims to provide a thorough understanding of how ECG, EEG, and EMG signals respond to various stimuli by combining these two approaches. It has been used various weights as a stimulus and using a hand dynamometer to understand the response of muscles and also have used dark chocolate as a stimulus to understand the response of the brain and heart. For analysing the changes in muscles, brain and heart, frequency and time domain analysis of EMG, EEG and ECG signals under stimulus is performed. The thesis is organized into chapters, each of which covers an essential stage of this whole study.

In the first chapter, the basic physiology of human muscles, the heart and the brain, as well as the corresponding biosignals EMG, ECG and EEG, have been briefly introduced.

In the second chapter, the objective and motivation of this thesis have been discussed.

In the third chapter, a literature review which is helping to lead to the thesis has been described. Signal acquisition, different linear and non-linear analyses and various previous research that are related to this work have been studied.

In the fourth chapter, the methodology as well as the experimental approach have been established. Each step taken during this study has been thoroughly described. The signal acquisition systems employed in the experimental technique have been discussed. The tools

and techniques required for this thesis, as well as their operating principles, have been thoroughly explained.

Results from this experiment are presented in the fifth chapter, along with a pattern that will help in future studies.

The results have been evaluated from a physiological perspective in the sixth and seventh chapters, and certain conclusions have been established.

The future scope of this study has been described in the last chapter.

CONTENTS

LIST OF FIGURES

LIST OF TABLES

Chapter: 1

INTRODUCTION

1. Biomedical Signal

Any detectable and trackable signal found inside living things is referred to as a "biomedical signal" or "biological signal." These signals may have electrical or nonelectrical properties [1], [2]. Electrical biological signals, often referred to as bioelectrical time signals, are produced by applied potential variations in particular tissues, organs, or cell systems, such as the nervous system. [3]. Electrical bio-signals, a large subset of biomedical signals, are particularly important because of their close relationship to physiological processes occurring within the body. These signals, also known as bioelectrical time signals, come from applied potential changes occurring within particular biological structures. A thorough investigation of biological signals dives into their different forms, origins, and effects. Researchers and medical practitioners can better understand health, sickness, and the effects of various interventions on biological systems by unravelling the complexities of these signals. The bioelectrical signals ECG, EEG, EMG, EOG, and GSR are all widely recognized. ECG, EEG and EMG data may be collected through a differential amplifier, which keeps a record of the variations in voltage between two electrodes placed against the skin [4].

2. Electromyography (EMG)

Our muscle cell generates rhythmical action potentials, which are represented as a waveform; this waveform is called electromyogram (EMG). Surface electromyography (sEMG) is a non-invasive method for acquiring myoelectric signals that use surface electrodes placed on the surface of the skin. These signals can be analysed to better understand muscle activity during various physical activities [1], [5]. Signals from EMG serve a purpose in both clinical and biological applications [6]. Currently, an analysis of the EMG signal's frequency spectrum is used to figure out the muscle's strength, evaluate its activation time, and determine its fatigue index. These uses listed above are the most essential and prevalent ways that EMG signals are used nowadays.

2.1. Anatomical Position of Muscles of Upper Limb:

Our upper limbs have three primary muscle associations: the triceps, biceps, and forearms [7], [8]. Extensors play a role in elongating the arm and elevating the joint angle,

while flexors aid in bending the arm and decreasing the joint angle. The biceps are one of the upper arm muscles, and it has two unique heads: a shorter head and a longer head. Proximal biceps tendons connect the biceps muscle to the bones in the arm. In addition, the distal biceps tendon joins the biceps to the radius and ulna, the forearm bones [9]. Biceps contraction causes the forearm to be raised and turned outward. The forearm joins the upper extremity's elbow along with the wrist [10]. The radius and the ulna are two very important bones that make up the skeletal structure of the forearm, which is an important part of the upper limb. The forearm is divided into two separate segments by this dynamic arrangement: the anterior segment, which is in charge of flexion, and the posterior segment, which is predominantly involved in extension. Amazingly, each of these compartments has a complex assembly of 20 different muscles, displaying a tremendous level of intricacy. The forearm is a unique nexus of anatomical plasticity and functional dexterity because of this complex musculature, which works together to coordinate a broad range of movements [11].

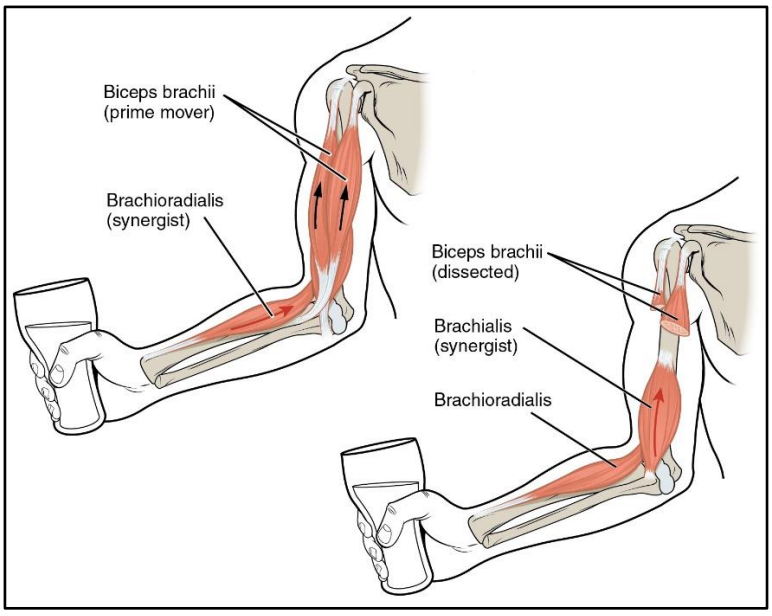

Figure 1: Muscles of the upper limb [4]

2.2. <u>Generation of EMG signal:</u>

Electromyogram (EMG) signals are generated by the interaction of nerves and muscles. At the neuromuscular junction, neurotransmitters are released in response to nerve signals from contracting muscles. Through the release of calcium, this starts the stimulation of muscle fibers and sarcomere contraction. Ions like sodium and potassium transfer as muscle fibers contract, causing regional voltage changes. These minor electrical potentials on the surface of the skin are recorded by surface EMG electrodes. The EMG signal can be amplified and processed to

reveal information about muscle activity that can be used to diagnose illnesses, gauge function, and investigate motor control [12]. Electrodes have been placed on the skin for recording muscle electrical activity during the detection and conditioning of surface electromyography (EMG) signals. These weak signals are amplified, and the noise is removed by filtering, and occasionally rectified for analysis. The generated signal is then normalized, smoothed, and its features are retrieved. This signal processing aids in the comprehension of muscle behavior and is utilized in medical, scientific, and athletic applications [13].

3. Human Heart and Electrocardiography (ECG)

The rhythmic contractions of the cardiac muscle are triggered by the heart's electrical activity, which allows the heart to pump blood throughout the body. This electrical activity, which is produced by specialised cardiac cells, is essential for maintaining a regular pulse and efficient blood circulation [1], [2], [14].

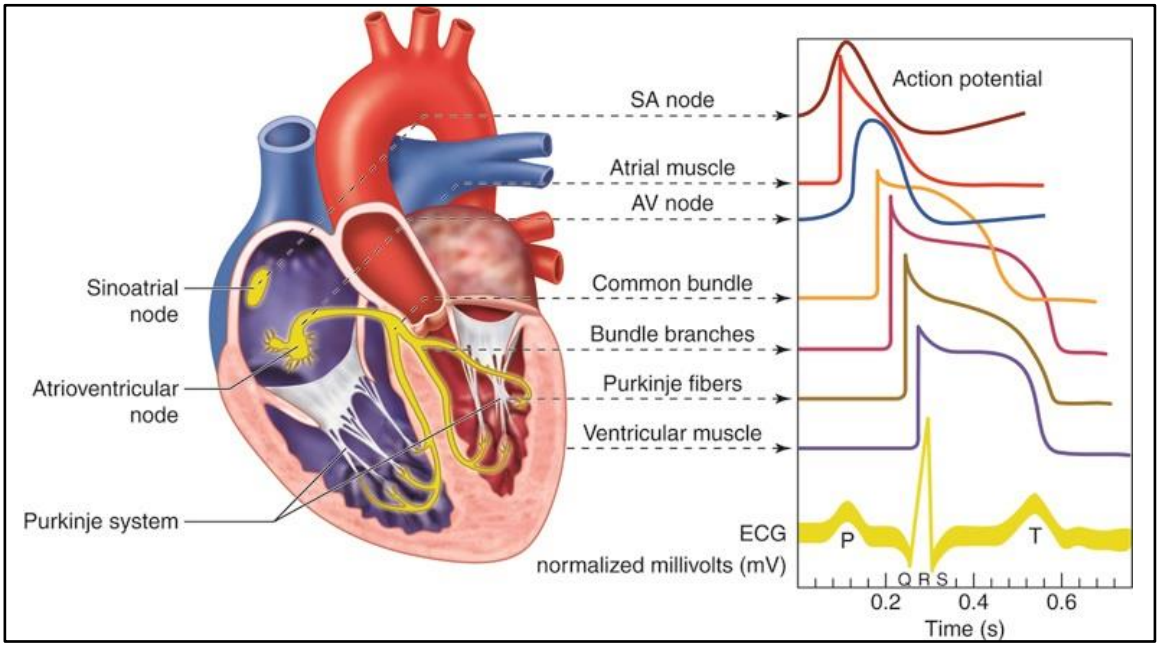

Figure 2: Conduction system of the heart and ECG [14]

3.1. Cardiac Conduction System:

The cardiac conduction system is a network of specialized cells that regulates the heart's electrical activity. This system comprises several crucial parts, including:

Sinoatrial (SA) Node: It is located in the right atrium and is referred to as the "natural pacemaker" of the heart. Each heartbeat is initiated by electrical impulses that it produces. The SA node produces impulses at a regular rate, which establishes the basic heartbeat.

Atria: As a result of the electrical impulses produced by the SA node, the atria rapidly contract and push blood into the ventricles.

Atrioventricular (AV) Node: The AV node serves as a delay mechanism, allowing the atria to contract and fill the ventricles before they contract. It is situated between the atria and ventricles.

Bundle of His: The AV node sends electrical impulses to the ventricles via a network of specialised conducting fibres.

Purkinje Fibres: These fibres, which spread throughout the ventricles, transmit electrical impulses, causing the ventricles to contract and force blood out of the heart.

3.2. Action Potentials:

Action potentials are quick changes in the electrical charge across cell membranes that cause the electrical activity of the heart. The special characteristic allows cardiomyocytes to produce action potentials on their own and without external stimulation.

3.3. Depolarization and Repolarization:

Depolarization and repolarization phases constitute the cardiac action potential:

Depolarization: Sodium ions enter the cardiac cell during depolarization, increasing the positive voltage across the cell membrane. The opening of sodium channels in response to an electrical stimulation starts this process. The sharp increase in voltage seen in the QRS complex of the ECG is an indication of depolarization.

Plateau Phase: Next depolarization, the cell enters a brief plateau phase during which calcium ions maintain the cell's positive charge. By extending the action potential's duration, this phase enables the heart muscle to contract and pump blood efficiently.

Repolarization: Repolarization is the process by which the cell membrane's voltage returns to its resting state after potassium ions have left the cell. The T wave that is visible in the ECG is caused by repolarization [14], [15], [16].

3.4. Electrocardiogram (ECG):

Electrocardiography is a non-invasive technique for monitoring the electrical activity of the heart. The electrocardiogram (ECG) graphically represents the electrical impulses generated by the heart's electrical system, which cause contraction and relaxation of the heart muscles, resulting in rhythmic pumping of blood through the circulatory system.

In ECG waveform, each wave and interval represents a different phase of the cardiac cycle. The P wave denotes atrial depolarization, the QRS complex ventricular depolarization, and the T wave ventricular repolarization. These waveforms reveal any irregularities or disturbances in the heart's pace and rhythm. The frequency range of ECG is 0.05Hz to 150Hz. ECG is used in the medical field for various purposes, such as diagnosis of cardiac diseases, monitoring the overall health of the heart during check-ups or surgeries, and assessing the effects of medications on the heart. These are crucial in determining medical decisions [1], [2].

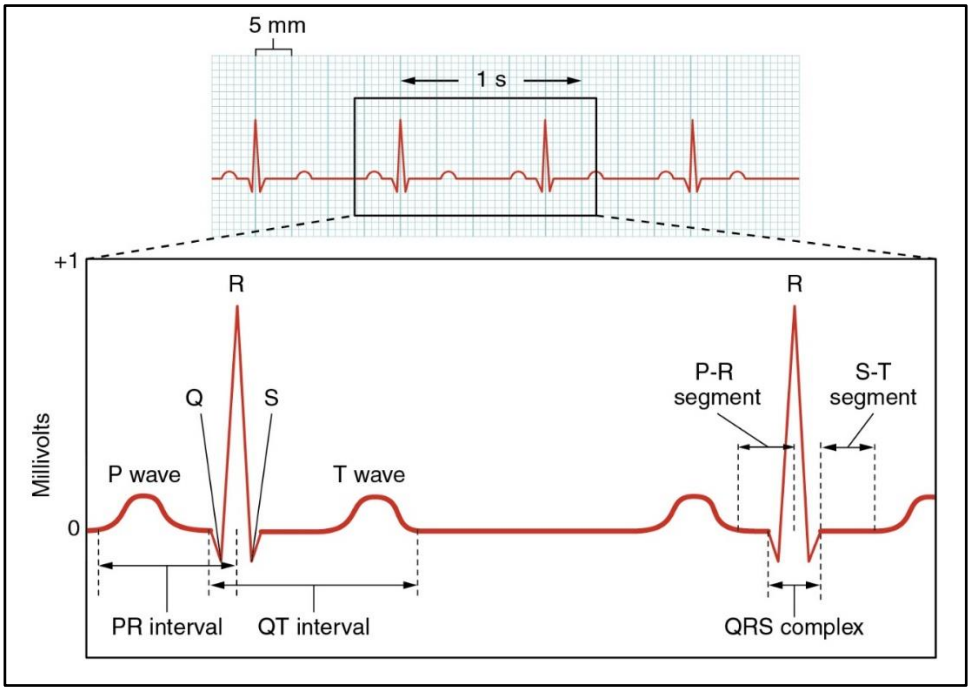

Figure 3: ECG Signal [14]

4. Human Brain and Electroencephalography (EEG)

The human brain is composed of billions of neurons and orchestrates various bodily functions such as thoughts, emotions, behaviours, and movements through intricate electrical activity. Each neuron generates small electrical potentials that collectively shape the brain's overall activity. While individual neuron signals are too weak to capture, the simultaneous electrical behaviour of numerous neurons can be recorded using electrodes on the scalp, a method known as Electroencephalography (EEG) [1], [14].

The human brain is divided into three sections:

- Cerebrum
- Cerebellum
- Brain stem

The Cerebrum is the largest part that is divided into distinct left and right hemispheres connected by the corpus callosum. Each hemisphere has four lobes with different functions: the Frontal lobe for reasoning and motor skills, the Parietal lobe for touch and language, the Temporal lobe for memory and hearing, and the Occipital lobe for vision.

It's worth noting that brain functions are interconnected rather than confined to specific points. Brain activity involves intricate systems, with different areas contributing to various functions [14], [17], [18].

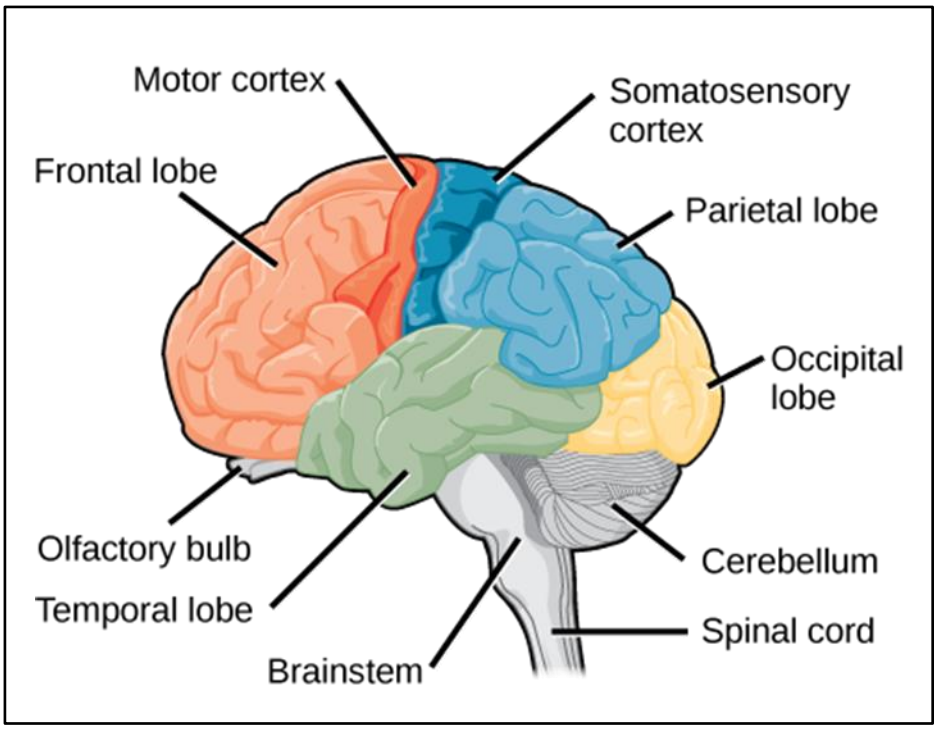

Figure 4: Different parts of the brain [14]

4.1. EEG Signal Generation:

The origin of EEG signals lies in neurons, the fundamental units of the nervous system. Neurons are electrically polarized, maintaining a resting potential. When stimulated above a threshold, neurons depolarize, creating a wave of electrical activity that flows through the neuron and to other neurons through synaptic junctions.

Electrical potentials in the brain result from the interactions between excitatory and inhibitory post-synaptic potentials in neurons' cell bodies and dendrites. All brain processes involve information transmission through electrical currents across neurons. This synchronized neuronal activity generates rhythmic potentials, which, when aggregated, can be captured using surface electrodes on the scalp [1], [2], [19], [20], [21], [22].

4.2. EEG Signal:

EEG, or Electroencephalogram, records the brain's electrical activity. Electrodes on the scalp or directly on the cerebral cortex (invasive method) pick up EEG signals. EEG signals span a frequency range from 0.5 to 50 Hz and are categorized into different waves [1]:

- Delta (0.5-4 Hz): Associated with deep sleep.
- Theta (4-8 Hz): Present during early sleep stages and subconscious activity.
- Alpha (8-13 Hz): Predominant at rest and decreases with increased mental activity.
- Beta (13-22 Hz): Linked to cognitive tasks and engaged mental states.
- Gamma (22-30 Hz): Involved in processing complex tasks.

These brainwave states fluctuate based on activities. For instance, reading engages beta waves, relaxation increases alpha waves, daydreaming raises theta waves, and deep sleep induces delta waves. Despite one wave predominating, all waves coexist in the brain's mix.

The human brain's intricate workings are governed by the collective electrical activity of neurons. EEG captures this activity, with different brainwaves indicating various mental states and activities. The brain's functionality relies on a dynamic interplay between its components, and EEG provides insights into this complex dance of electrical impulses [19], [20], [21], [22].

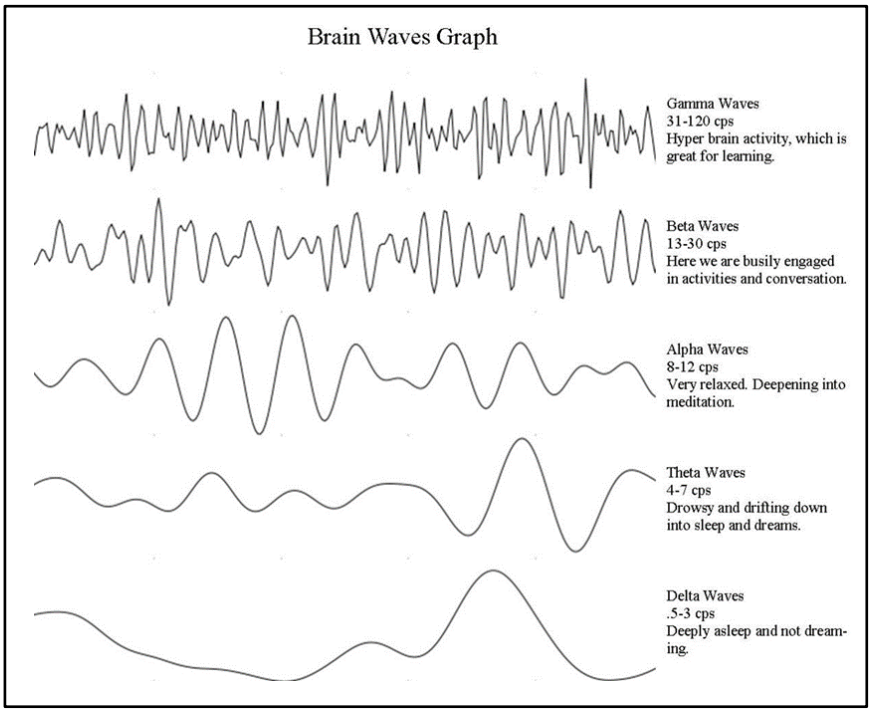

Figure 5: Different waveforms of the EEG signal [3]

Chapter: 2

MOTIVATION AND OBJECTIVE

Signal analysis of the Electromyogram (EMG), Electroencephalogram (EEG) and Electrocardiogram (ECG) is done for both biological and clinical diagnostic purposes. EMG tests evaluate muscle health and efficiency, EEG tests diagnose epilepsy, seizures, sleep disorders, and brain tumors, while ECG provides information about cardiac rhythm and overall heart health.

However, biomedical signals have complex characteristics like non-linearity, non-stationarity, and transience due to the inherently non-linear nature of cellular activity that generates biopotentials. These signals, which include measurements such as EMG, ECG, and EEG, frequently have complicated characteristics that complicate analysis and interpretation. The interaction of non-linearity, non-stationarity, and transience has a significant impact on signal behaviour.

The primary goal of this thesis is to investigate how muscle dynamics change as a person lifts varying weights and using a hand dynamometer and also to investigate how the dynamics of the brain and heart under the stimulus of dark chocolate. EMG, EEG and ECG data from certain subjects have been acquired for this study. A methodology is developed for this thesis that makes use of these data. It is necessary to have a basic understanding of how the brain, muscles and hearts function as well as the techniques used to analyse biosignals in order to carry out this experiment.

The main objective of this research was to determine how the dynamics of the muscles, brain and heart changed. Various linear and nonlinear analysis methods were used in this work. In this work, the heart rate was linearly calculated using R-peaks of ECG signal, and the band powers of different bands of EEG were calculated. The fractal dimension of the sEMG signal during the activity of the biceps and forearm muscles was estimated using the Higuchi's Fractal Dimension (HFD) and Katz's Fractal Dimension (KFD) methods. The fractal dimension of the EEG and ECG signals was also calculated using HFD.

Detrended Fluctuation Analysis (DFA), a nonlinear analysis technique, was used to detect changes in the sEMG, EEG and ECG signals with stimulus. Multifractal Detrended Fluctuation Analysis (MFDFA) of EEG and ECG signals was observed under dark chocolate stimulus.

Chapter: 3

LITERATURE REVIEW

This chapter discuses about EMG, ECG and EEG signal acquisition, various processing and different analysis. An overview of recent EMG, ECG and EEG research is presented in this section.

The paper [23] provides a comprehensive overview of electromyography (EMG) signal acquisition and processing techniques, methods, and advancements. The authors of this paper investigate the importance of EMG signals in understanding muscle activity and movement patterns. The paper covers various aspects of signal acquisition in detail, emphasizing the importance of electrode placement, signal amplification, and noise reduction techniques. This section is an excellent resource for researchers looking to collect accurate and reliable EMG data.

The research of [24] includes a variety of signal processing techniques, ranging from feature extraction to classification algorithms that are used to identify stress patterns in ECG and EMG data. The authors provide insights into the strengths and limitations of each approach by comparing different methodologies. This paper emphasizes the value of combining ECG and EMG signals in improving the accuracy of stress detection models. This integrated strategy provides a multidimensional view of stress-related physiological responses, contributing to a more comprehensive understanding of stress detection mechanisms.

Sidharth Pancholi and Amit M. Joshi proposed a method for conducting a focused investigation of a portable electromyography (EMG) data acquisition module designed for upper limb prosthesis applications [25]. The authors address the critical need for effective EMG signal acquisition in the field of prosthetics, where accurate muscle signal interpretation is required for controlling prosthetic devices. This paper describes the design and development of a small and portable module for capturing EMG signals from residual limb muscles.

The authors of [26] address the critical need for effective control mechanisms in prosthetics, focusing on the use of sEMG signals as a user-friendly interface for prosthetic limb operation. The research explores into the complexities of sEMG signal acquisition, discussing electrode placement, signal processing techniques, and the difficulties in extracting meaningful control signals from residual muscles.

The literature [27] investigate the complex relationship between various types of muscle contractions and their effects on the corticospinal pathway. The research looks at how isometric wrist flexion and extension maximal voluntary contractions (MVCs) modulate corticospinal excitability to the forearm muscles in the context of low-intensity hand-gripping tasks.

The authors [28] demonstrate the importance of collecting EEG and ECG data at the same time because these signals provide complementary insights into both brain and cardiac activity. The paper describes the dataset creation process, including the experimental setup and data acquisition methods used to capture EEG and ECG signals simultaneously.

The paper [29] discusses the technical aspects of wearable EEG and ECG acquisition technologies, including sensor designs, signal processing methods, power management, and communication protocols. The authors provide insights into the challenges of designing wearable devices capable of accurate and reliable signal acquisition while taking comfort and usability into consideration.

Bohao Li et al. present a comprehensive examination of the field that includes electroencephalography (EEG) signal acquisition, processing techniques, and a wide range of applications. The authors acknowledge the importance of EEG in revealing insights into brain activity and its implications for a variety of disciplines. The paper delves into the complex process of EEG signal acquisition, shedding light on the various sensors, electrode placements, and measurement setups used to capture brainwave activity [30].

One group of researchers contributes to the field of biomechanics and neural network applications by studying the prediction of wrist angles under varying loads using a hybrid GA-ELM neural network approach and surface electromyography (sEMG) signals. The authors understand the value of accurate wrist angle prediction in fields such as rehabilitation and prosthetics. The use of a GA-ELM neural network in conjunction with sEMG signals in the study reflects the intersection of machine learning and physiological data, promising a robust predictive model [31].

By investigating the fusion of electroencephalography (EEG) and electromyography (EMG) signals to classify task weight during dynamic movements, the literature [32] significantly contributes to the field of neuroengineering. The paper explores into the technical complexities of EEG-EMG integration, signal processing, and classification algorithms to provide in-depth insights into the fusion process. The authors provide transparency into their

approach and contribute to the larger discussion of multi-modal signal fusion by detailing their methodology.

The paper [33] innovations the field of biomechanics by investigating the use of electromyography (EMG) data for load classification. This research focuses on using empirical mode decomposition (EMD) and feature analysis to classify various loads based on EMG signals. Recognizing the importance of accurate load classification in fields such as ergonomics and rehabilitation, the authors present a methodology for improving the classification accuracy of EMG data using signal processing techniques. This study will use EMD to decompose EMG signals into intrinsic mode functions for more effective feature extraction.

M. Chakraborty and D. Parbat contribute to electromyography (EMG) signal analysis by investigating the use of chaos, fractals and entropy analysis for extracting features during dynamic contraction for the biceps muscles under different loads [34]. The technical complexities of chaos, fractal and entropy characterization of EMG signals are explained in this paper. The researchers demonstrate how to transform raw EMG data into parametric features that reflect the underlying complexity of muscle contractions.

Recognizing the importance of understanding how muscle behaviour changes with load, the authors of literature [35] investigate fractal analysis as a tool for identifying the underlying complexity of sEMG signals. The purpose of this paper is to elucidate the intricate patterns and dynamics within sEMG data when subjected to various loads. This paper discusses the technical aspects of fractal analysis and its application to sEMG signals. The authors provide insight into the process of transforming raw sEMG data into fractal features that capture the variations caused by different load conditions by detailing the methodology.

The literature [36] discusses the relationship between EMG signals and force generated during biceps and flexor digitorum profundus muscle contractions through hand dynamometer. The purpose of this paper is to investigate the dynamic relationship between EMG measurements and the forces generated by these muscles.

The authors of paper [37] investigate the effects of basic taste stimuli on physiological signals (EEG and ECG) because they recognize how crucial it is to comprehend how various tastes cause biological reactions. The goal of the study is to learn more about how our bodies respond to basic tastes by examining the complex relationships between taste perception and biological processes.

The paper [38] examines how consumers' perceptions and assessments of healthy and unhealthy snacks are affected by virtual eating environments. The study focuses on how people's preferences and assessments are virtually influenced by the context in which snacks are presented. The methodologies used to investigate the effects of virtual eating environments on snack evaluations are discussed in this paper. The author provides a glimpse into the process of examining how digital contexts can affect consumers' snack choices by outlining the experimental design and data analysis techniques.

The authors of paper [39] go over the methodologies and concepts that were used to investigate the effects of digital immersive technology on sensory experiences during product testing. The paper provides a window into the process of investigating how digital contexts can alter sensory perceptions of products such as white, milk and dark chocolates by describing the theoretical underpinnings and research approaches.

The paper [40] investigates the feasibility of monitoring heart rate responses elicited by taste stimuli using a noncontact approach, specifically a video camera. The noncontact method of monitoring heart rate responses to taste stimuli has the potential to improve data collection and understanding of individuals' physiological reactions to different tastes.

The authors of literature [41] recognize the complex interplay between cognitive load and food preferences, as well as the potential role of affective computing in solving these dynamics. The study aims to discover how cognitive strain influences people's emotional responses, which in turn influences their food preferences and decisions.

In [42], the authors find the significance of accurate RR interval measurements in predicting heart rate variability and overall cardiovascular health. The purpose of the study is to compare the performance of a heart rate monitor and an ECG Holter device in capturing RR interval data under different physiological states.

The development of a robust algorithm for detecting R peaks in electrocardiogram (ECG) signals is addressed in the literature [43]. The research focuses on using wavelet transform as a tool to improve the accuracy of R peak detection, particularly in heart rate variability studies.

The paper [44] investigates through the technical methodologies that are used to analyse EEG spectral bands and determine emotional states. The authors provide insights into the steps

taken to differentiate between pleasure and displeasure based on EEG data by detailing the calculation of power spectral density and the analysis of spectral bands.

This article [53] gives a general overview of the ways in which fractal analysis has been used to analyse different biomedical signals, including EEG, ECG, and others.

The authors talk about how fractal analysis may offer new perspectives on the underlying complexity of physiological processes.

The review [45] starts off by outlining the idea of fractals and how important they are for analysing complex signals, especially in the field of neurophysiology. The importance of fractal dimension measures as a tool to assess the irregularity and complexity of signals derived from the nervous system is probably covered by the authors.

Most likely, the authors of the paper [47] give a general overview of DFA as a technique for studying time series data. They might clarify how DFA is suitable for analysing complex systems like neuronal oscillations because it can spot long-range correlations or fractal-like characteristics in signals.

The review [48] would probably started by talking about how difficult it is to understand the intricate responses of the human brain, especially when it comes to music. The idea of non-linear techniques like Wavelet transform, DFA and MFDFA and their potential to reveal hidden patterns in complex systems may be discussed by the authors.

The authors of literature [49] may discuss fractal analysis and its application to characterizing complex physiological signals such as ECG. They would most likely explain how fractal measures can shed illuminate the underlying dynamics and complexities of heart rate variability.

In [50], the authors would explain MFDFA, a method for accounting for multifractality that extends the detrended fluctuation analysis (DFA) technique. They could talk about how MFDFA is useful for capturing a signal's varying scaling properties at different time scales.

Chapter: 4

METHODOLOGY

In this chapter, the process of taking data, processing and then analysis of this data is discussed. The basic stages of recording, processing and analysis of a bio-signal is depicted in the given flowchart:

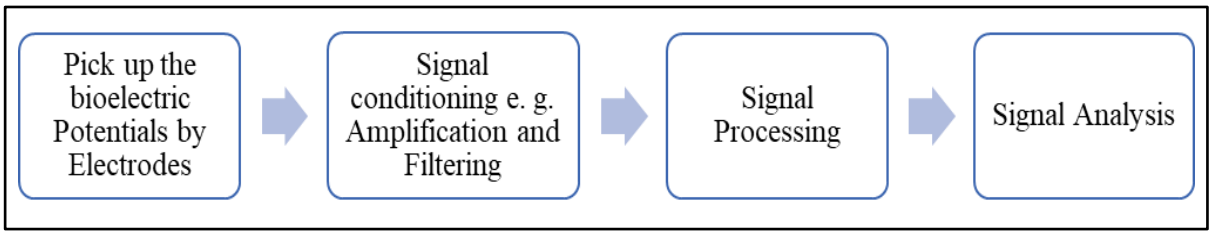

Figure 6: Representation of procedure of a bio-signal

1. Stimulus

A stimulus is a trigger that causes a distinct response within a person's body, originating from external factors and temporarily interfering with the body's normal functions. This interaction between external elements and the body's internal processes points out the dynamic nature of human physiology, emphasizing the ability to make immediate adaptations and changes in response to various stimuli. In the whole thesis, it has been used three different stimuli according to the different protocols. In the experiment of sEMG, a variety of weights, ranging from 0 to 5 kg, are used as the stimulus, with a 1-minute break between each weightlifting. In another experiment of sEMG, using a hand dynamometer external force is applied as the stimulus repeatedly. In the experiment of ECG and EEG, 15gm dark chocolate (50%) is used as the stimulus per subject. The details and composition of this dark chocolate are given in Table 1.

Table 1 - Detail and composition of Dark Chocolate that is used in the study

	50% Dark Chocolate
Company Name	Cadbury Bournville
Nutrition Information (per 100g)	Energy 543 kcal, Protein 5.5 g, Carbohydrate 55.1 g, Total Sugars 45.1 g, Added Sugars 44.1 g, Total Fat 35 g, Saturated Fat 23.4 g, Trans Fat 0.1 g, Cholesterol 4.8 mg, Sodium 10 mg.
Composition	Sugar, Cocoa Solids (42%), Cocoa Butter (9%), Milk Solids, Emulsifiers (442, 476), Lactose, Nature Identical Flavouring Substances.
	Allergen Information: Contains Milk.
	May Contain Tree Nuts, Soy.

In this study, it has been devised two distinct experimental setups.

1. Study of sEMG under varying weights and using a hand dynamometer
2. Study of ECG and EEG signals under the influence of dark chocolate.

2. Study of sEMG under varying weights and using hand dynamometer

In this section of the study, it has been designed three different protocols that would help me better understand the effects on muscles under varying weights and using hand dynamometer. These three protocols are:

- Study of sEMG during flexion movement of the upper limb with varying weights
- Study of sEMG during static holding fatigue of the upper limb with varying weights
- Study of sEMG during handgrip fatigue of the upper limb using hand dynamometer

These protocols followed to record the sEMG signals are shown in Figure 7.

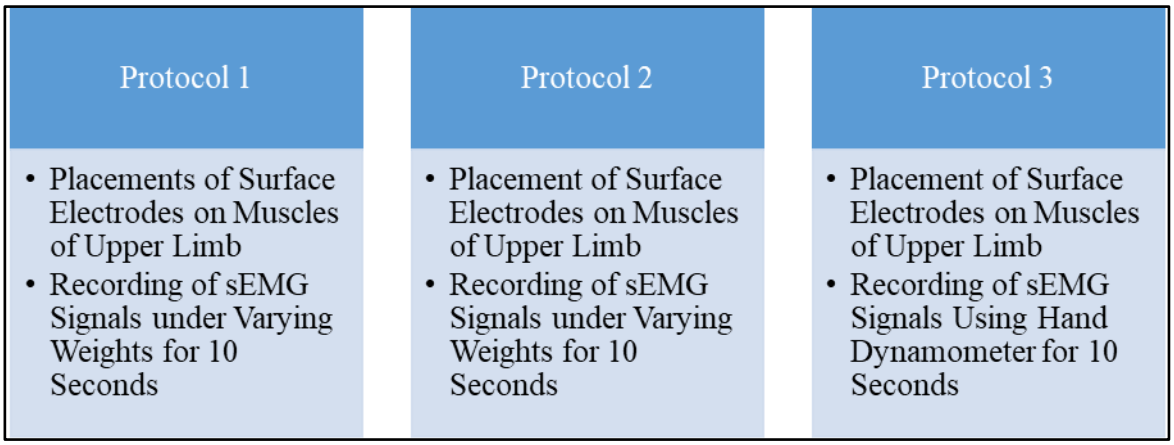

Figure 7: Protocols followed to record the effects on muscles under varying weights and using hand dynamometer

The subjects were instructed to sit quietly and breathe normally throughout these three protocols. Following skin preparation and electrode placement, sEMG signals are then recorded for 10 seconds in accordance with these protocols.

Using the experimental set-up the acquisitions of sEMG signals for these three different protocols are shown in Figure 8, 9 and 10.

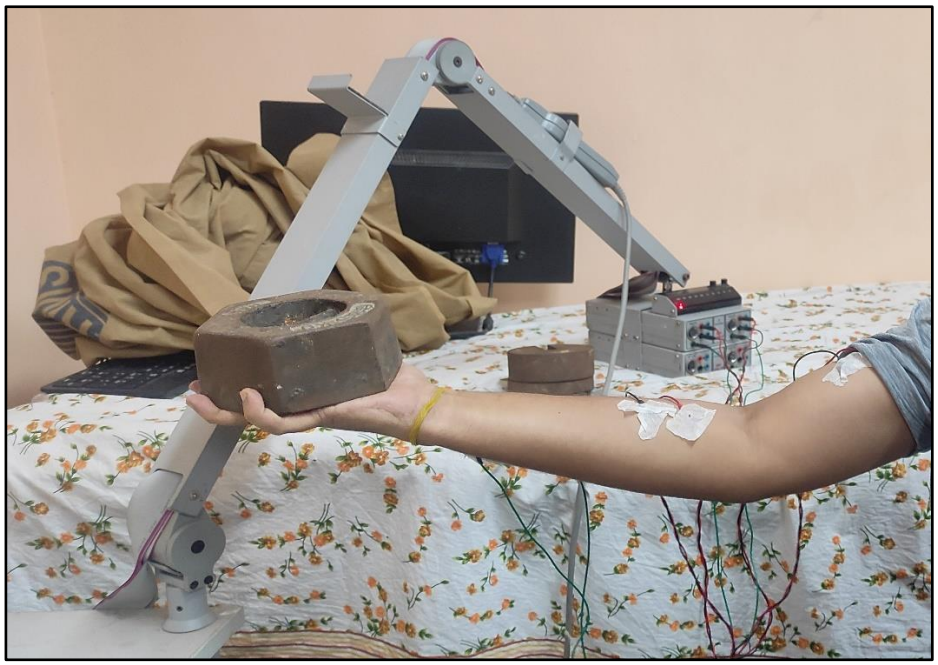

Figure 8: Acquisition of sEMG during flexion movement with weight

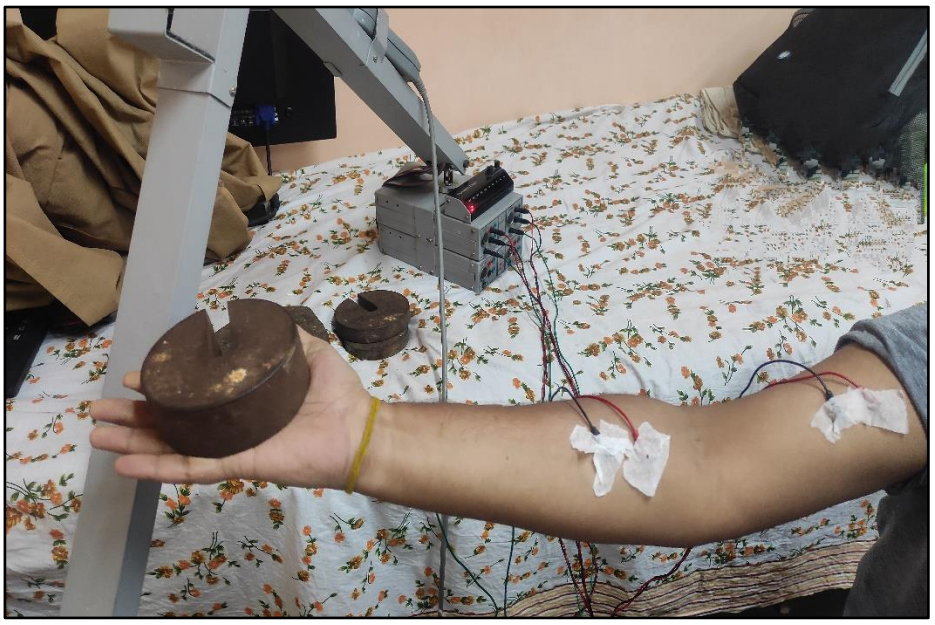

Figure 9: Acquisition of sEMG during static holding fatigue with weight

Figure 10: Hand dynamometer used in handgrip fatigue for acquisition of sEMG

The reusable clamp type metallic electrodes were used to place the active electrodes after the necessary skin preparation. Four surface electrodes (E1, E2, E3, and E4) were positioned on the subject's upper limb (biceps and forearm muscles) for the purpose of sEMG signal acquisition, and a reference electrode was positioned on the subject's neutral point (see Figure 11). E1 and E2 electrode signals were used to create Channel 1 and Channel 2 was created using E3 and E4 electrode signals. After acquiring the signals, they were amplified and filtered, and the output was recorded in the special device RMS Aleron 401. The sampling frequency of this EMG system is 4500 samples/sec.

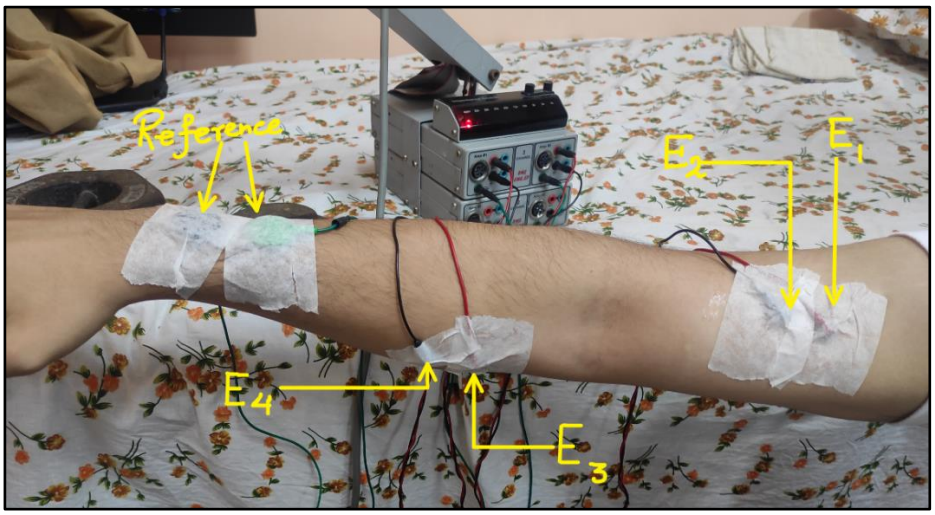

Figure 11: Placement of sEMG electrodes according to the protocols

Eight healthy subjects who took part in the study provided EMG recordings. The subject was told to take it easy and breathe normally throughout the test. In protocol 1, the person was given instructions to lift a range of weights, starting at no load and progressing to 0.5 kg, 1 kg, 1.5 kg, 2 kg, 2.5 kg, 3 kg, 3.5 kg, and 5 kg. This study took into account arm flexion movement with different weights, so the subjects were instructed to flex their arms for 10 seconds. In Protocol 2, the subject was told to hold a variety of weights, no load to 0.5 kg, 1 kg, 1.5 kg, 2 kg, 2.5 kg, 3 kg and 3.5 kg. The subjects were told to hold these loads for 10 seconds in order to compensate for the static holding fatigue with various weights in this study. In Protocol 3, the subject was directed to continuously exert force through a hand dynamometer. This study used a hand dynamometer to measure handgrip fatigue, so the subjects were told to exert force repeatedly for 10 seconds. The entire research methodology of this study is represented as block diagram in Figure 12.

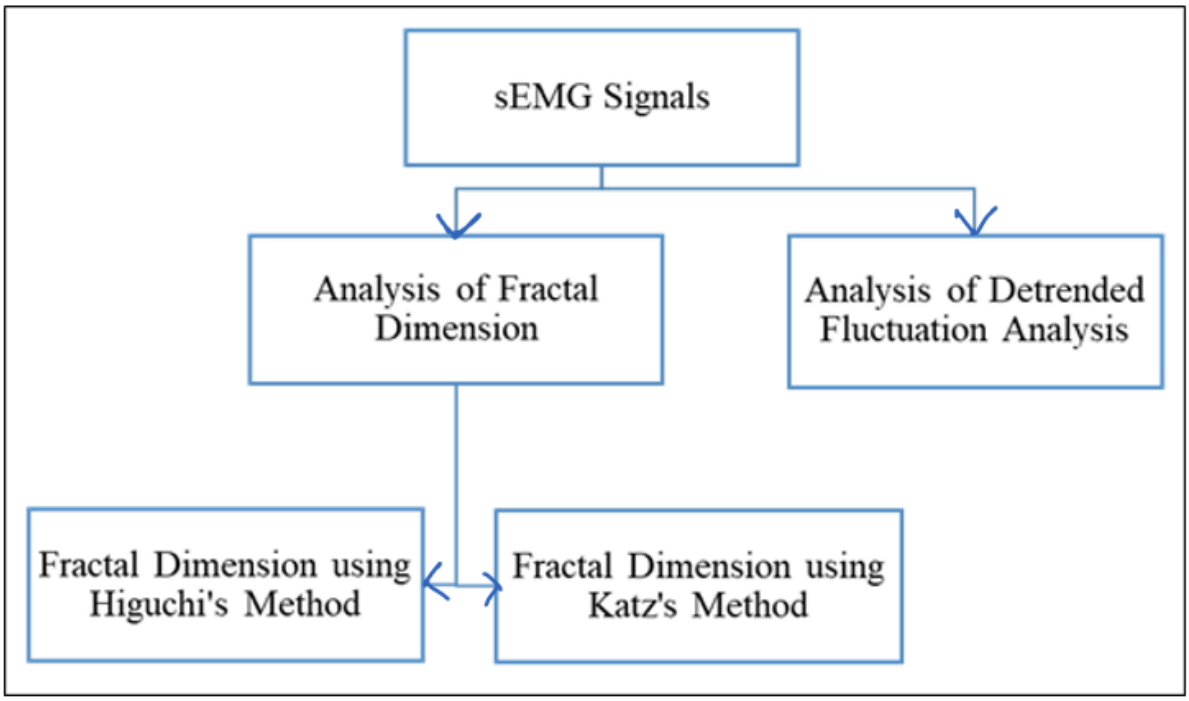

Figure 12: Block Diagram of Methodology for Analysis of sEMG Signal

The sEMG signals were loaded into MATLAB software for additional processing and analysis after the sEMG signals were acquired with the help of specially designed software from RMS. The sample sEMG results of three protocols are shown in Figure 13, 14, 15, 16, 17 and 18.

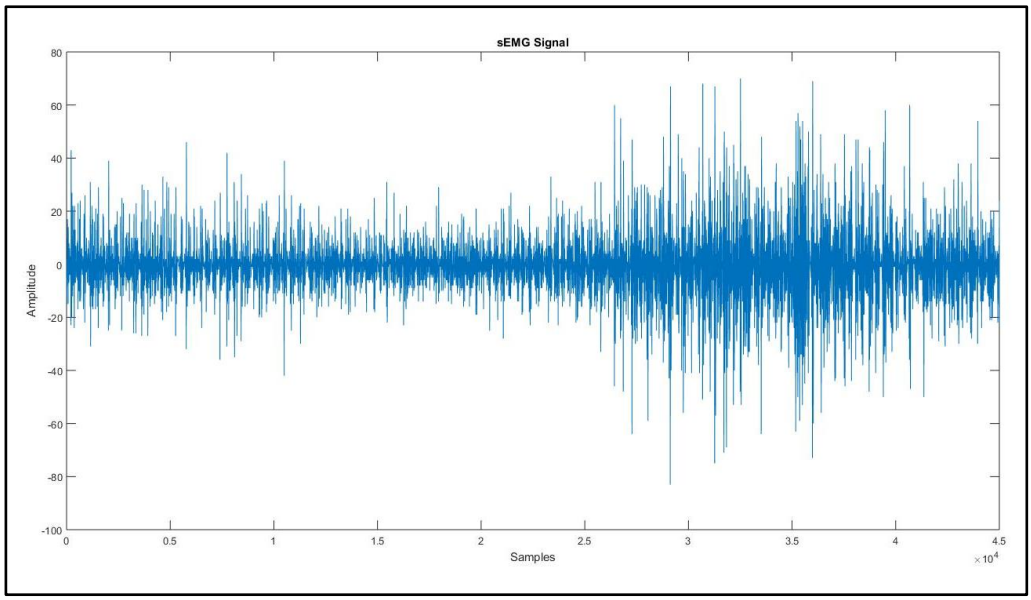

Figure 13: sEMG Signal of Channel 1 during flexion movement under weight

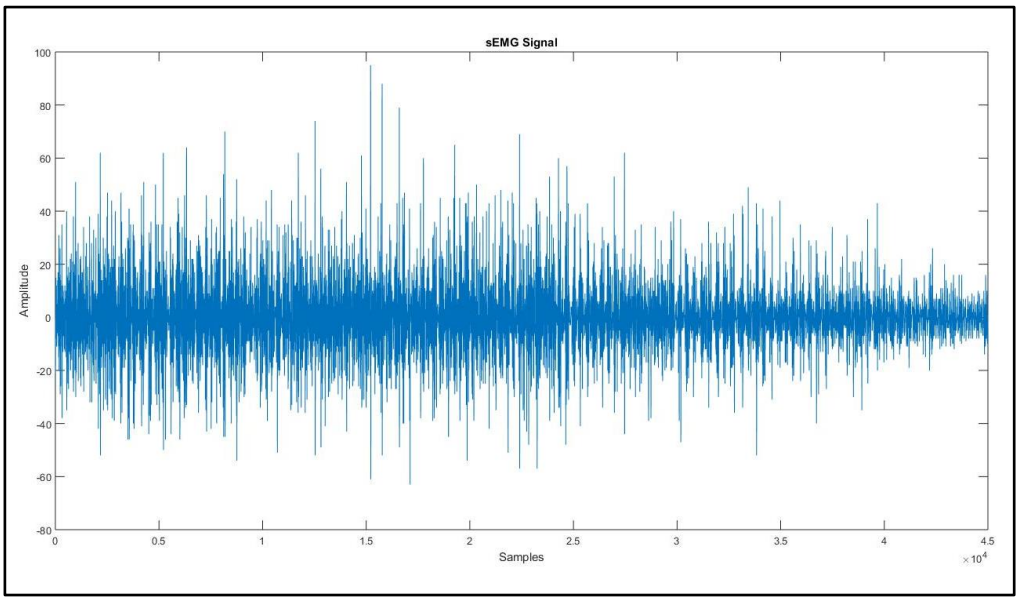

Figure 14: sEMG Signal of Channel 2 during flexion movement under weight

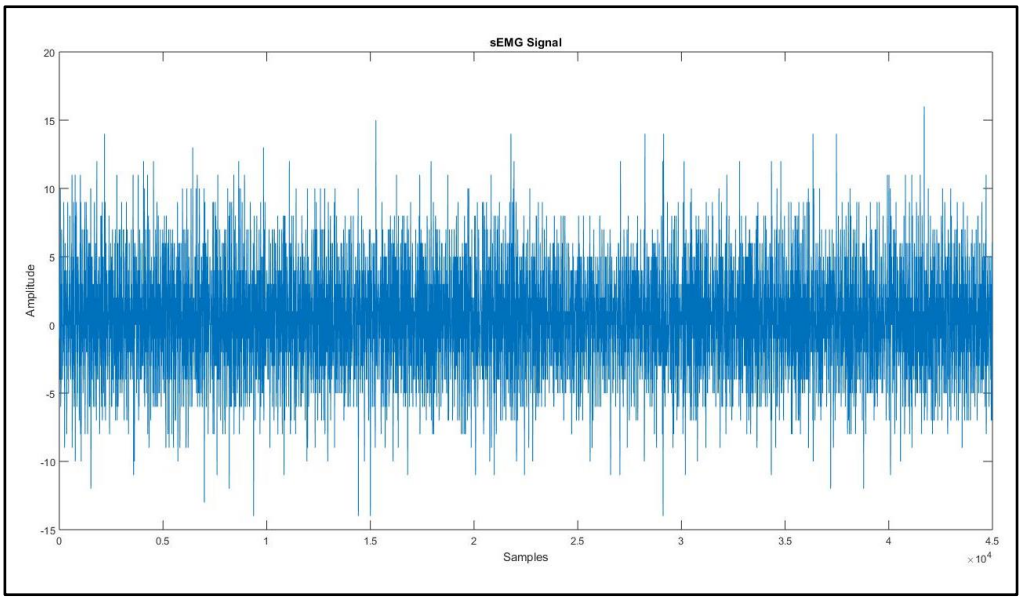

Figure 15: sEMG Signal of Channel 1 during static holding fatigue under weight

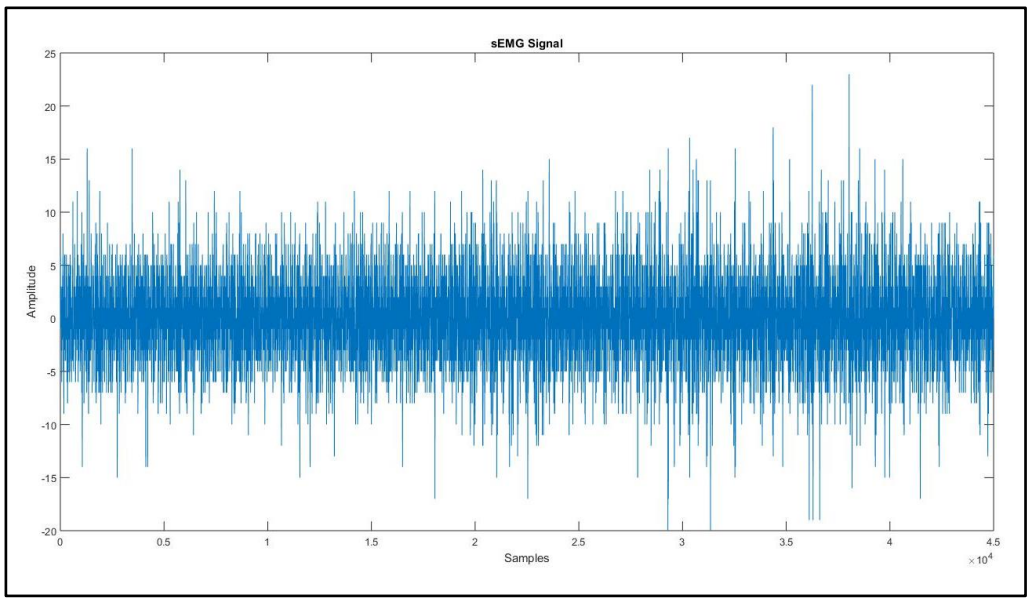

Figure 16: sEMG Signal of Channel 2 during static holding fatigue under weight

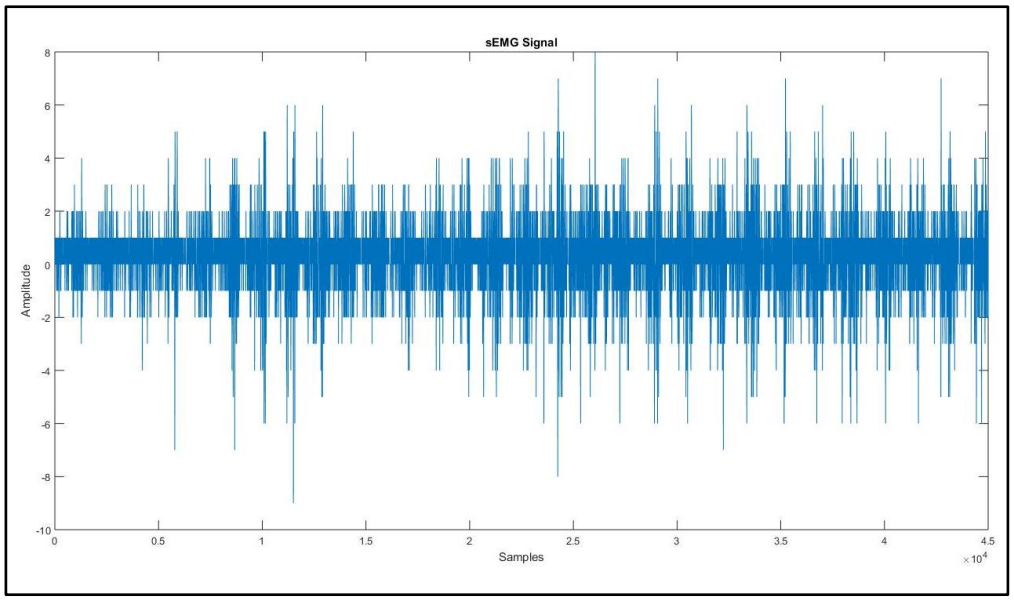

Figure 17: sEMG Signal of Channel 1 during handgrip fatigue using hand dynamometer

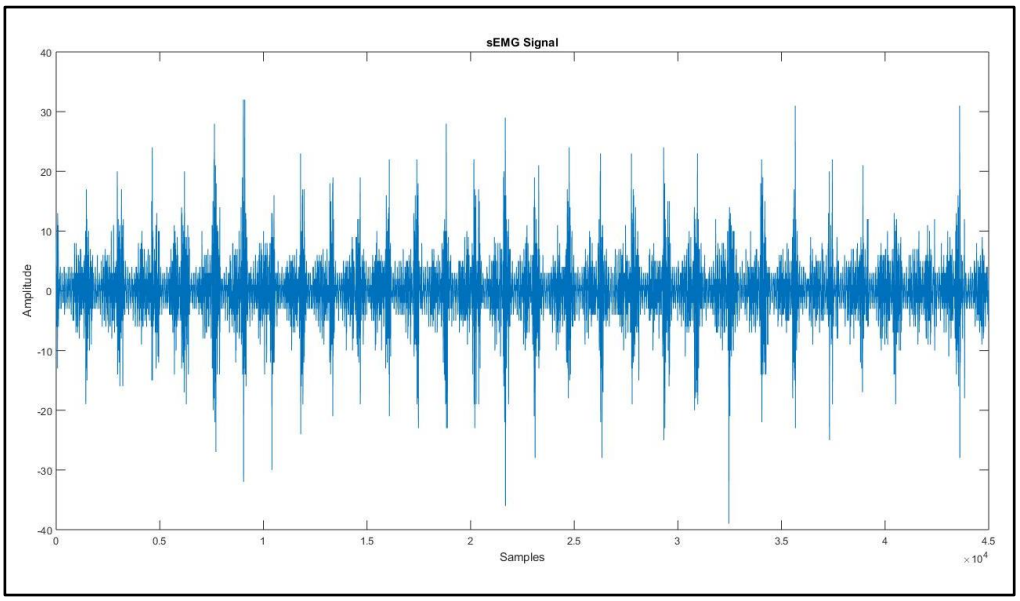

Figure 18: sEMG Signal of Channel 2 during handgrip fatigue using hand dynamometer

3. Study of ECG and EEG signals under the influence of dark chocolate

In this study, it has been designed a protocol that would help us understand the effect of dark chocolate as a stimulus on our heart and brain. The protocol followed to record the effect of dark chocolate on human body is shown in Figure 19.

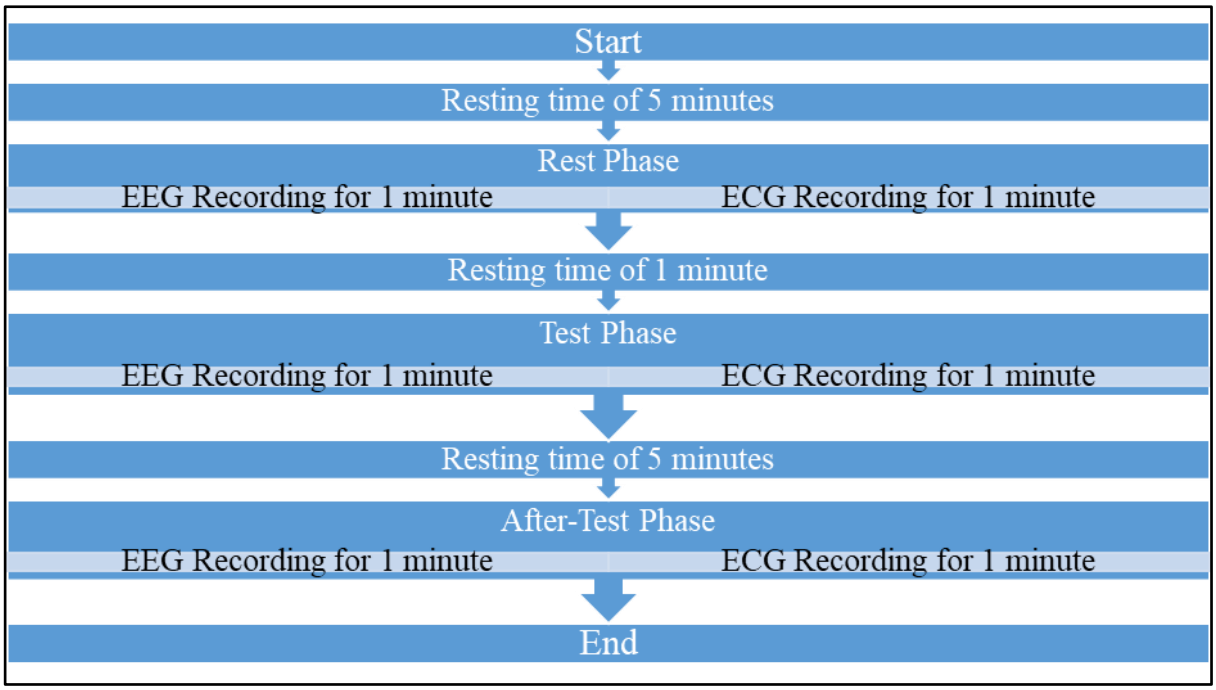

Figure 19: Protocol followed to record the effect of dark chocolate on human brain and heart

In this study, it has been used dark chocolate (50%) as a stimulus. The whole experimental protocol is divided into three phases: rest phase, test phase and after-test phase. During rest phase the subjects were asked to sit quietly, breath normally and close their eyes. Then after skin preparation and electrodes placements, EEG and ECG both are recorded for 1 minute. After completion of the rest phase, the subjects were given a resting time of 1 minute. Then test phase is started. In this phase, the subjects were given the 15gm dark chocolate and told to chew it and hold it in their mouth and then EEG and ECG signals are recorded for 1 minute. After test phase, the subjects were asked finish this chocolate and given a resting time for 5 minutes. Later the subjects were asked to relax and close their eyes and then EEG and ECG are again recorded for 1 minute. In this study, 50 seconds data has been used in three phases for both EEG and ECG signals.

Using the experimental set-up the acquisition of EEG and ECG signals is shown in Figure 20.

Figure 20: Acquisition of EEG and ECG Signals

After proper skin preparation, the 21 EEG electrodes (Ag/AgCl scalp electrodes) were placed according to the International 10/20 system.

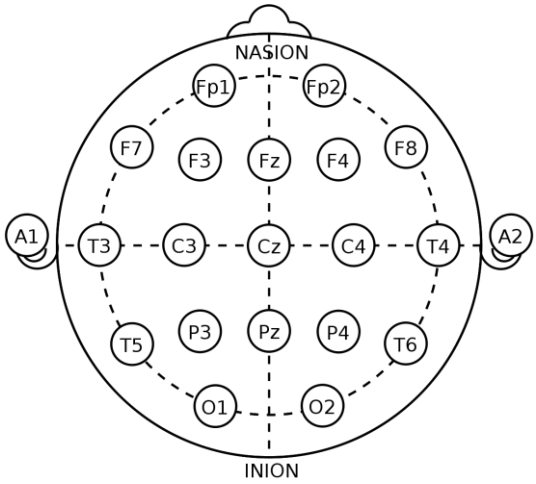

Figure 21: Placement of EEG electrodes according to International 10/20 system [1]

In 21 EEG electrodes, 19 measuring electrodes were placed on the scalp of the subjects and others two electrodes A1 and A2 were put on the earlobe and these two electrodes are used as reference electrodes. The impedance of electrodes were checked below 20 kilo ohms. In this study, common average referential montage for EEG recordings has been used. The signals acquired using these electrodes formed 19 different channels. After amplification and filtering the acquired signals were recorded in the dedicated EEG machine RMS EEG MAXIMUS. The sampling frequency of this EEG system is 256 samples/sec. ECG signals were recorded using ECG electrodes inbuilt into the RMS EEG MAXIMUS system. The ECG measuring electrodes

were put near elbow joint of right and left forearm and one ground electrode was placed on the right wrist of the subjects. In this study, lead I has been used for ECG recording that provided clean ECG signal.

EEG and ECG recordings were obtained from five healthy adult subjects who took part in the study. During the procedure, each subject was asked to close their eyes and sit comfortably and relaxed in a chair. 15gm dark chocolate (50%) was used as stimulus during test phase. The whole methodology of this study is illustrated as block diagram in Figure 22.

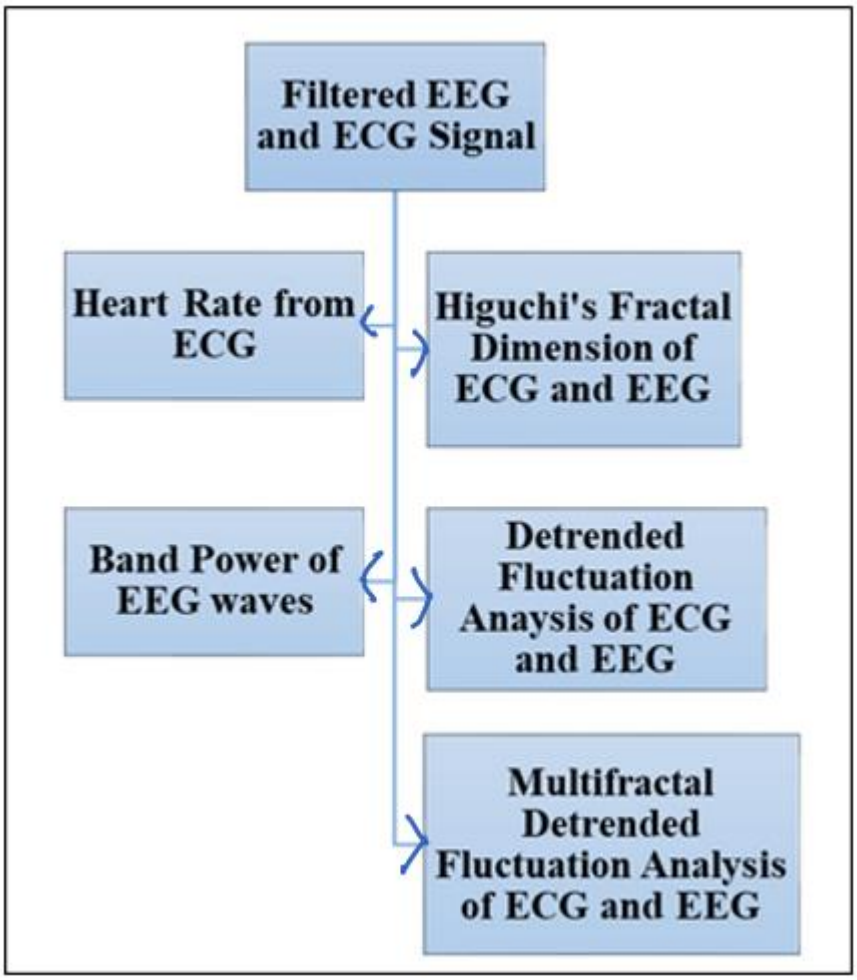

Figure 22: Block Diagram of Methodology for Analysis of EEG and ECG Signals

After acquisition of EEG and ECG signals with the help of customized software of RMS, the filtered signals were loaded into MATLAB software for further processing and analysis. Figure 23 and Figure 24 are the sample results of ECG and EEG respectively.

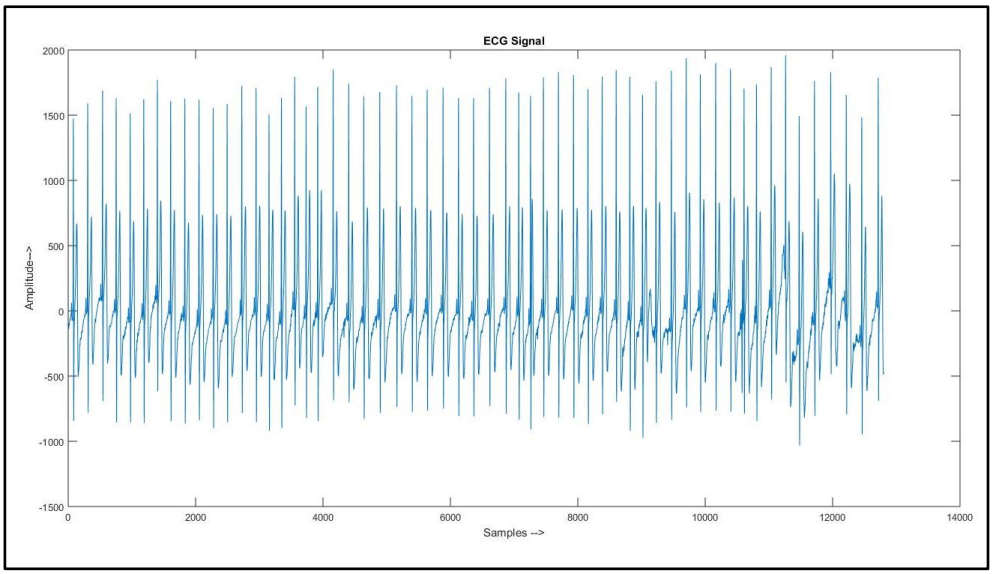

Figure 23: Filtered ECG Signal

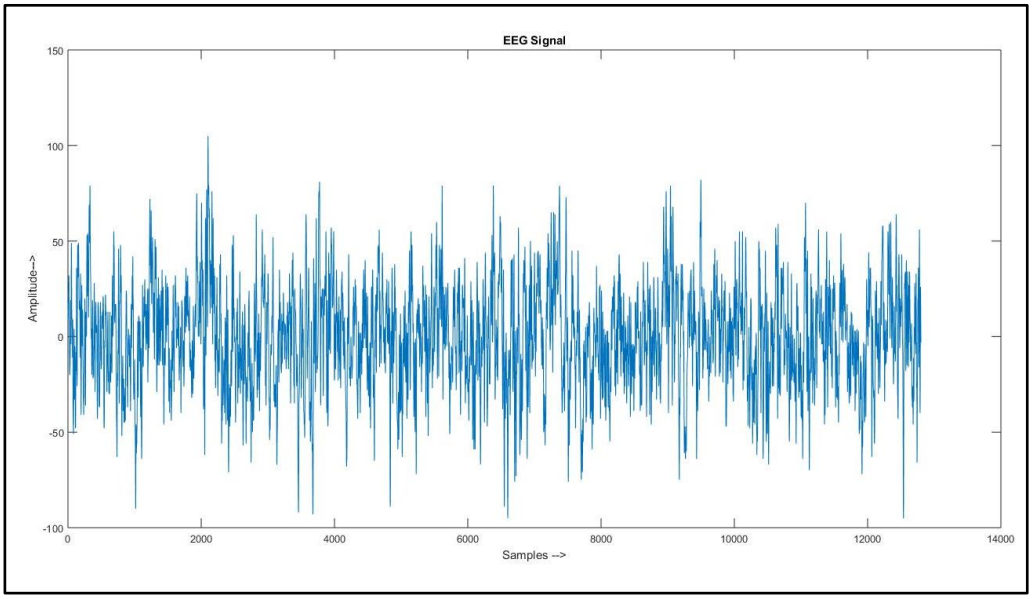

Figure 24: Filtered EEG Signal

3.1. Heart Rate from ECG:

The heart beat or heart rate (HR) is not constant. It changes according to the requirements of the body, with stress, sympathetic and parasympathetic stimulation. Using the beat-to-beat RR-intervals, analysis of the variation in HR is called as Heart Rate Variability (HRV) analysis. The activity of HR results occurring in the two branches of Autonomic Nervous System (ANS) – Parasympathetic and Sympathetic nervous system. These nerves are active at rest condition. At any point of time, the HR estimation represents the net effect of

these both nervous system, where parasympathetic nervous system decelerates the heart rate while sympathetic nervous system accelerates it. There is a direct relationship between HR and HRV. When HR rises there is less time between heartbeats for variability to occur, so HRV decreases, while HR decreases there is more time between heartbeats, so HRV naturally rises [1], [2], [42], [43], [51].

The following formula can be used to calculate the heart rate (HR) from the R-R interval of ECG:

$$HR = \frac{60}{R{-}R\ interval} \qquad (1)$$

Where,

HR is the heart rate in beats per minute (bpm).

R-R interval is the time duration between two successive R peaks in seconds.

3.2. Analysis of Band Power of EEG Signals:

The signal's power is the total of the modulus squares of its time-domain samples divided by the RMS level or length of the signal. The band power represents the estimation of signal power in one step. Band power is the amount of activity of specific frequency bands of a signal. The average power of EEG signals in various conditions of this work has been estimated according to the location of the electrodes [44]. The EEG electrodes have been put on the basis of its location, that is, frontal, frontal-polar, central, temporal, parietal and occipital. The power of electrodes in these regions have been estimated and compared. The average band power of delta, theta, alpha and beta waves of EEG signals have been calculated on MATLAB platform.

4. Application of non-linear dynamical methods

4.1. Analysis of Higuchi's Fractal Dimension (HFD):

To analyse the variation of the fractal dimension (FD) with dark chocolate stimulus, the Higuchi's Fractal dimension method is used. As a nonlinear method for analysing biomedical signals, this method plays an important role. In addition to linear technique, this method can also be used for stationary, transient, stochastic, deterministic, synthetic, and natural signals. Determining the optimal Kmax is important because the HFD result is calculated by Kmax value, not the duration of the signal [45], [52], [53].

A time series X(t) is converted into a new time series i.e. X_k^m with the help of HFD method, where,

$$X_k^m \in \left\{X(m), X(m+k) \ldots . X\left(m + \frac{(N-m)}{k}\right)\right\} \quad (2)$$

Where, $\frac{(N-m)}{k}$ is Gaussian notation and both *m* and *k* are integers. Thus, at time intervals with *k* values each, get a new set of *k* time series. The curved length formed by X_k^m is represented by equation *(3).*

$$L_m(k) = \frac{(N-1)}{int\left[\frac{N-m}{k}\right]k^2} \sum_{i=1}^{int\left[\frac{N-m}{k}\right]} |X(m+ik) - X(m+(i-1)k)| \quad (3)$$

The normalized coefficient of curve length for the partial time series is given in the following term in equation *(4)*

$$\frac{(N-1)}{int\left[\frac{N-m}{k}\right]k} \quad (4)$$

L(k) is the length that is determined by the mean value of $L_1(k), L_2(k) \ldots, L_k(k)$ of *k*, which is represented by the equation *(5)*

$$L(k) = \frac{1}{k} \sum_{m=1}^{k} L_m(k) \quad (5)$$

To determine the Higuchi fractal dimension, find the slope of the *ln(L(k))* versus *ln(1/k)* curve shown in *(6),*

$$HFD = \frac{ln(L(k))}{ln\left(\frac{1}{k}\right)} \quad (6)$$

Higuchi's fractal dimension, which is indicated by the index D, is the fractal dimension identified by Higuchi's method [45].

4.2. Analysis of Katz's Fractal Dimension (KFD):

The Katz algorithm is important for fractal analysis because it accurately estimates the fractal dimensions of various datasets and images, which is a measure essential for evaluating the complexity and self-similarity of fractal structures. The mathematical basis and practical steps of the Katz algorithm are clarified in this section. This algorithm's simplicity shines through, making it adaptable to both one-dimensional and two-dimensional data. It works by examining the interaction between curve segment lengths and corresponding observation scales

within datasets. Analysing the slope of the logarithmic plot of segment lengths versus scales will reveal the fractal dimension [46].

Let $L(l)$ represents the length of the curve segments observed at scale l within the dataset. The Katz algorithm yields an estimation of the fractal dimension D through the following equation:

$$D = \frac{\log\left(\frac{L(l)}{L(1)}\right)}{(\log(l))} \qquad (7)$$

Where:

D = The estimated fractal dimension.

l = The scale or size of the segments.

$L(l)$ = The average length of curve segments at the given scale l.

$L(1)$ = The length of the smallest segments within the dataset.

4.3. Analysis of Detrended Fluctuation Analysis (DFA):

The study of Detrended fluctuation analysis (DFA) is used to examine the scaling nature of time series. It is used to study the fractal behaviour of a signal. The steps of DFA algorithm are illustrated in a block diagram as follows:

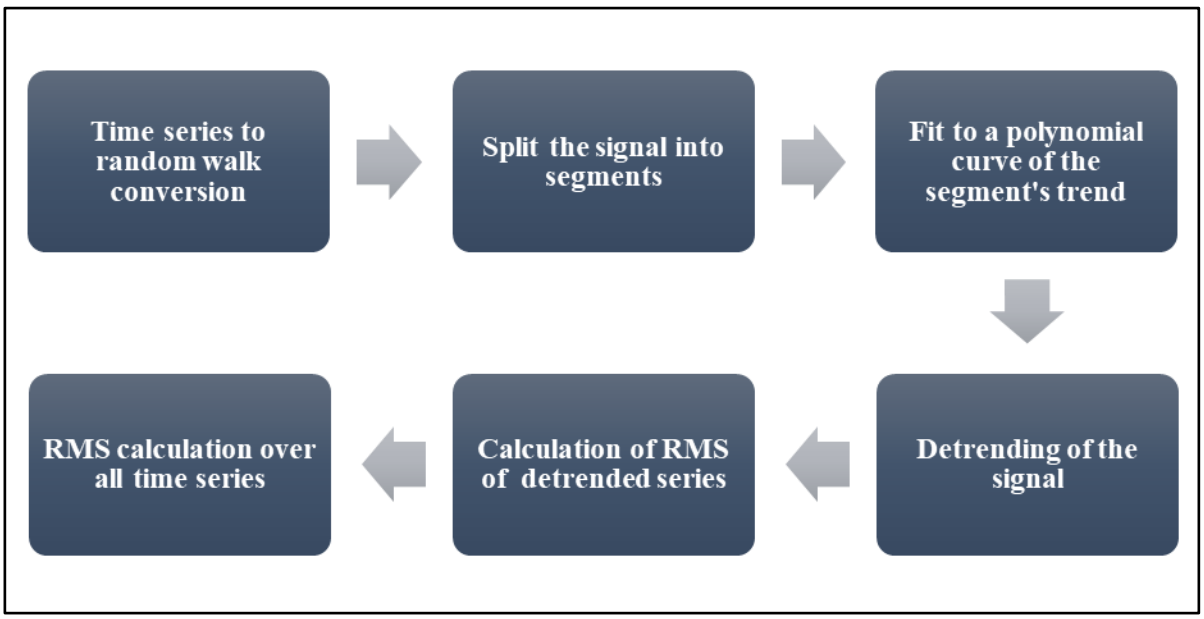

Figure 25: Block Diagram of steps of DFA algorithm

The signal is initially integrated in the DFA algorithm. The signal is integrated in order to transform it from a noise-like signal to a random walk-like signal. The signal is split into smaller parts after integration. The signal in each segment is then fitted to a polynomial curve that depicts the segment's trend. After that, the signal is detrended by subtracting the segment's local trend from the integrated signal. The root mean square of the detrended series is then computed. Finally, the RMS fluctuation is calculated for all-time series. A linear relationship may be seen in the logarithmic plot of fluctuation versus segment length of signal. The slope of this linear line is called as scaling exponent *(α)* of DFA.

The time series of a signal are considered to be 'white noise' when the scaling component *(α)* equals *0.5*, it means the time series is uncorrelated. The time series is positively correlated when $0.5 < \alpha < 1$, which indicates that greater fluctuations are occurring on longer time spans. If $\alpha < 0.5$, the time series is anti-correlated, which means smaller fluctuations are occurring over a wider time span. The long-range temporal correlation no longer reflects the nature of power law when the scaling exponent *(α)* is larger than *1* [47], [48], [49].

4.4. Analysis of Multifractal Detrended Fluctuation Analysis (MFDFA):

When any time series show multifractality, then it is analysed by multifractal detrended fluctuation analysis (MFDFA). A q-order exponent is introduced in MFDFA and the equation is given as:

$$F(n) = \left\{\frac{1}{N}\sum_{k=1}^{N}[y(k) - y_n(k)]^{q/2}\right\}^{1/q} \qquad (8)$$

Except for zero, the q-order exponent can take values ranging from any negative to positive integers. When $q = 2$, it means the time series is monofractal in nature. In MFDFA, scaling exponent is determined for a range of value of q. When q is negative, smaller fluctuation is detected and when q is positive, then larger fluctuation is detected. MFDFA produces a range of scaling component $h(q)$ that represents the scaling component of q^{th} order. The width of a multifractal spectrum is defined as the difference between the maximum and minimum values of *h(q)*. When the width of multifractal spectrum rises, the fluctuation also increases of any time series [48], [49], [50].

Chapter: 5

EXPERIMENTAL RESULTS

1. Analysis of sEMG Characteristics

1.1. Protocol 1 – Flexion Movement of Upper Limb with Variable Weights:

1.1.1. Calculating Fractal Dimension using Higuchi's Method:

Selecting K_{Max}:

The K_{Max} value has a significant role in Higuchi's Fractal Dimension (HFD). The optimal K_{Max} value is determined from the graph saturation point. In Figure 26, the saturation point is K=100, so the K_{Max} is 100 for sEMG signal during the flexion movement of upper limb at no load condition.

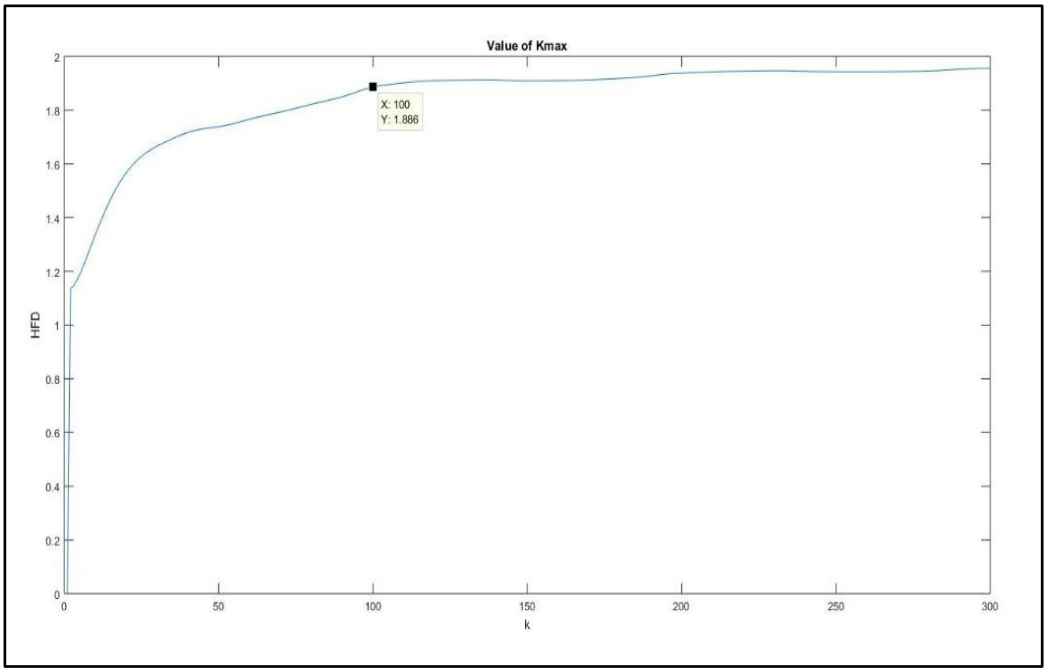

Figure 26: HFD vs K plot shows that Kmax value 100 for sEMG signal during the flexion movement of upper limb at no load condition

Calculation of Higuchi's Fractal Dimension of sEMG Signal:

Table 2 - Average HFD of sEMG signals for each weight for all subjects during the flexion movement of upper limb for channel 1 and channel 2

Weight	***Channel 1***	***Channel 2***
0kg	1.815621979	1.843447559
0.5kg	1.824968259	1.852719799
1kg	1.830263224	1.859330173
1.5kg	1.837081237	1.86275962
2kg	1.842579181	1.865653896
2.5kg	1.840588853	1.867414767
3kg	1.849706689	1.860141643
3.5kg	1.848764522	1.852830197
5kg	1.843267284	1.857822435

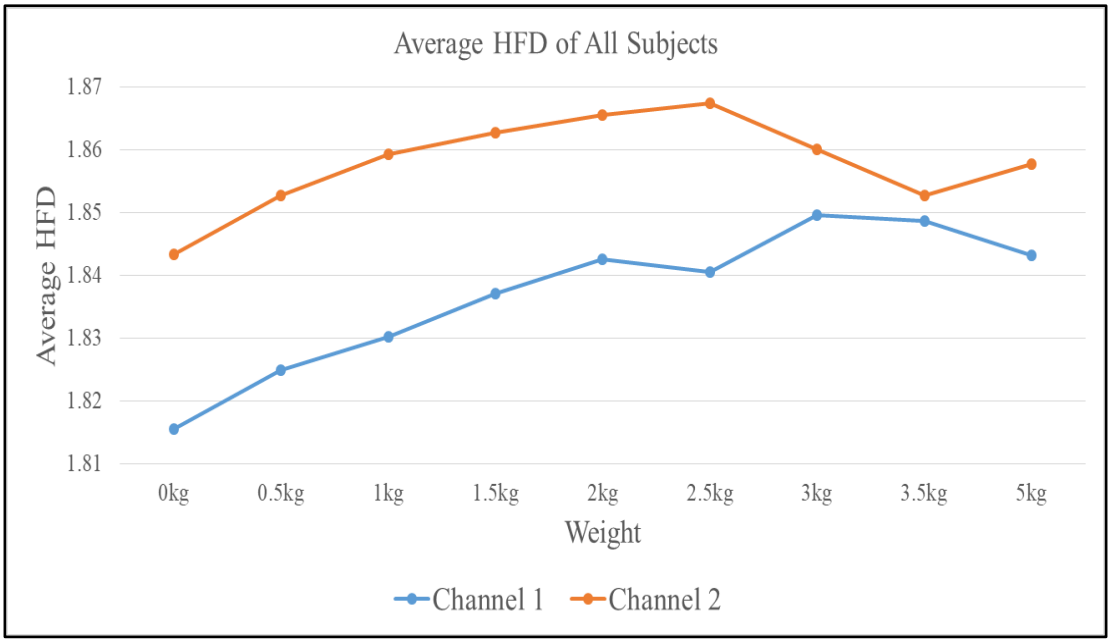

Figure 27: Average HFD of sEMG signals for each weight for all subjects during the flexion movement of upper limb for channel 1 and channel 2

The findings from the above table and charts are-

The average HFD of sEMG signals for each weight for all subjects was determined. The average HFD was shown to rise with increasing weight for all subjects for both channels in Table 2 and Figure 27.

1.1.2. Calculating Fractal Dimension using Katz's Method:

Table 3 - Average KFD of sEMG signals for each weight for all subjects during the flexion movement of upper limb for channel 1 and channel 2

Weight	***Channel 1***	***Channel 2***
0kg	1.01108835	1.006511333
0.5kg	1.013624901	1.009591711
1kg	1.015433219	1.012192419
1.5kg	1.017952534	1.017570088
2kg	1.020252453	1.018784078
2.5kg	1.02264886	1.023908695
3kg	1.049924505	1.027193654
3.5kg	1.059237175	1.028949096
5kg	1.060350064	1.034553003

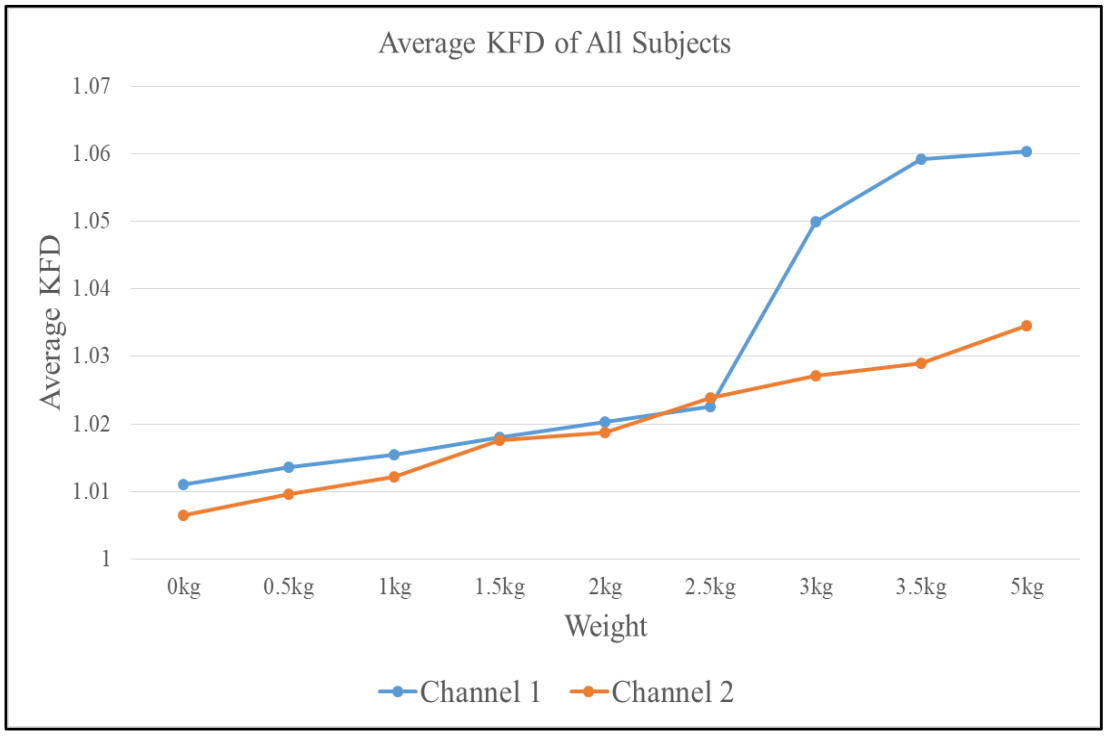

Figure 28: Average KFD of sEMG signals for each weight for all subjects during the flexion movement of upper limb for channel 1 and channel 2

The findings from the above table and charts are-

The average KFD of sEMG signals for each weight was calculated for all individuals. Table 3 and Figure 28 demonstrate that the average KFD increases with increasing weight for all patients in both channels.

1.1.3. Calculation of Scaling Exponent (α) using Detrended Fluctuation Analysis (DFA) of sEMG Signal:

Table 4 - Average Scaling Exponent of sEMG signals for each weight for all subjects during the flexion movement of upper limb for channel 1 and channel 2

Weight	Channel 1	Channel 2
0kg	1.36443115	1.2380572
0.5kg	1.32602382	1.27164541
1kg	1.30088466	1.28898587
1.5kg	1.25465954	1.26302572
2kg	1.25708458	1.21686126
2.5kg	1.24363313	1.20889858
3kg	1.10538599	1.1884111
3.5kg	1.08112925	1.17736003
5kg	1.02852562	1.13464346

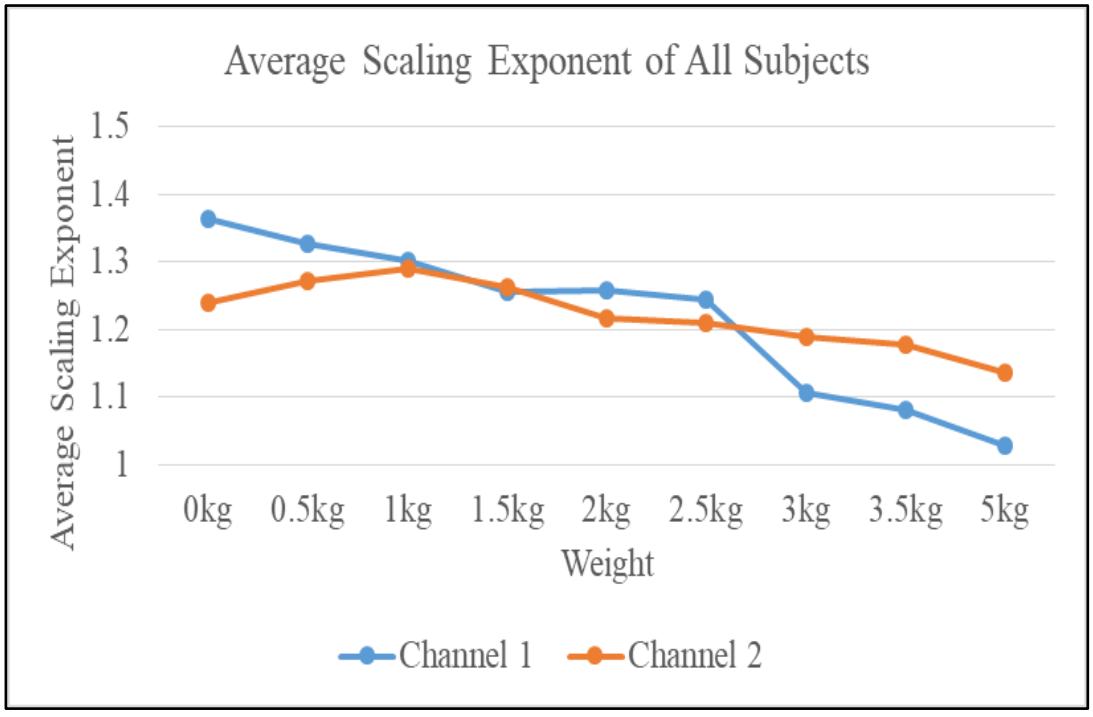

Figure 29: Average Scaling Exponent of sEMG signals for each weight for all subjects during the flexion movement of upper limb for channel 1 and channel 2

The findings from the above table and charts are-

As demonstrated in Table 4 and Figure 29, the average of scaling component (α) shows a decreasing trend with increasing load for all subjects and both channels.

1.1.4. Summary of Experiment

The complexity of sEMG signal increases with increase in weight for both the biceps and forearm muscles during the flexion movement using both Higuchi's and Katz's Methods. This is occurred due to changes in muscle recruitment patterns, muscle fiber recruitment, and the complexity of muscle activation with weight variation. The scaling exponent of DFA for biceps and forearm muscles decreases during flexion movement due to related to changing dynamics of muscles under varying loads.

1.2. Protocol 2 – Static Holding Fatigue of Upper Limb with Variable Weights:

1.2.1. Calculating Fractal Dimension using Katz's Method:

Table 5 - Average KFD of sEMG signals for each weight for all subjects during the static holding fatigue of upper limb for channel 1 and channel 2

Weight	***Channel 1***	***Channel 2***
0kg	1.00890548	1.007425221
0.5kg	1.01183576	1.010339386
1kg	1.014297729	1.012962841
1.5kg	1.017147515	1.014896342
2kg	1.021374644	1.01628131
2.5kg	1.02541744	1.023513911
3kg	1.030701582	1.02245156
3.5kg	1.036886514	1.02831218

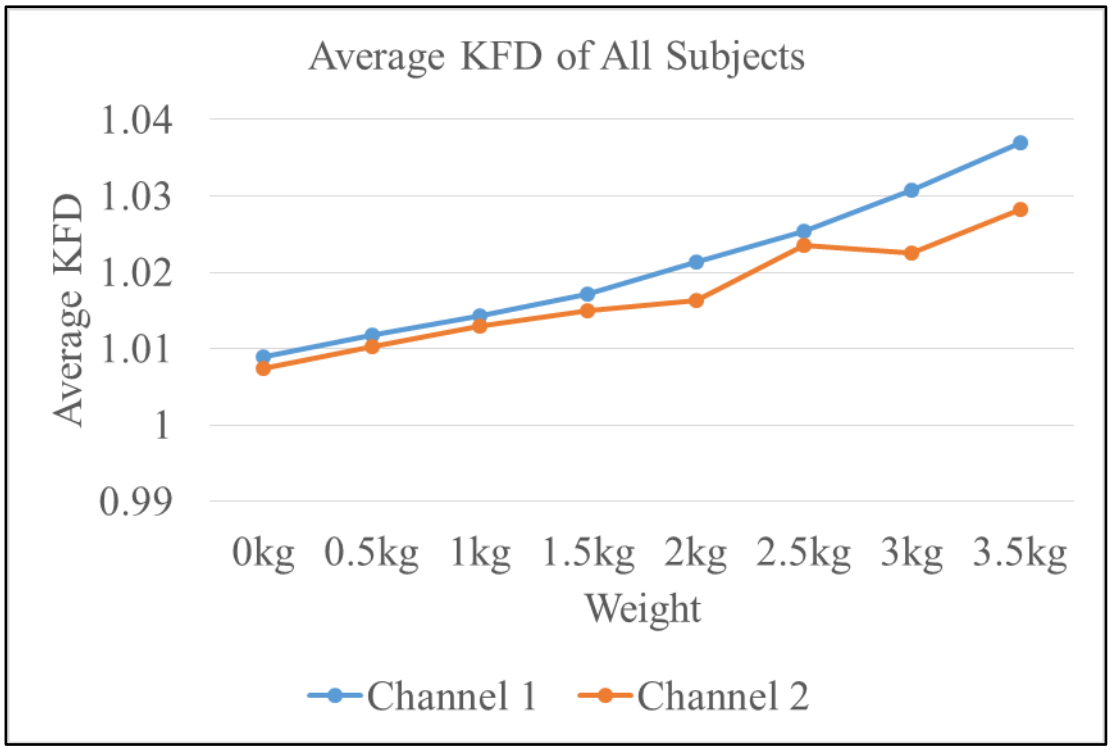

Figure 30: Average KFD of sEMG signals for each weight for all subjects during the static holding fatigue of upper limb for channel 1 and channel 2

The findings from the above table and charts are-

For each weight, the average KFD of sEMG signals was determined for all subjects. Table 5 and Figure 30 show that the average KFD increases with increasing weight in both channels for all subjects during the static holding fatigue of upper limb.

1.2.2. *Calculation of Scaling Exponent (α) using Detrended Fluctuation Analysis (DFA) of sEMG Signal:*

Table 6 - Average Scaling Exponent of sEMG signals for each weight for all subjects during the static holding fatigue of upper limb for channel 1 and channel 2

Weight	***Channel 1***	***Channel 2***
0kg	1.312327748	1.350642454
0.5kg	1.271692503	1.295055942
1kg	1.235286655	1.302158127
1.5kg	1.223357966	1.287527659
2kg	1.195185487	1.268033788
2.5kg	1.166266739	1.202376141
3kg	1.149426147	1.196083607
3.5kg	1.110400786	1.184011075

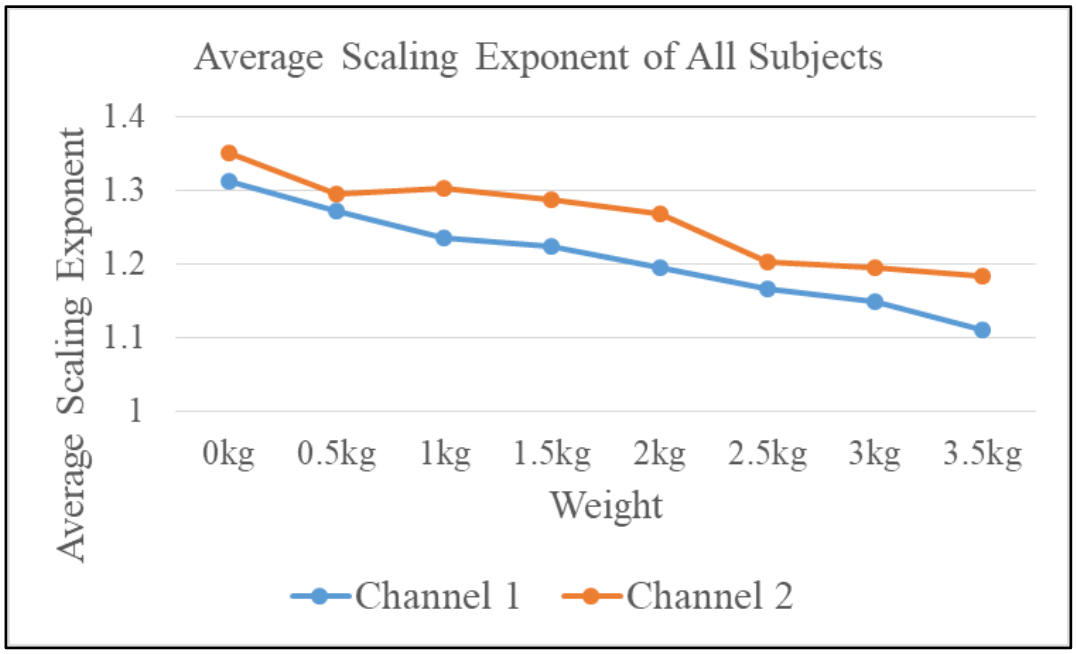

Figure 31: Average Scaling Exponent of sEMG signals for each weight for all subjects during the static holding fatigue of upper limb for channel 1 and channel 2

The findings from the above table and charts are-

For each weight, the average scaling exponent using DFA of sEMG signals was determined for all subjects during the static holding fatigue of upper limb. As seen in Table 6 and Figure

31, the average of the scaling exponent (α) decreases with increasing load for all subjects and both channel 1 and 2.

1.2.3. Summary of Experiment

The Fractal analysis shows that the complexity of sEMG signal rises with increase in weight for both the biceps and forearm muscles during the static holding fatigue due to changes in muscle recruitment patterns and activation under varying weights. The scaling exponent of DFA for these muscles decreases due to related to changing dynamics of muscles with load variation.

1.3. Protocol 3 – Handgrip Fatigue through Hand Dynamometer:

1.3.1. Calculating Fractal Dimension using Higuchi's Method:

Selecting K_{max}:

In Figure 32, the saturation point is K=100, so the K_{Max} is 100 for sEMG signal during the handgrip fatigue through hand dynamometer.

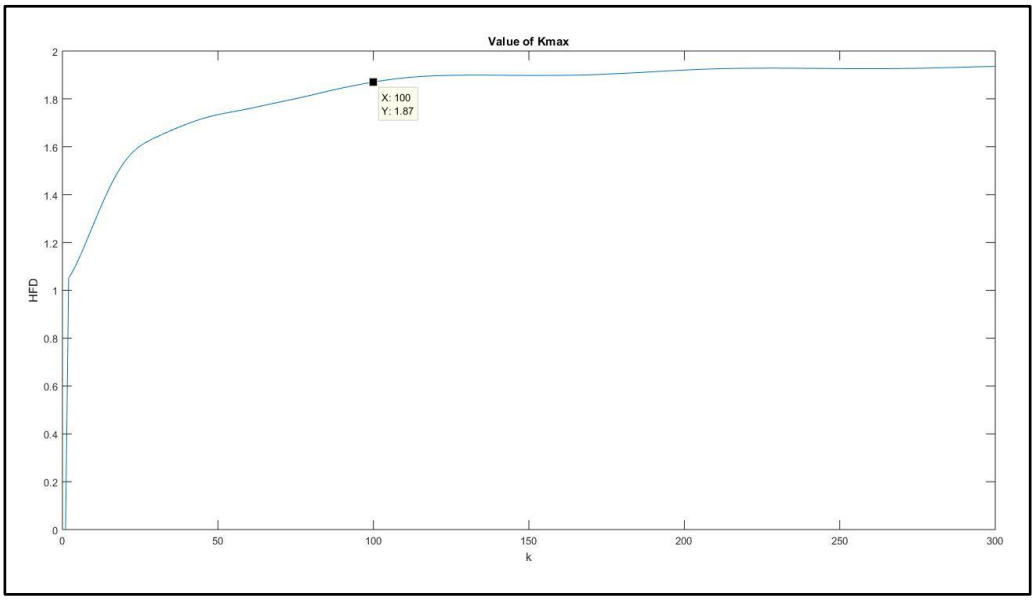

Figure 32: HFD vs K plot shows that Kmax value 100 for sEMG signal during the handgrip fatigue through hand dynamometer

Calculation of Higuchi's Fractal Dimension of sEMG Signal:

Table 7 - HFD of sEMG signals for each subject during the handgrip fatigue through hand dynamometer for channel 1 and channel 2

	Channel 1	***Channel 2***
Subject 1	1.864704237	1.870298974
Subject 2	1.754290932	1.884965449
Subject 3	1.800748396	1.816234912
Subject 4	1.803039563	1.839350858
Subject 5	1.854392382	1.912113518
Subject 6	1.758220292	1.882085972
Subject 7	1.866715813	1.90826187
Subject 8	1.794914965	1.826108965
Average	**1.812128322**	**1.867427565**

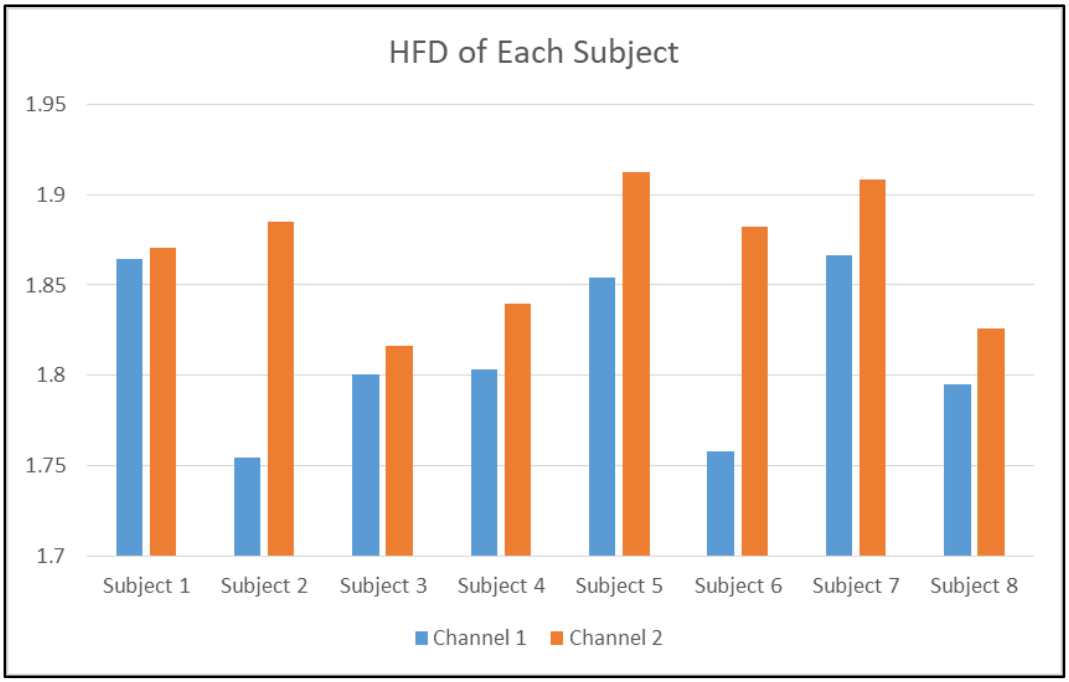

Figure 33: HFD of sEMG signals for each subject during the handgrip fatigue through hand dynamometer for channel 1 and channel 2

The findings from the above table and charts are-

As shown in Table 7 and Figure 33, the HFD of Channel 2 increases when compared to all persons and both channels during handgrip fatigue as measured by a hand dynamometer.

Furthermore, the same scenario is analysed with an average value of HFD for both channels, as shown in Table 7.

1.3.2. Calculating Fractal Dimension using Katz's Method:

Table 8 - KFD of sEMG signals for each subject during the handgrip fatigue through hand dynamometer for channel 1 and channel 2

	Channel 1	***Channel 2***
Subject 1	1.009617084	1.036902618
Subject 2	1.006384303	1.019701691
Subject 3	1.003801608	1.013598225
Subject 4	1.011810595	1.01539087
Subject 5	1.004439114	1.025301568
Subject 6	1.012886772	1.019173966
Subject 7	1.010750467	1.019244479
Subject 8	1.009767397	1.01991956
Average	**1.008682168**	**1.021154122**

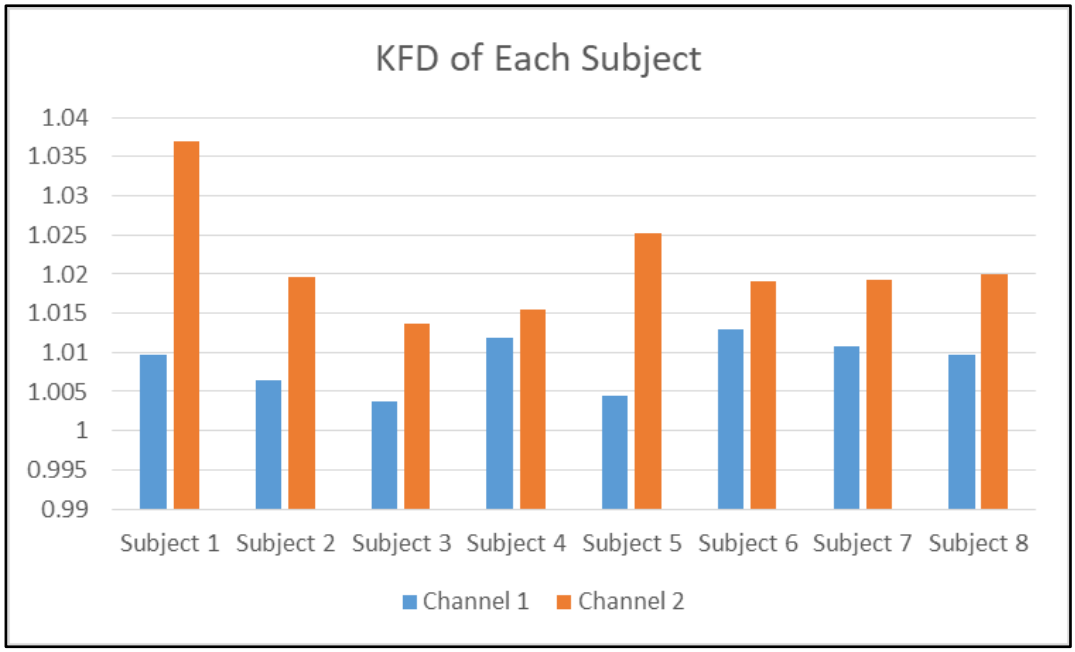

Figure 34: KFD of sEMG signals for each subject during the handgrip fatigue through hand dynamometer for channel 1 and channel 2

The findings from the above table and charts are-

The KFD of Channel 2 increases as compared to for all persons and both channels during handgrip fatigue as measured by a hand dynamometer, as shown in Table 8 and Figure 34. Table 8 shows an average value of KFD of Channel 2 is higher than Channel 1.

1.3.3. Calculation of Scaling Exponent (α) using Detrended Fluctuation Analysis (DFA) of sEMG Signal:

Table 9 - Scaling Exponent of sEMG signals for each subject during the handgrip fatigue through hand dynamometer for channel 1 and channel 2

	Channel 1	***Channel 2***
Subject 1	1.229572822	1.11292694
Subject 2	1.351686741	1.256161128
Subject 3	1.121335849	1.455863944
Subject 4	1.37845456	1.384027841
Subject 5	1.132659166	1.193589256
Subject 6	1.376441338	1.343338539
Subject 7	1.208540966	1.240384707
Subject 8	1.362007987	1.213701819
Average	**1.270087429**	**1.274999272**

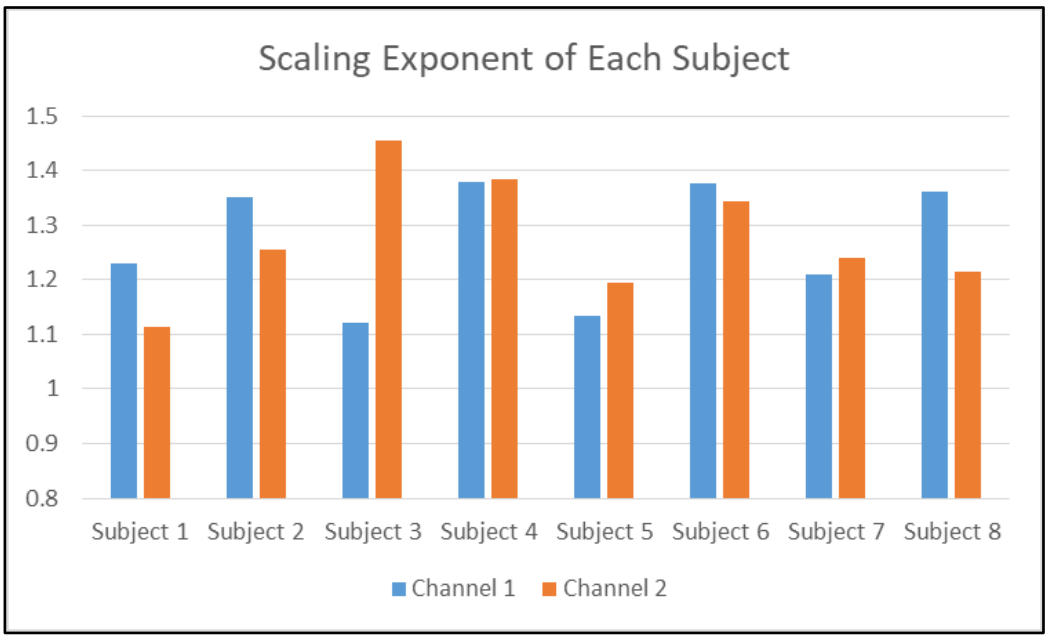

Figure 35: Scaling Exponent of sEMG signals for each subject during the handgrip fatigue through hand dynamometer for channel 1 and channel 2

The findings from the above table and charts are-

During the handgrip fatigue through hand dynamometer, the scaling exponent of sEMG signals was obtained for all participants using DFA. The scaling exponent of Channel 2 is greater than Channel 1 for Subject 3, 4, 5 and 8 while the scaling component of Channel 2 is lower than Channel 1 for others subjects.

The average of the scaling exponent of Channel 2 is slightly higher compared to Channel 1, as shown in Table 9.

1.3.4. Summary of Experiment

The complexity is greater for forearm muscles than biceps muscles during the handgrip fatigue as related to the different roles and muscle fiber compositions of these muscle groups. When handgrip fatigue is measured with a hand dynamometer, variation in the scaling exponent of DFA between the forearm and biceps muscles can be attributed to variations in muscle mobilization patterns, biomechanics, and individual physiological differences.

2. Effects of Dark Chocolate Consumption on ECG and EEG Parameters

2.1. Calculating Heart Rate from ECG Signal:

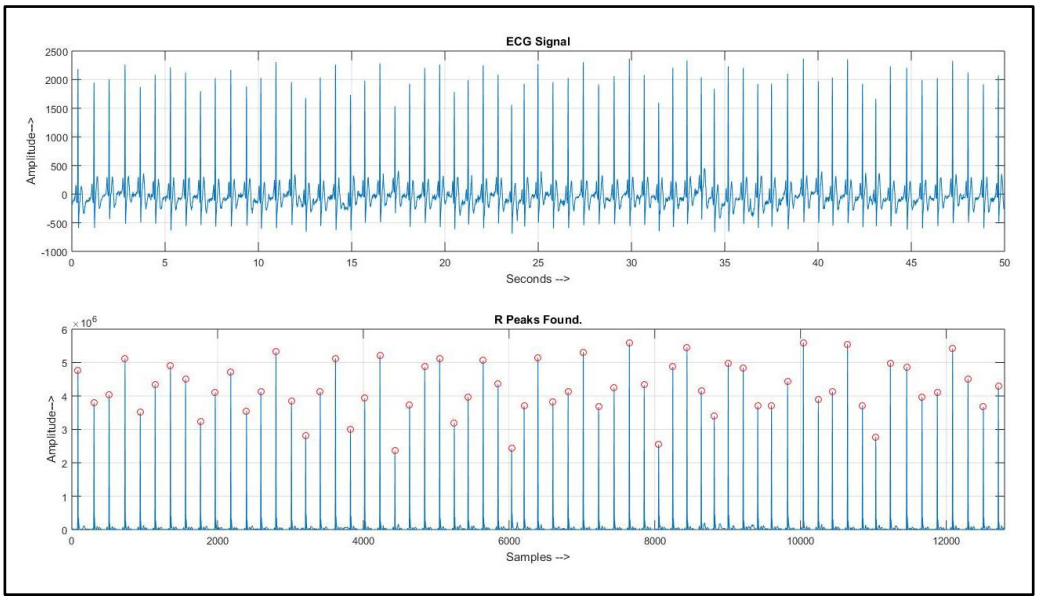

Figure 36: ECG Signal and R peaks of a subject during rest condition

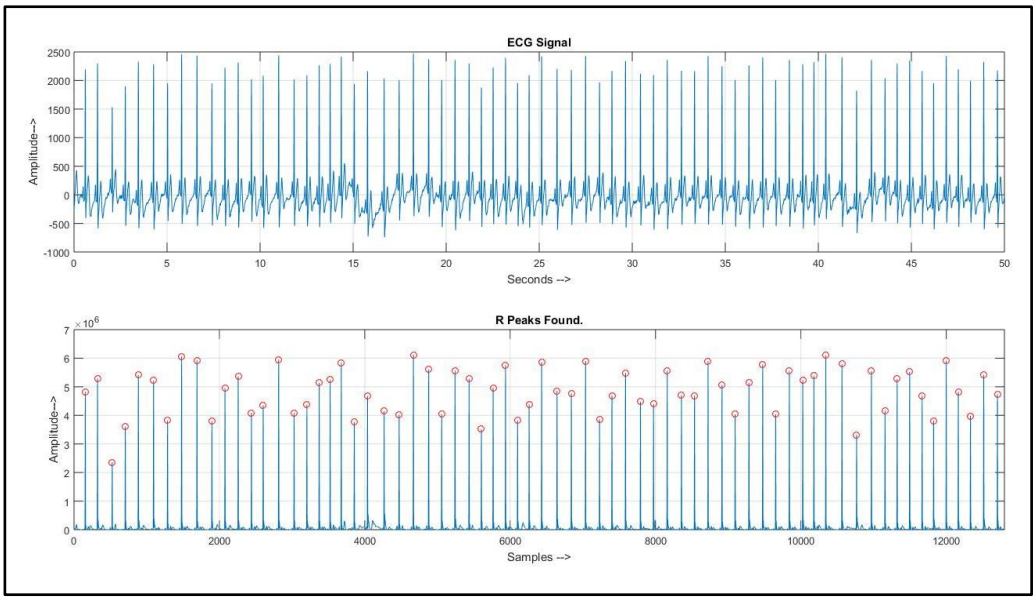

Figure 37: ECG Signal and R peaks of a subject during test condition

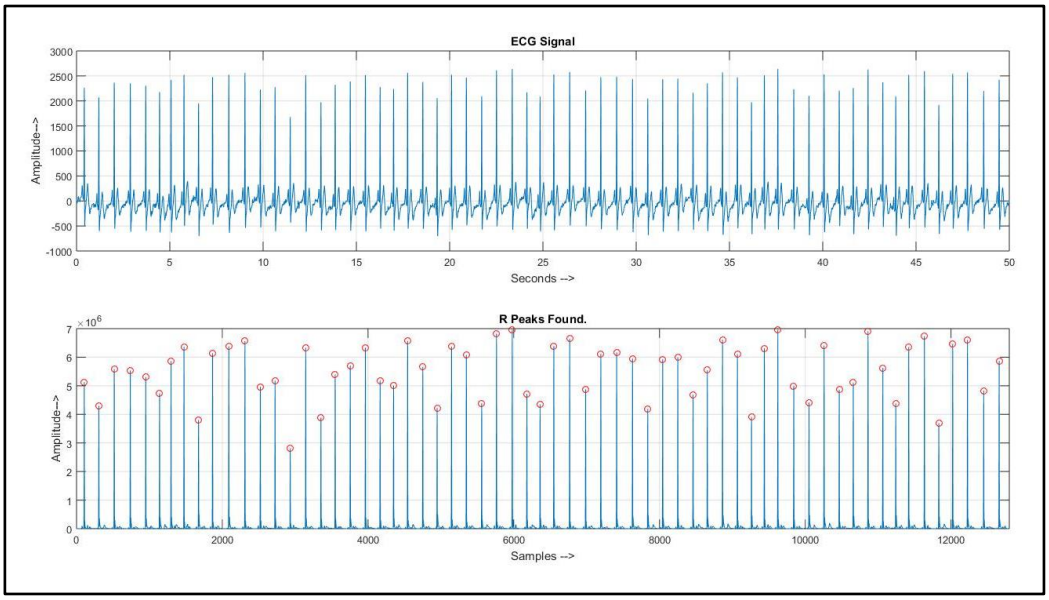

Figure 38: ECG Signal and R peaks of a subject during after-test condition

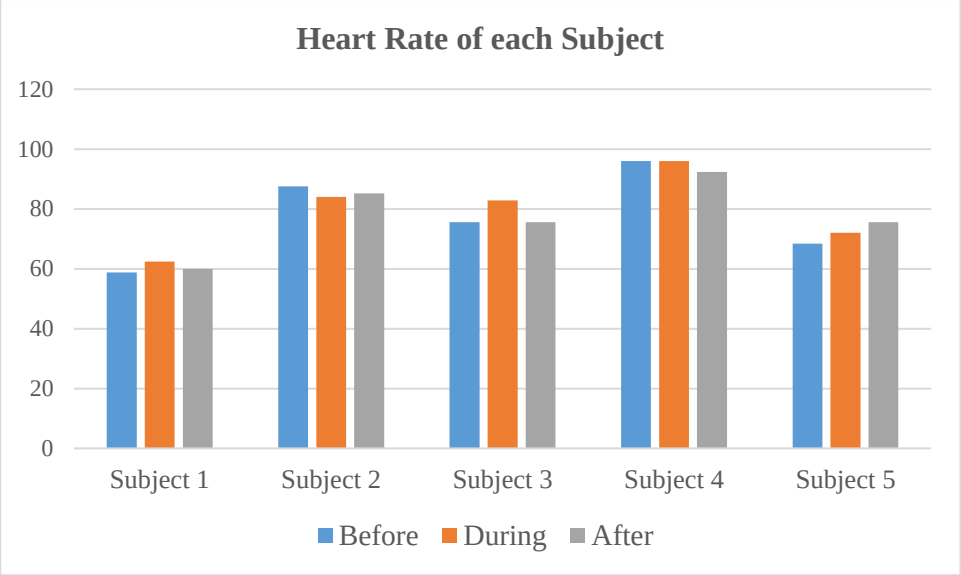

Figure 39: Heart Rate of each Subject among three conditions

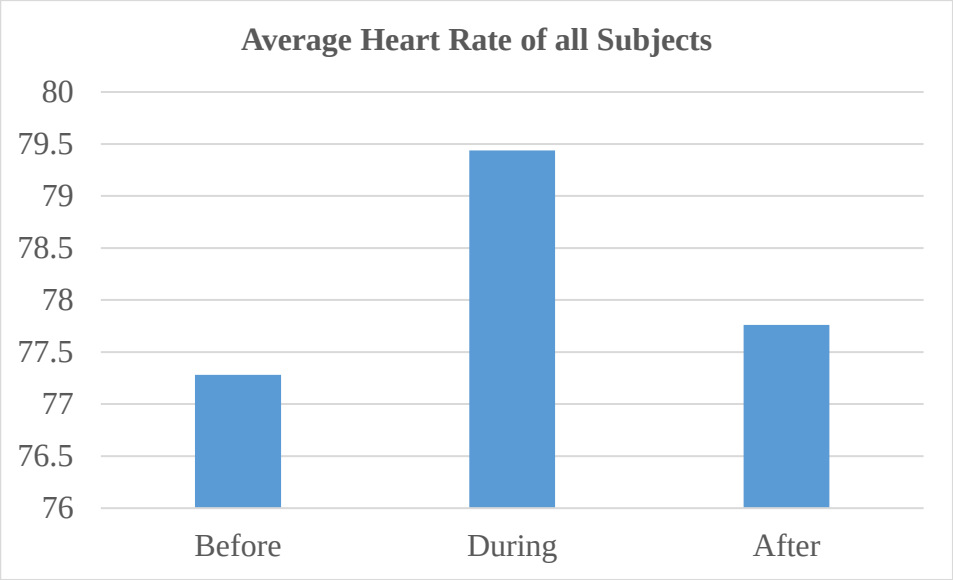

Figure 40: Average Heart Rate of all Subjects among three conditions

The findings from the above charts are-

- In all the subjects except Subject 2, the Heart Rate increases slightly when dark chocolate stimulus is applied.
- In Subject 2, Heart Rate decreases slightly when the stimulus is applied.
- When the stimulus is stopped, the Heart Rate is slightly decreased for all subjects except Subject 2 and Subject 5.
- In Subject 2 and Subject 5, the Heart Rate is marginally increased when the stimulus is stopped.

- It is seen from Figure 40 that an average Heart Rate for all subjects rises when the dark chocolate stimulus is applied.
- In Figure 40, an average Heart Rate for all subject is decreased when the stimulus is stopped.

2.2. Calculation of Band Power of EEG Signal:

2.2.1. Calculation of Band Power of Delta Wave from EEG Signal:

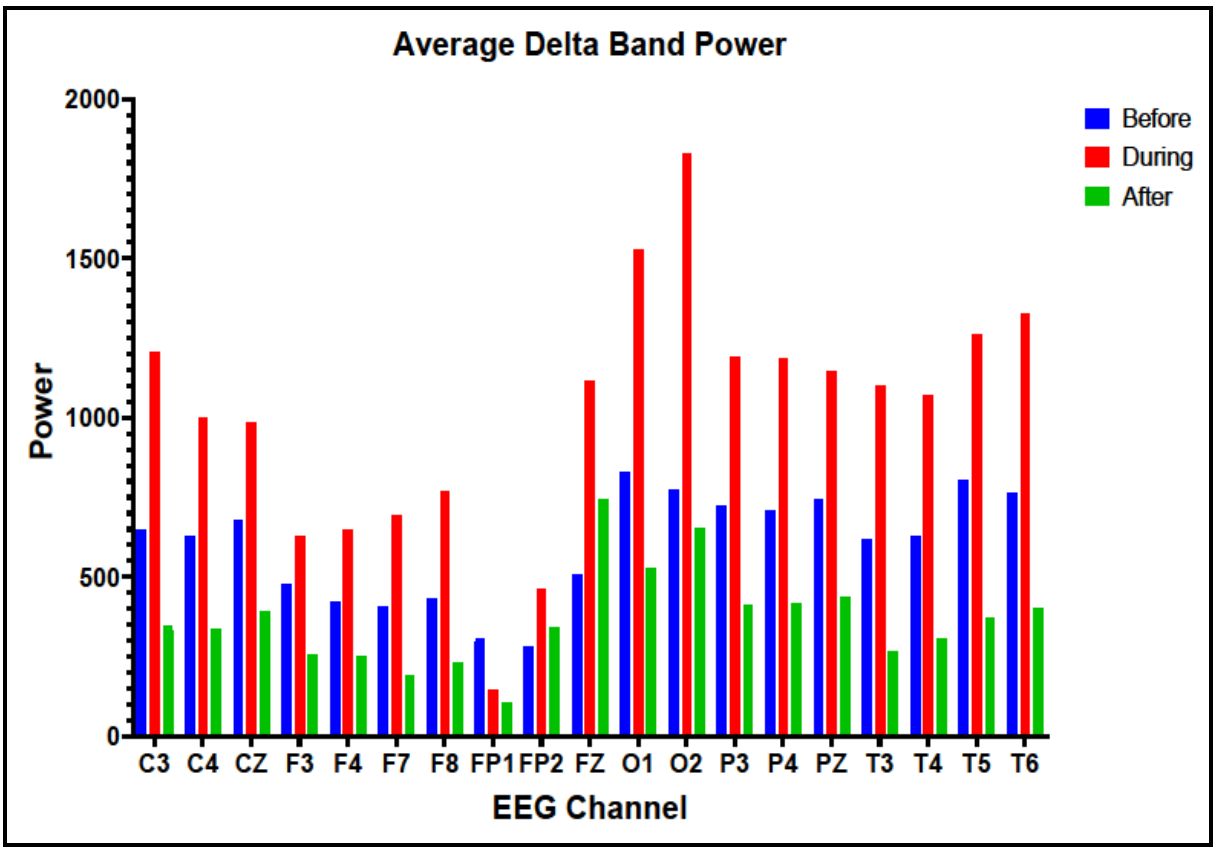

Figure 41: Average Delta Band Power of all EEG Channels for all Subjects among three conditions

The findings from the above charts are-

- Average band power of delta wave rises in all subjects during stimulus phase for all EEG channels except FP1-REF channel.
- FP1-REF channel shows a decreasing pattern of average delta band power for all subjects when stimulus is applied.
- In after-test phase, the average delta band power for all subjects decreases with respect to normal condition of all channels except FP2-REF and FZ-REF channels. FP2-REF

and FZ-REF channels show an increasing trend with respect to rest condition for all subjects.

- In after-test phase, the average delta power decreases with compare to stimulus phase for all subjects of all 19 channels.

2.2.2. Calculation of Band Power of Theta Wave from EEG Signal:

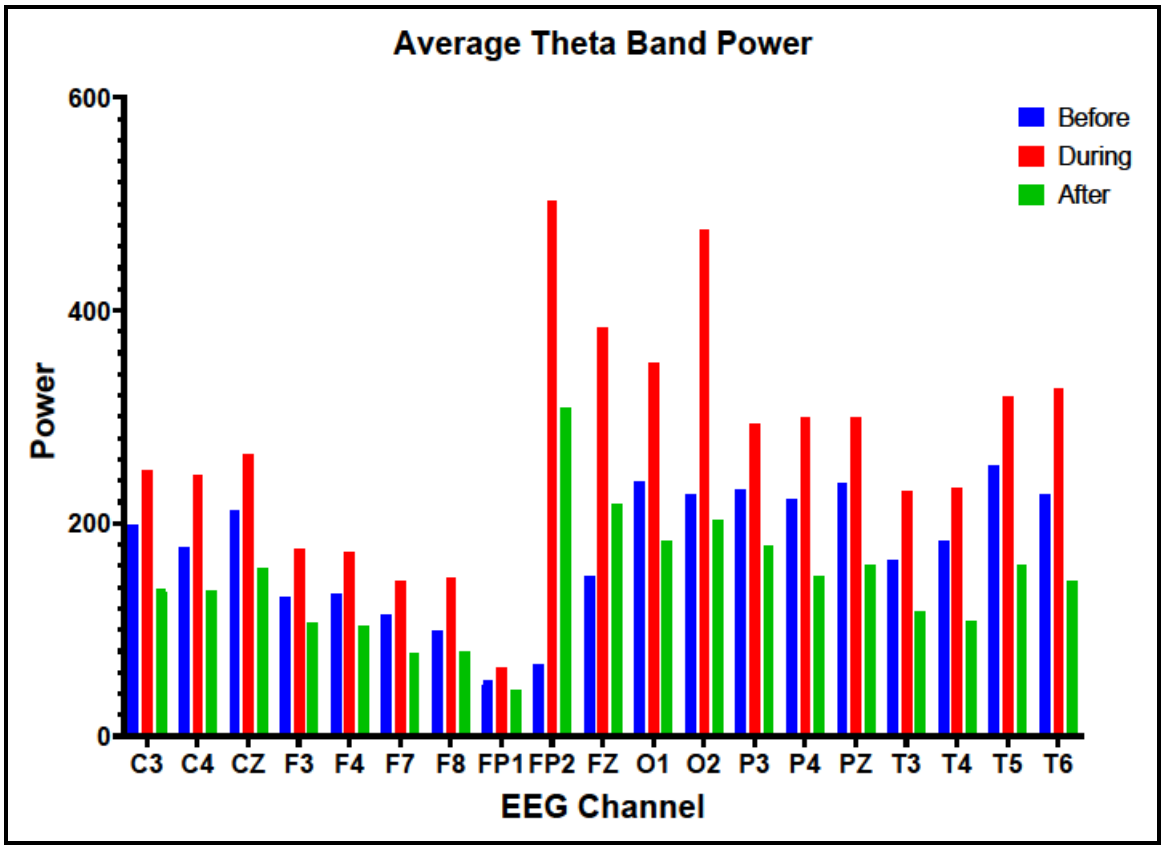

Figure 42: Average Theta Band Power of all EEG Channels for all Subjects among three conditions

The findings from the above charts are-

- The average band power of theta wave increases in all subjects during stimulus phase for all 19 EEG channels.
- In after-test phase, the average theta band power decreases with compare to normal condition of all channels except FP2-REF and FZ-REF channels. FP2-REF and FZ-REF channels show an increasing average theta band power with respect to rest condition for all subjects.

- In after-test phase, the average theta band power decreases with compare to stimulus phase for all subjects of all 19 channels.

2.2.3. Calculation of Band Power of Alpha Wave from EEG Signal:

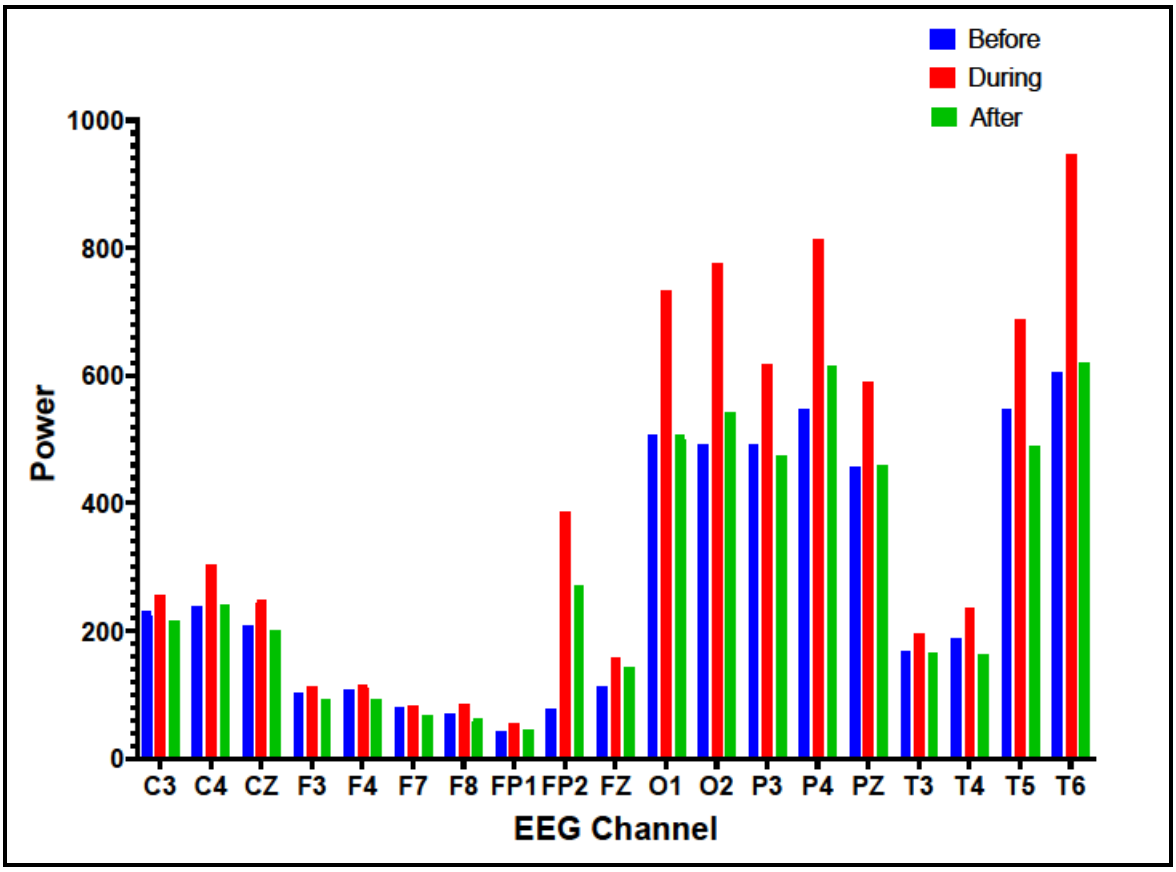

Figure 43: Average Alpha Band Power of all EEG Channels for all Subjects among three conditions

The findings from the above charts are-

- Average band power of alpha EEG wave rises in all subjects during stimulus phase for all EEG channels.
- In after-test phase, the average delta band power decreases with respect to normal condition for all subjects of all channels except FP1-REF, FP2-REF, FZ-REF, O2-REF, P4-REF, PZ-REF and T6-REF channels. These channels show an increasing trend with respect to rest condition for all subjects.
- In after-test phase, the average delta power decreases with compare to stimulus phase for all subjects of all 19 channels.

2.2.4. ***Calculation of Band Power of Beta Wave from EEG Signal:***

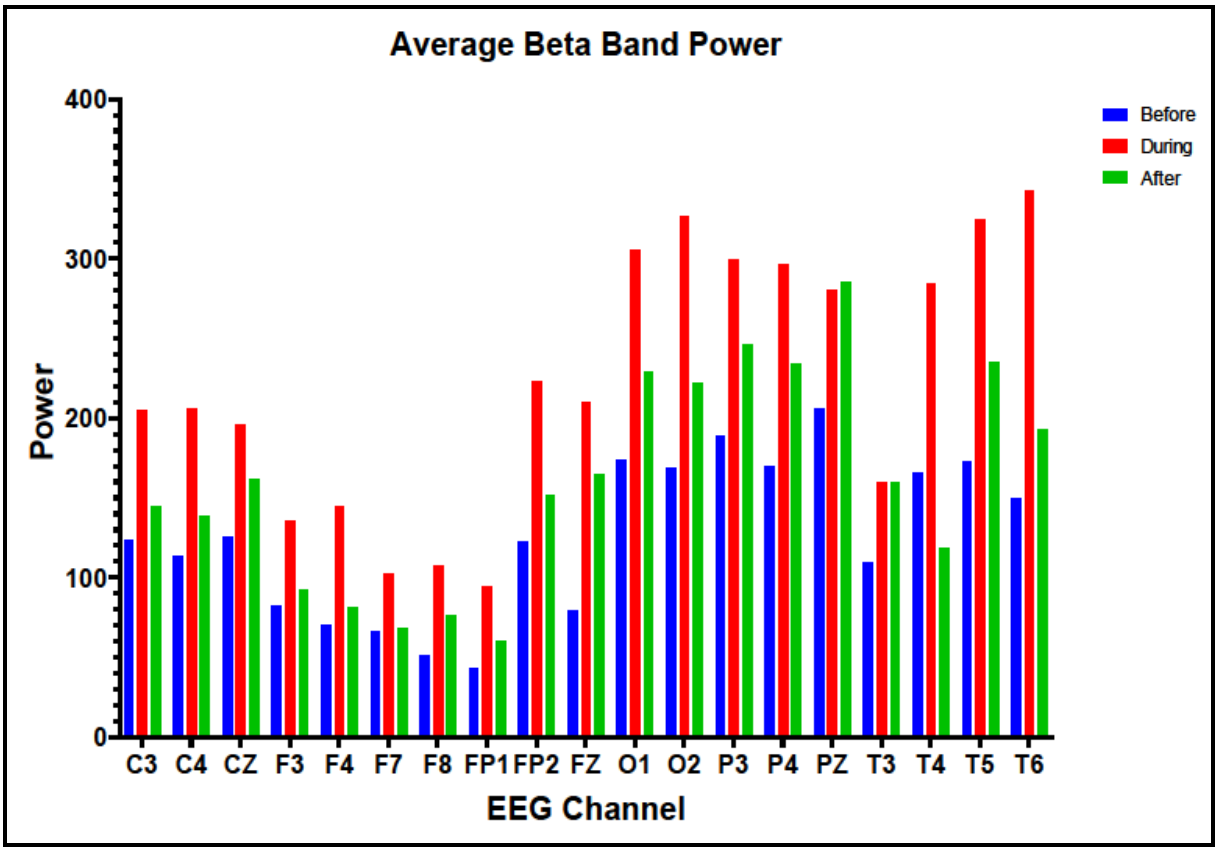

Figure 44: Average Beta Band Power of all EEG Channels for all Subjects among three conditions

The findings from the above charts are-

- The average band power of beta wave increases in all subjects during stimulus phase for all 19 EEG channels.
- In after-test phase, the average beta band power rises with compare to normal condition of all channels except T4-REF channel. T4-REF channel shows a decreasing average beta band power with respect to rest condition for all subjects.
- In after-test phase, the average beta band power decreases with compare to stimulus phase for all subjects of all channels except PZ-REF and T3-REF channels. PZ-REF channel shows an increasing average beta band power and T3-REF channel shows no change with respect to test condition for all subjects when the stimulus is stopped.

2.3. ***Calculating Fractal Dimension using Higuchi's Method:***

2.3.1. ***Selecting K_{Max}:***

In Figure 45, the saturation point is K=300, so the K_{Max} is 300 for ECG signal. In Figure 46, the saturation point is K=50, so the K_{Max} is 50 for EEG signal.

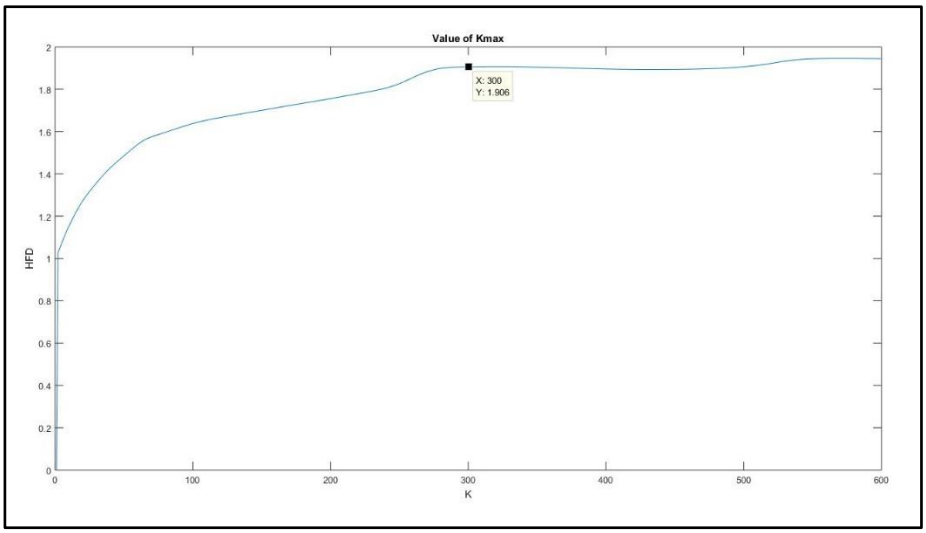

Figure 45: HFD vs K plot shows that Kmax value 300 for ECG signal

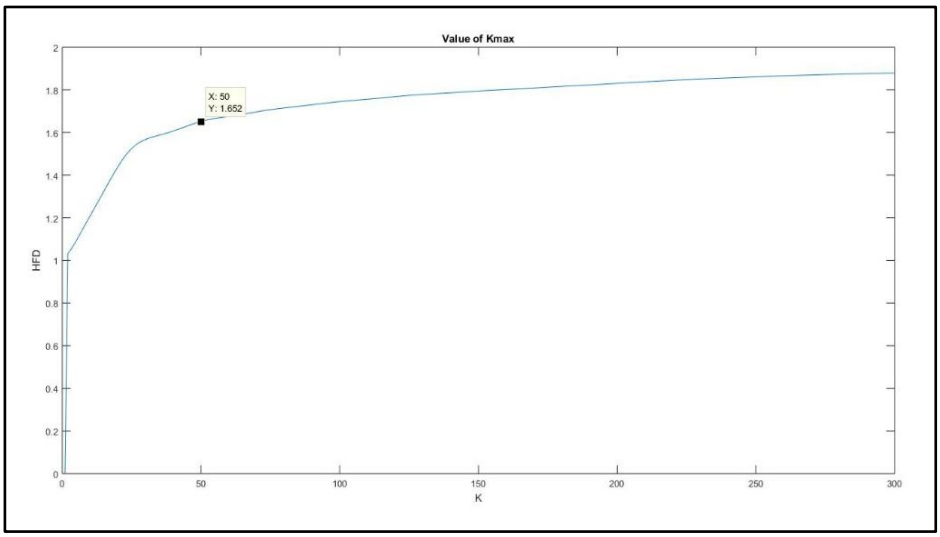

Figure 46: HFD vs K plot shows that Kmax value 50 for EEG signal

2.3.2. ***Calculation of Higuchi's Fractal Dimension of ECG Signal:***

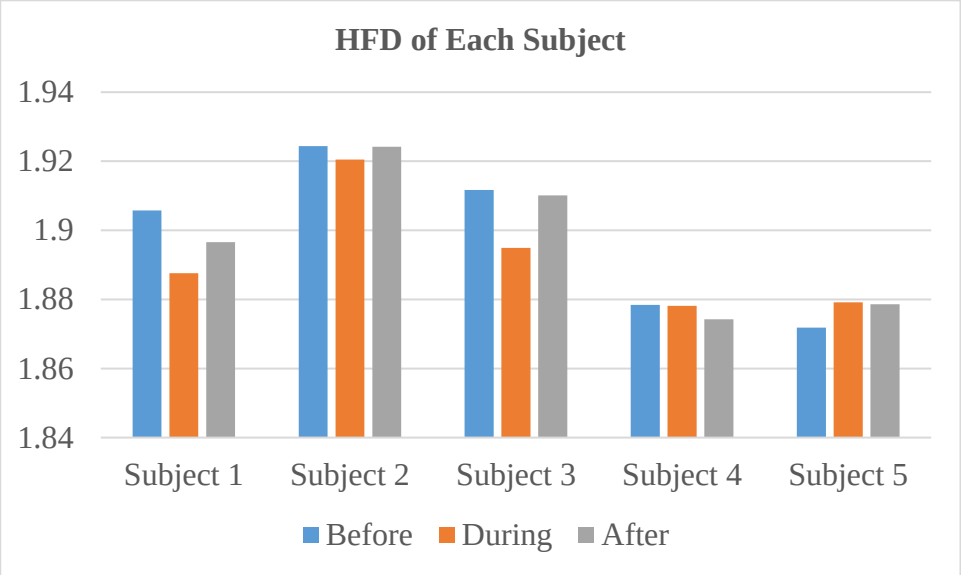

Figure 47: Higuchi's Fractal Dimension of each Subject among three conditions

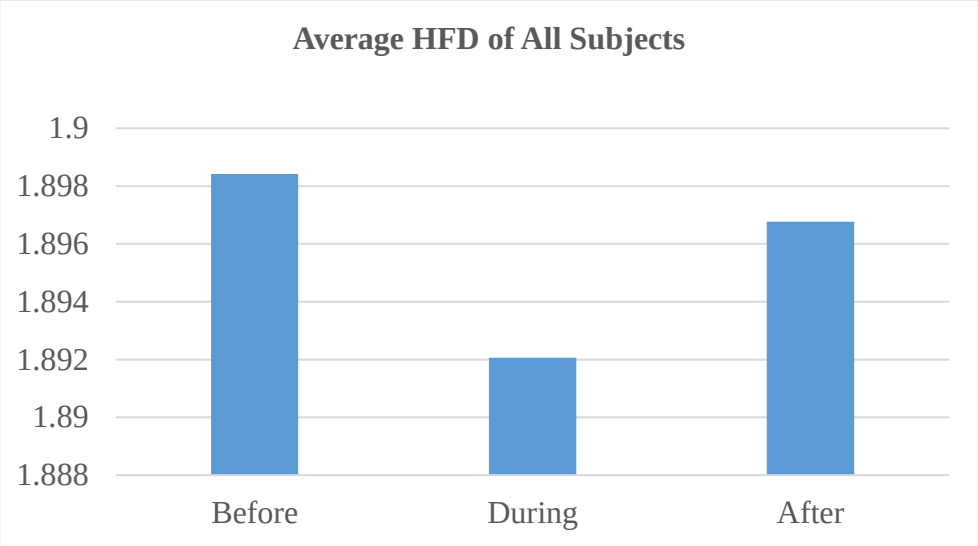

Figure 48: Average Higuchi's Fractal Dimension of all Subjects among three conditions

The findings from the above the charts are-

- In all subjects except Subject 5, there is a decrease in Higuchi's Fractal Dimension (HFD) with dark chocolate stimulus. Subject 5 shows an increasing HFD with stimulus.
- When the stimulus is stopped, all subjects except Subject 4 and Subject 5 show an increasing HFD. Subject 4 and Subject 5 show a decrease in HFD when stimulus is stopped.
- The average HFD is decreased for all subjects with stimulus.

- In after-test phase, average HFD decreases with respect to rest condition and the average HFD increases with compare to test phase.

2.3.3. Calculation of Higuchi's Fractal Dimension of EEG Signal:

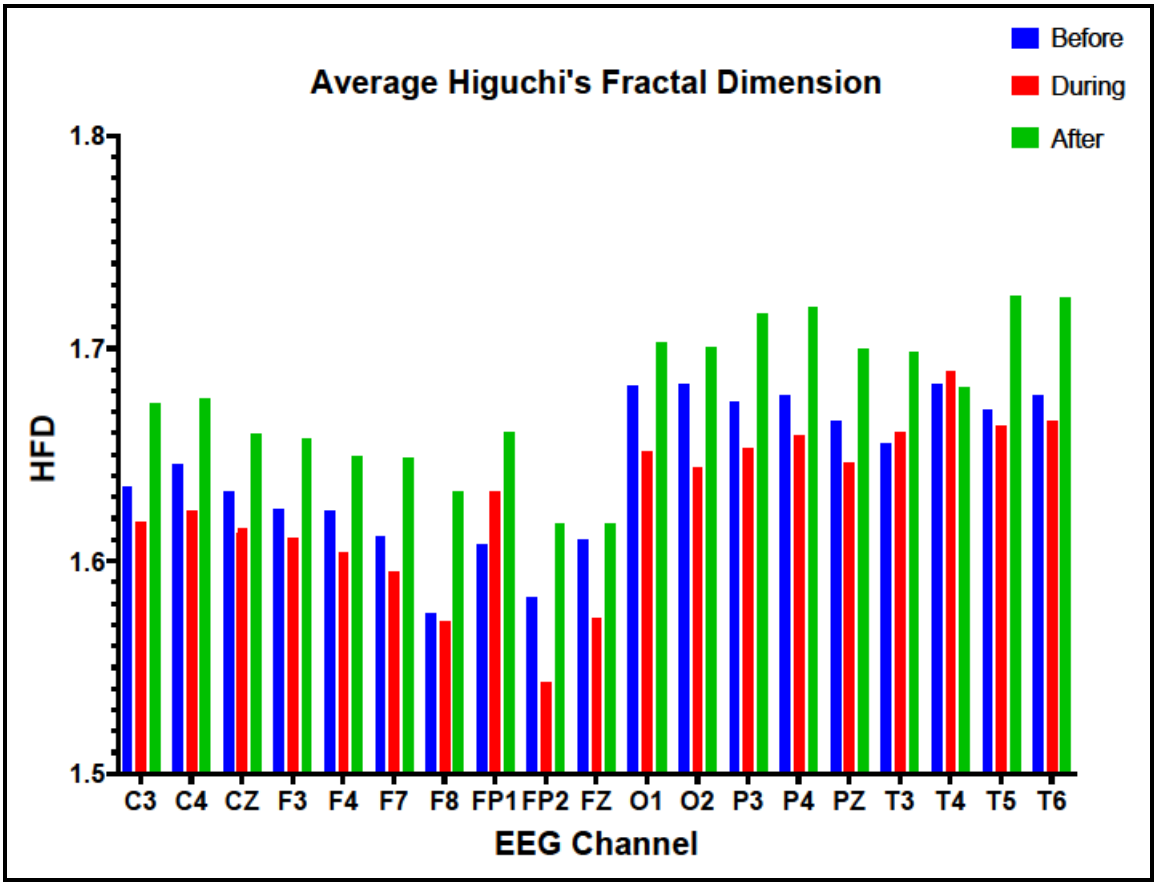

Figure 49: Average HFD of all EEG Channels for all Subjects among three conditions

The findings from the above charts are-

- The average HFD decreases for all subjects of all EEG channels except FP1-REF, T3-REF and T4-REF channels when dark chocolate stimulus is applied. FP1-REF, T3-REF and T4-REF channels show an increasing HFD with stimulus.
- When the stimulus is stopped, average HFD increases with compare to rest condition for all subjects of all channels except T4-REF channel. This channel shows a decreasing HFD.
- The average HFD rises with respect to test condition for all subjects of all channels except T4-REF channel in after-test condition. This channel shows a decreasing HFD when the stimulus is stopped.

2.4. Calculating Detrended Fluctuation Analysis (DFA):

2.4.1. Calculation of Scaling Exponent (α) using DFA of ECG Signal:

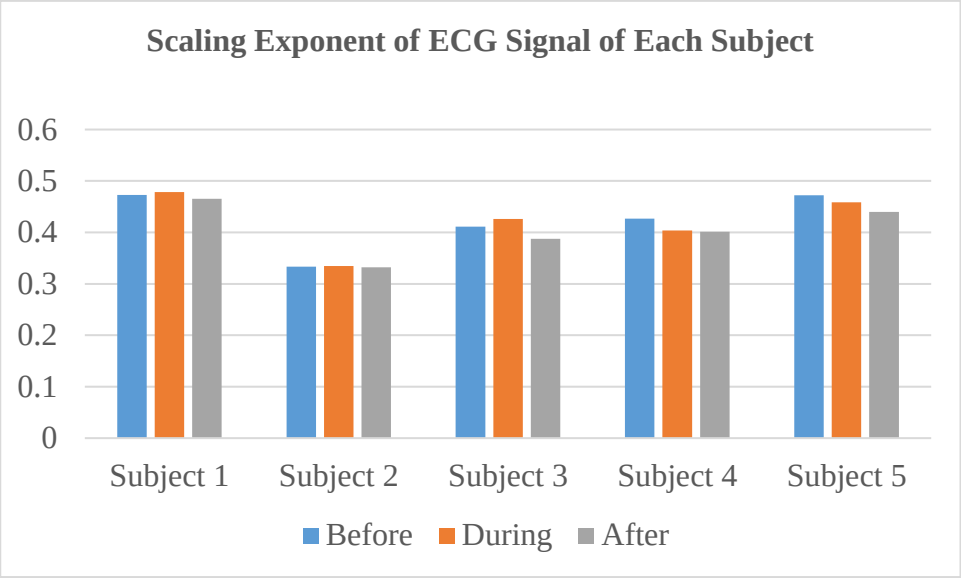

Figure 50: Scaling Exponent of ECG Signal of Each Subject among three conditions

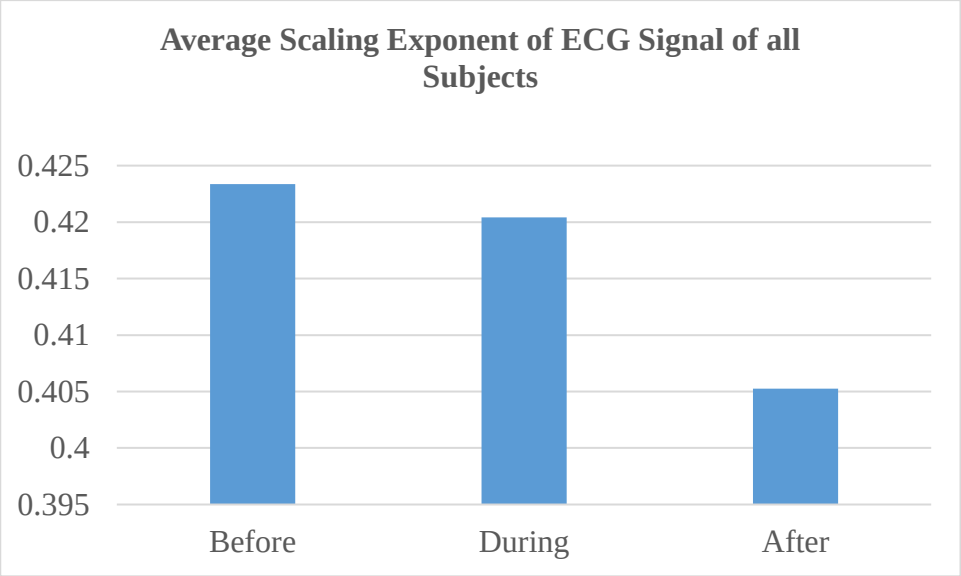

Figure 51: Average Scaling Exponent of ECG Signal of all Subjects among three conditions

The findings from the above the charts are-

- In Subject 4 and Subject 5, there is a decrease in scaling exponent of DFA with dark chocolate stimulus.
- Subject 1, Subject 2 and Subject 3 show an increasing scaling exponent of DFA with stimulus.
- When the stimulus is stopped, all subjects show a decreasing scaling exponent of DFA.

- The average scaling exponent of DFA is decreased for all subjects with stimulus.
- In after-test phase, average scaling exponent of DFA decreases with respect to rest condition as well as test condition.

2.4.2. Calculation of Scaling Exponent (α) using DFA of EEG Signal:

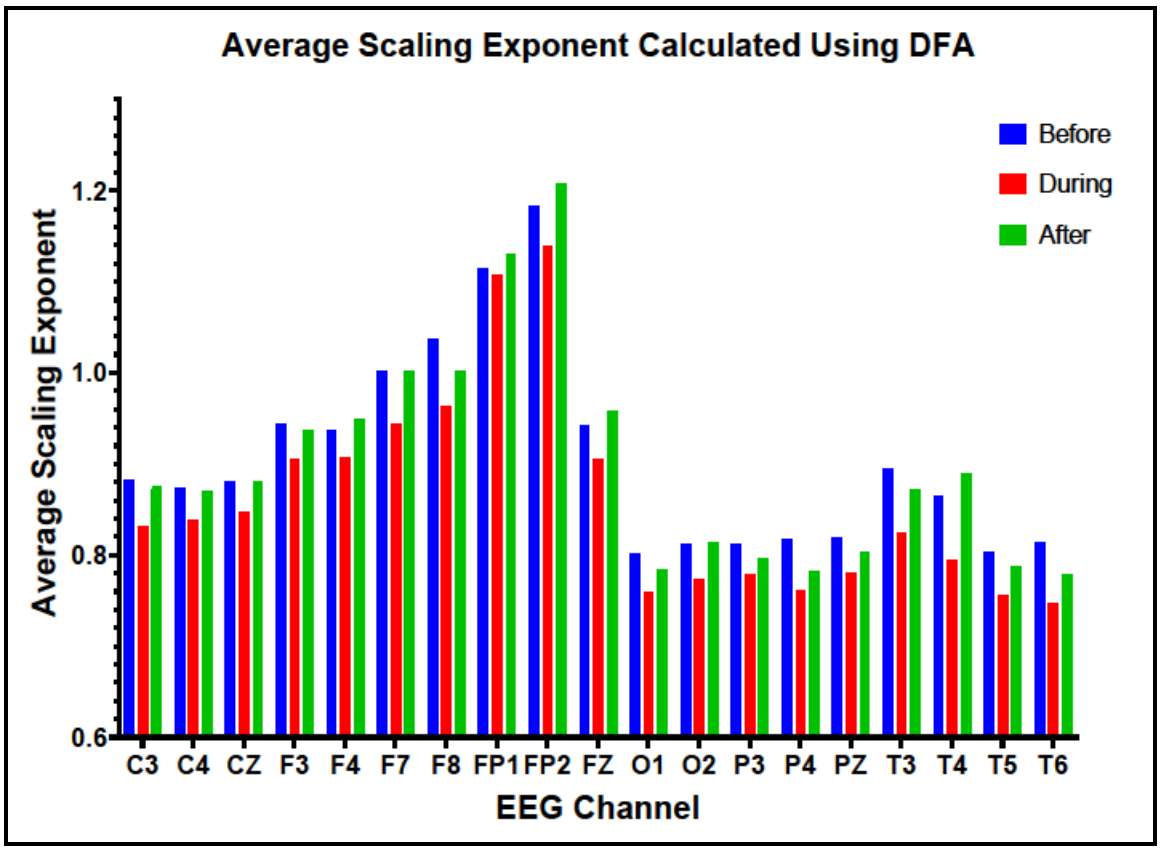

Figure 52: Average Scaling Exponent of all EEG Channels for all Subjects among three conditions

The findings from the above the charts are-

- When the dark chocolate stimulus is applied, there is a decrease in average scaling exponent of DFA for all subjects of all EEG 19 channels.
- In after-test phase, average scaling exponent of DFA decreases with respect to rest condition for all channels except F4-REF, FP1-REF, FP2-REF, FZ-REF, O2-REF and T4-REF channels. These channels show an increasing average scaling exponent with respect to rest condition when the stimulus is stopped.
- In after-test condition, the average scaling exponent of DFA rises with compare to test condition for all subjects for all 19 EEG channels.

2.5. Calculating Multifractal Detrended Fluctuation Analysis (MFDFA):

2.5.1. MFDFA of ECG Signal:

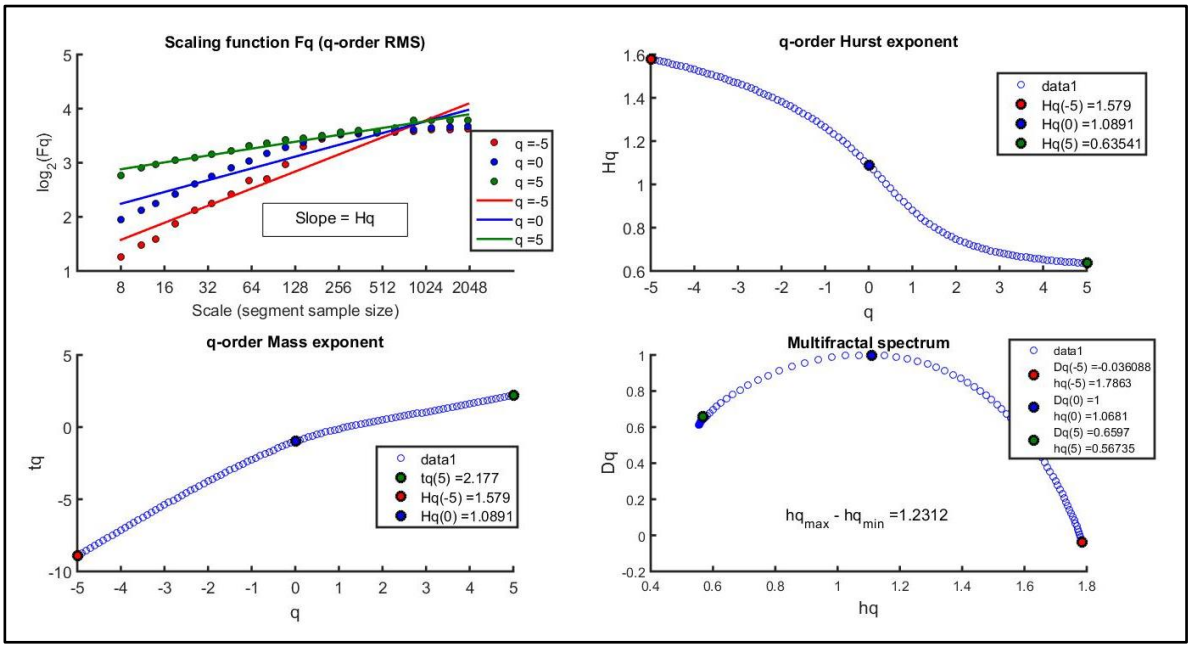

Figure 53: MFDFA of ECG Signal of a Subject during rest condition

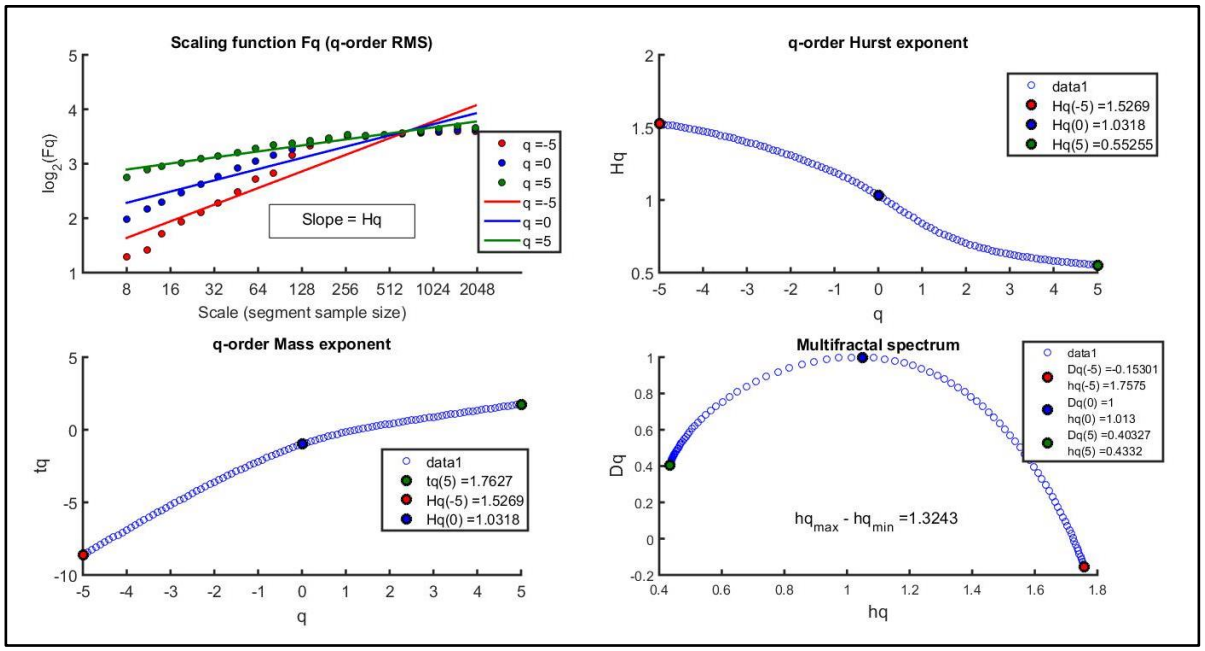

Figure 54: MFDFA of ECG Signal of a Subject during test condition

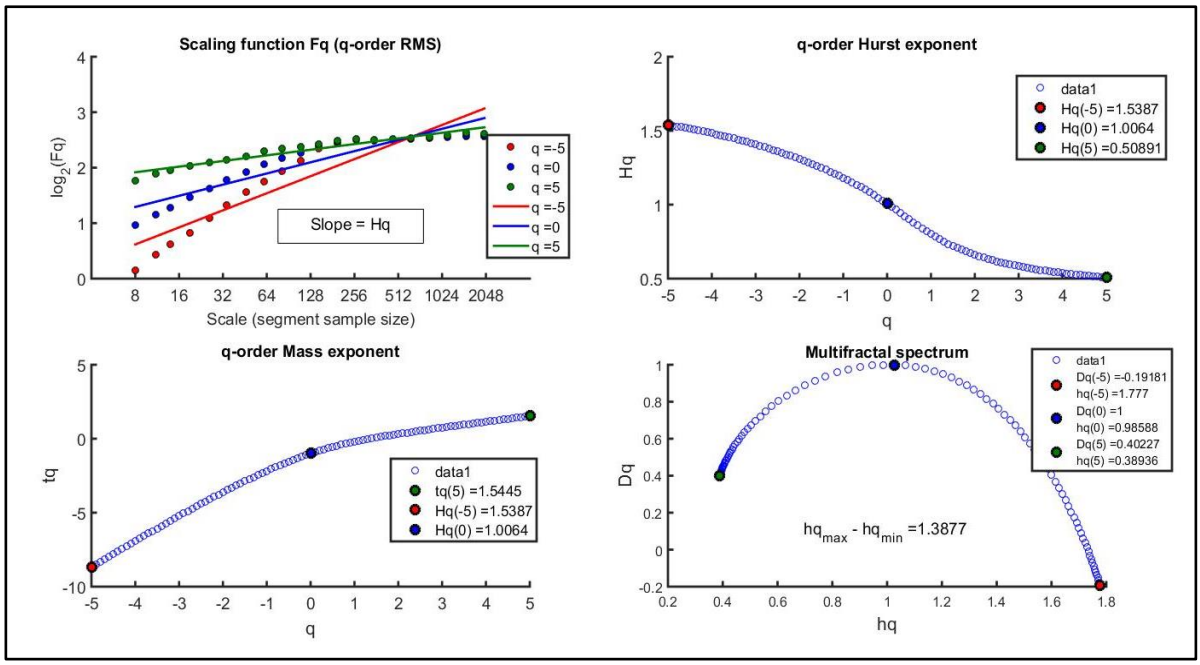

Figure 55: MFDFA of ECG Signal of a Subject during after-test condition

2.5.2. ***Calculation of Multifractal Spectrum Width of ECG Signal:***

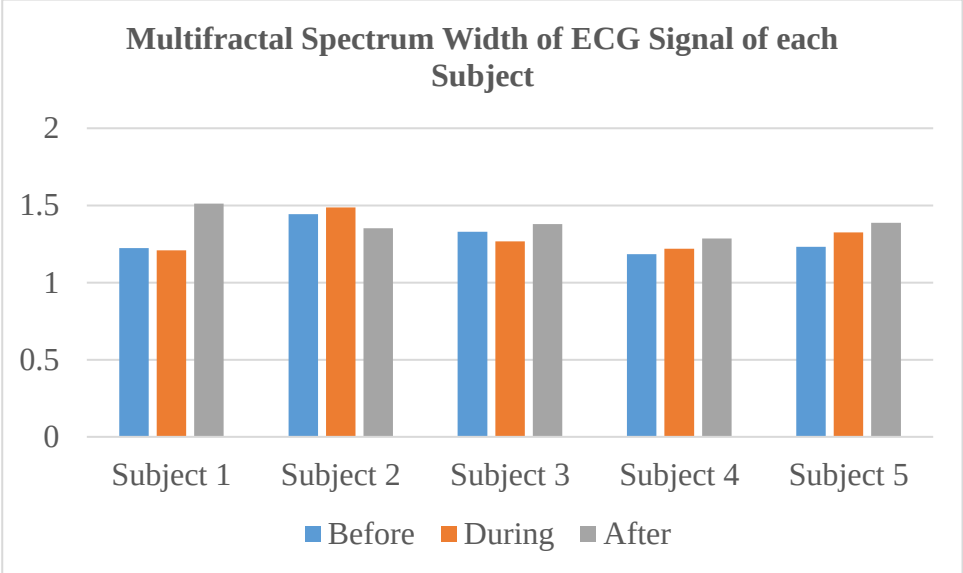

Figure 56: Multifractal Spectrum Width of ECG Signal of each Subject

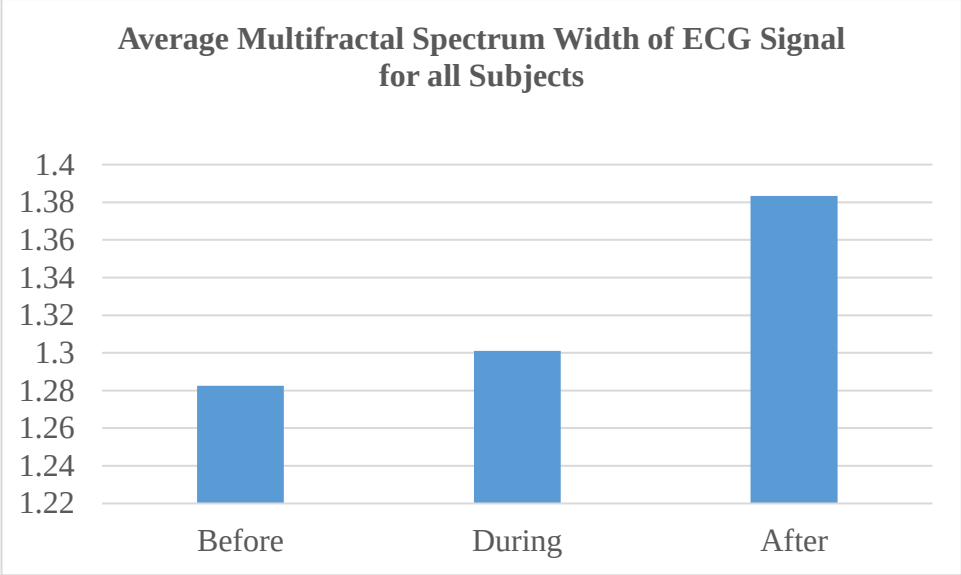

Figure 57: Average Multifractal Spectrum Width of ECG Signal for all Subjects among three conditions

The findings from the above the charts are-

- In all subjects except Subject 1 and Subject 3, there is a rise in multifractal spectrum width of MFDFA with dark chocolate stimulus.
- Subject 1 and Subject 3 show a decreasing width of multifractal spectrum with stimulus.
- When the stimulus is stopped, all subjects except Subject 2 show an increasing multifractal spectrum width of MFDFA. Subject 2 shows a decreasing trend in after-test condition.
- The average width of multifractal spectrum of MFDFA is increased for all subjects with stimulus.
- In after-test phase, average multifractal spectrum width of MFDFA rises with respect to rest condition as well as test condition.

2.5.3. ***MFDFA of EEG Signal:***

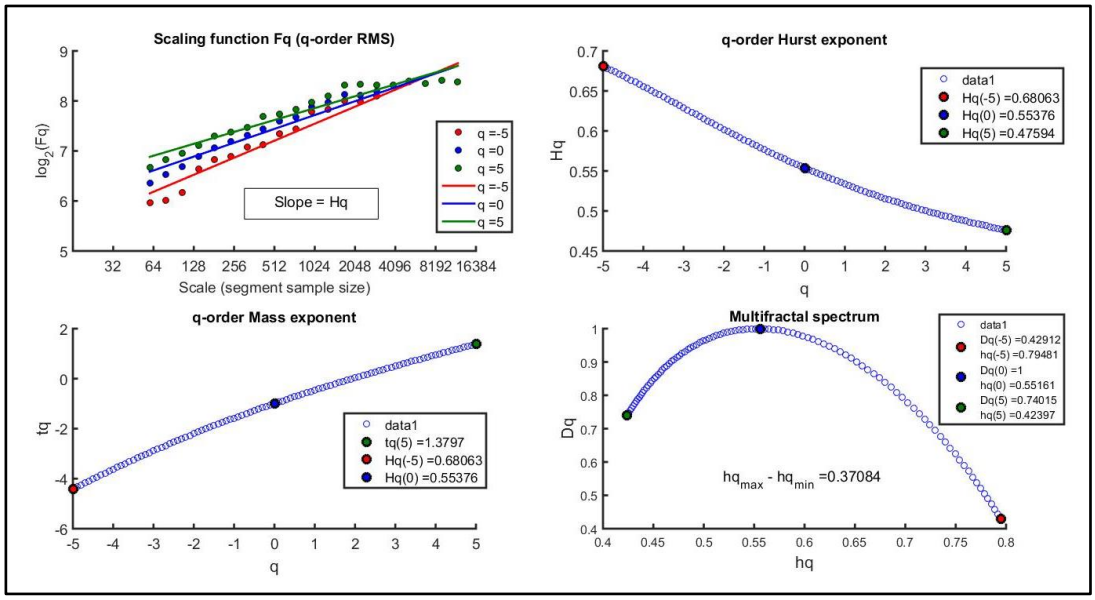

Figure 58: MFDFA of EEG Signal of a Subject during rest condition

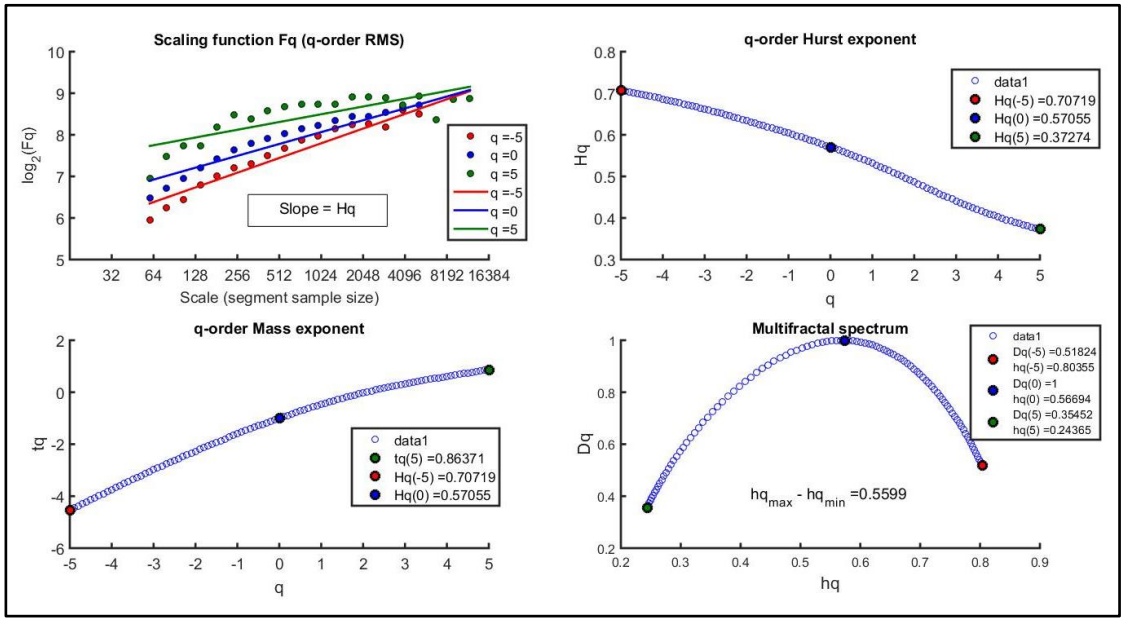

Figure 59: MFDFA of EEG Signal of a Subject during test condition

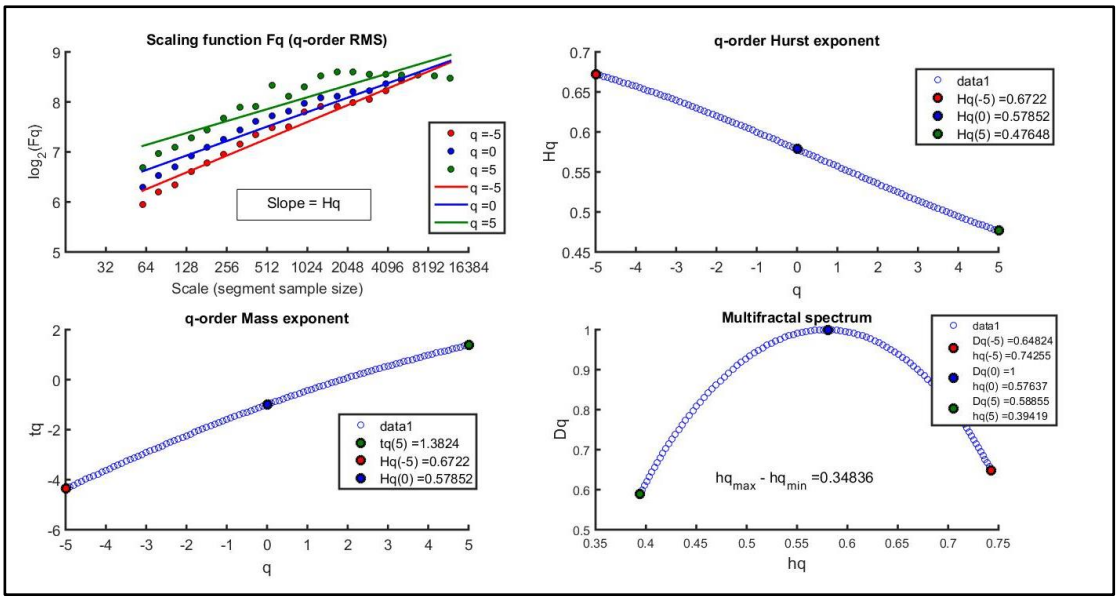

Figure 60: MFDFA of EEG Signal of a Subject during after-test condition

2.5.4. ***Calculation of Multifractal Spectrum Width of EEG Signal:***

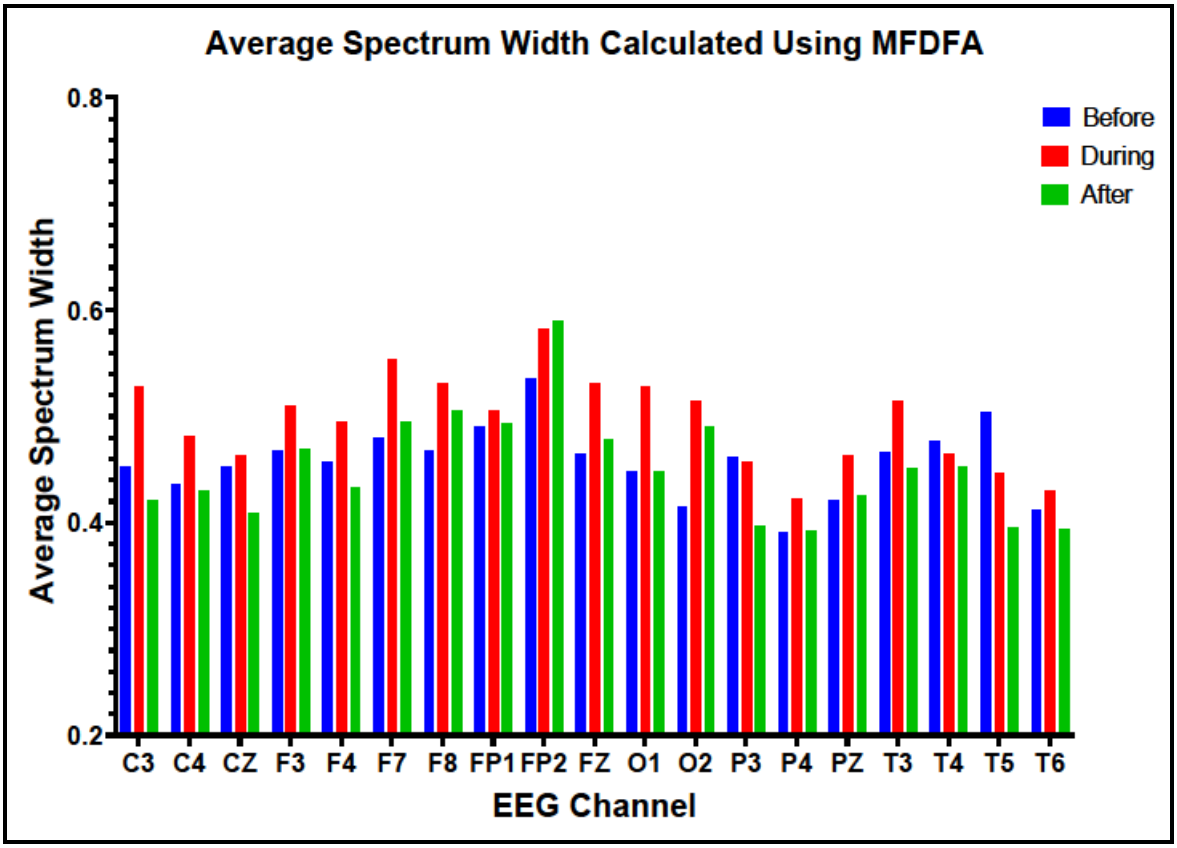

Figure 61: Average Multifractal Spectrum Width of all EEG Channels for all Subjects among three conditions

The findings from the above the charts are-

- When the dark chocolate stimulus is applied, there is an increase in average multifractal spectrum width of MFDFA for all subjects of all 19 EEG channels except P3-REF, T4-REF and T5-REF channels. These channels show a decreasing trend with stimulus.
- In after-test phase, average width of multifractal spectrum rises with respect to rest condition for F3-REF, F7-REF, F8-REF, FP1-REF, FP2-REF, FZ-REF, O1-REF, O2-REF, P4-REF and PZ-REF channels.
- C3-REF, C4-REF, CZ-REF, F4-REF, P3-REF, T3-REF, T4-REF, T5-REF and T6-REF channels show a decreasing average multifractal spectrum width of MFDFA with respect to rest condition when the stimulus is stopped.
- In after-test condition, the average width of multifractal spectrum decreases with compare to test condition for all subjects for all 19 EEG channels except FP2-REF channel. FP2-REF channel shows an increasing pattern with respect to test phase.

Chapter: 6

DISCUSSION

In the first part of the study, it has been studied sEMG parameters during three different protocols.

Fractal analysis shows that the complexity of sEMG signal increases with increase in weight for both the biceps and forearm muscles during the flexion movement as well as during the static holding fatigue of these muscles using both Higuchi's and Katz's Methods. The rise in fractal dimension for bicep and forearm muscles with increasing weight during flexion movement could be due to changes in muscle recruitment patterns, muscle fiber recruitment, and the complexity of muscle activation as the load grows greater.

During handgrip fatigue using a hand dynamometer, the observation that the fractal dimension is greater for forearm muscles than biceps muscles. So the complexity of forearm muscles is higher than that of biceps muscles due to attributed to the different roles and muscle fiber compositions of these muscle groups, as well as the specific biomechanics of the handgrip task.

The scaling exponent of Detrended Fluctuation Analysis (DFA) for sEMG is greater than one during these three protocols, this suggests that the presence of long-term correlations or persistent behaviour in the data. This implies that biosignals display self-similarity and patterns that are not random, but rather have some predictability and structure over longer time scales.

The decreased scaling exponent of DFA for biceps and forearm muscles during flexion movement and during static holding fatigue due to related to changing dynamics of muscle activation patterns and coordination under varying weights.

Differences in the scaling exponent of DFA between forearm and biceps muscles during handgrip fatigue measured with a hand dynamometer can be due to variations in muscle recruitment patterns, biomechanics, and individual physiological differences.

In the next part of the study, it has been studied dynamics of ECG signal with dark chocolate stimulus. It was seen that the heart rate marginally increases with this stimulus, and then slightly decreases when the stimulus is stopped. So, cardiac output is increased with stimulus. These results were consistent among almost all subjects.

While applying the dark chocolate stimulus it was seen that the average band power across various regions of the brain increased significantly. A consistent increase of delta band power with stimulus in all subjects tell that dark chocolate causes the effect of relaxation in subjects. When the stimulus is stopped, average delta band power is decreased for all subjects. The average band power of theta is increased when the stimulus is applied and when this stimulus is removed average theta power is decreased. An increase in alpha band power was seen with dark chocolate stimulus. But there was a decreasing trend in average alpha power when the stimulus is stopped and it is reveal that this stimulus causes the effect of arousal in subjects. During stimulus phase the average beta power is increased that indicates raised cortical activity and cognitive engagement in response to the stimulus and after test condition the average power of beta is decreased for almost all 19 EEG channels which implies a change in cognitive state, such as a shift from focused attention to a more relaxed state.

Fractal analysis shows that the complexity of ECG signal decreases with dark chocolate stimulus. The variation of fractal dimension is not consistent in test and after test conditions. In after test phase, complexity of ECG signal is decreased with respect to rest condition and is increased with compare to test condition.

Variation of fractal dimension show that there is a decrease in the complex nature of EEG signals with dark chocolate stimulus in almost all regions of brain. The front left side of frontal lobe, slightly left and right temporal lobe regions of brain are an increase in complex nature with stimulus. When the stimulus is removed, the complexity of almost all regions of brain is increased with respect to rest as well as test conditions, except the right temporal lobe of brain is decreased in that case.

The results of DFA of ECG signal show that scaling exponent (α). When dark chocolate stimulus is applied, the average value of α is lesser than α values of rest condition. This result means that when the subject is eating dark chocolate the anti-correlated nature of ECG signal reduces, that is the signal becomes more anti-correlated. When the dark chocolate stimulus is stopped, the average α value is smaller than the rest condition as well as test condition, it means the signal becomes more anti-correlated.

During stimulus phase, the average value of α is smaller than α values of rest condition. This results means that when the subject is under stimulus the correlated nature of EEG signal reduces, that is the signal becomes more uncorrelated. When the dark chocolate stimulus is removed, the average α value is greater than the test condition.

The results of MFDFA show that ECG is multifractal in nature and the average multifractal spectrum width increases with dark chocolate stimulus. It means the degree of multifractality of ECG signal increases with this stimulus. When the stimulus is stopped the width of multifractal spectrum is increased with respect to rest as well as test conditions, it means the degree of multifractality more increases in that case.

When the dark chocolate stimulus is applied, there is an increase in average multifractal spectrum width of all 19 EEG channels except P3-REF, T4-REF and T5-REF channels. This result means the degree of mutifractality increases almost all regions of brain with stimulus, except in left parietal lobe and left and right temporal lobe regions of brain the degree of multifractality decreases. In after-test condition, the average width of multifractal spectrum decreases with compare to test condition for all subjects for all channels except FP2-REF channel. It means the degree of mutifractality decreases almost all regions of brain with stimulus, except in front right side of frontal lobe region the degree of multifractality increases.

Chapter: 7

CONCLUSION

In the first part of the study, the effects of varying weights and using hand dynamometer on biceps and forearm muscles were analysed.

In conclusion, the use of fractal analysis to study sEMG signals provides on the complex interactions between the biceps and forearm muscles. Both Higuchi's and Katz's methods show that there is a trend toward increasing complexity with heavier loads during flexion movement and static holding fatigue, which emphasizes the dynamic interaction between muscle activation, coordination, and effort as the load increases.

Additionally, using a hand dynamometer, it found that the fractal dimension of forearm muscles is greater than that of biceps muscles during handgrip fatigue, illustrating the distinct biomechanical roles and muscle activation patterns of these two muscle groups.

Across the protocols studied, the scaling exponent values obtained through Detrended Fluctuation Analysis (DFA) for sEMG signals exceed one, indicating the presence of long-term correlations or persistent patterns in the data. Under different weights, the scaling exponent for both the biceps and forearm muscles decreases during flexion movement and static holding fatigue. Using a hand dynamometer, variations in the scaling exponent between the forearm and biceps muscles are also observed during handgrip fatigue.

In the next part of this study, the effects of dark chocolate on heart and brain were analysed. The objective of this work to study the dynamics of heart and brain when dark chocolate stimulus is applied.

In this work, it has been found an average heart rate is slightly increased with dark chocolate stimulus while the stimulus is stopped the average heart rate decreases.

The average band power of delta, theta, alpha and beta waves of EEG is raised with dark chocolate stimulus.

Complexity of ECG and EEG signals calculated by HFD is found to show decreasing pattern with the dark chocolate stimulus.

The average value of scaling exponent using DFA of ECG signals is decreased in test and after test condition with dark chocolate stimulus. During stimulus phase, the average value

of scaling exponent is decreased in all EEG channels and when the dark chocolate stimulus is removed, the average α value is greater in all EEG channels.

The MFDFA shows that ECG and EEG are multifractal in nature. The average multifractal spectrum width increases with dark chocolate stimulus for both ECG and EEG signals.

Further research with much larger data sets and statistical analysis is required to establish the effects of stimulus on biosignals.

Chapter: 8

FUTURE SCOPE

The future potential for analysing electromyography (EMG) signals with varying weights and using a dynamometer is significant for advancing both research and practical applications in a variety of fields. It holds enormous promise for transforming fields ranging from rehabilitation and sports performance to robotics and healthcare. The perspectives gained from such analyses are likely to contribute to innovative solutions that improve human movement, well-being, and quality of life as technology advances and interdisciplinary collaborations flourish.

The future scope of analysing electrocardiogram (ECG) and electroencephalogram (EEG) signals with dark chocolate stimulus opens up exciting possibilities for research and application in a variety of fields. This novel approach has the potential to yield novel insights into physiological and cognitive responses. It has the potential to transform our understanding of the complex relationships between nutrition, cardiovascular health, and cognitive well-being.

REFERENCES

[1] R. S. Khandpur, *Handbook of Biomedical Instrumentation*, 3rd ed. Tata McGraw-Hill Education, 2014.

[2] Rao, C.R., & GUHA, S.K. (2001). *Principles of medical electronics and biomedical instrumentation.* Universities Press.

[3] Brooks, A. (2018). An HCI Approach in Contemporary Healthcare and (Re) habilitation. *The Wiley Handbook of Human Computer Interaction*, 2, 923-944.

[4] Soderberg, G.L. and Cook, T.M., 1984. Electromyography in biomechanics. *Physical Therapy*, 64(12), pp.1813-1820.

[5] J. D. Bronzino, *Biomedical Engineering Handbook*, Volume II. Boca Raton, FL: CRC Press, 1999.

[6] Gupta, S.D., Al Yusuf, S., Ammar, J.K. and Hasan, K., 2012, August. An analysis to generate EMG signal and its perspective: *A panoramic approach. In 2012 International Conference on Advances in Power Conversion and Energy Technologies* (APCET) (pp. 1-5). IEEE.

[7] Pradhan, G. N., Engineer, N., Nadin, M., & Prabhakaran, B. (2008, July). Analyzing motoric and physiological data in describing upper extremity movement in the aged. In *Proceedings of the 1st international conference on PErvasive Technologies Related to Assistive Environments* (pp. 1-8).

[8] Kobayashi, H., & Hiramatsu, K. (2004, April). Development of muscle suit for upper limb. In *IEEE International Conference on Robotics and Automation, 2004. Proceedings. ICRA'04. 2004* (Vol. 3, pp. 2480-2485). IEEE. [9] Legg, A.J., Stevens, R., Oakes, N.O. and Shahane, S.A., 2016. *A comparison of nonoperative vs. Endobutton repair of distal biceps ruptures. Journal of Shoulder and Elbow Surgery*, 25(3), pp.341-348.

[10] Crosby, J.W., 1957. *Course on Upper Extremity Prosthetics. Canadian Journal of Occupational Therapy*, 24(3), pp.93-98.

[11] Botte, M. J., & Gelberman, R. H. (1998). Acute compartment syndrome of the forearm. *Hand clinics*, *14*(3), 391-403. [12] R Merletti, P Parker., 2004 - Wiley-IEEE Press- "*Basic Physiology and Biophysics of EMG Signal Generation"*, pp.1 – 25.

[13] R. Merletti, A. Botter, U. Barone., 2016-John Wiley & Sons, Inc. "*Detection and Conditioning of Surface EMG Signals"*, pp. 54-90.

[14] Mahapatra, A. B. S. (1998). *Essentials of Medical physiology*. Current Books International.

[15] Geselowitz, D. B. (1989). On the theory of the electrocardiogram. *Proceedings of the IEEE*, *77*(6), 857-876. [16] Roberts, D. A. (2019). *Mastering the 12-Lead EKG* (2nd ed.). F. A. Davis Company.

[17] Niedermeyer, E., & da Silva, F. L. (2005). *Electroencephalography: Basic Principles, Clinical Applications, and Related Fields*. Lippincott Williams & Wilkins.

[18] Schomer, D. L., & da Silva, F. L. (Eds.). (2012). *Niedermeyer's Electroencephalography: Basic Principles, Clinical Applications, and Related Fields*. Lippincott Williams & Wilkins.

[19] Nunez, P. L., & Srinivasan, R. (2006). *Electric Fields of the Brain: The Neurophysics of EEG*. Oxford University Press.

[20] Sanei, S., & Chambers, J. A. (2007). *EEG Signal Processing*. Wiley.

[21] Daube, J. R. (Ed.). (2002). *Clinical neurophysiology* (Vol. 66). Oxford University Press.

[22] Sanei, S., & Chambers, J. A. (2021). *EEG signal processing and machine learning*. John Wiley & Sons.

[23] Gohel, V., & Mehendale, N. (2020). Review on electromyography signal acquisition and processing. *Biophysical Reviews*, *12*(6), 1361-1367.

[24] Pourmohammadi, S., & Maleki, A. (2020). Stress detection using ECG and EMG signals: A comprehensive study. *Computer methods and programs in biomedicine*, *193*, 105482.

[25] Pancholi, S., & Joshi, A. M. (2018). Portable EMG data acquisition module for upper limb prosthesis application. *IEEE Sensors Journal*, *18*(8), 3436-3443.

[26] Samarawickrama, K., Ranasinghe, S., Wickramasinghe, Y., Mallehevidana, W., Marasinghe, V., & Wijesinghe, K. (2018). Surface EMG signal acquisition analysis and classification for the operation of a prosthetic limb. *Int J Biosci Biochem Bioinformatics*, *8*, 32-41.

[27] Forman, D. A., Forman, G. N., Murphy, B. A., & Holmes, M. W. (2020). Sustained Isometric Wrist Flexion and Extension Maximal Voluntary Contractions on Corticospinal Excitability to Forearm Muscles during Low-Intensity Hand-Gripping. *Brain Sciences*, *10*(7), 445.

[28] Barra, S., Fraschini, M., Casanova, A., Castiglione, A., & Fenu, G. (2019). PhysioUnicaDB: A dataset of EEG and ECG simultaneously acquired. *Pattern Recognition Letters*, *126*, 119-122.

[29] Liu, J., Chen, Y., Zhou, Y., Wu, Q., Qiao, T., & Sun, B. (2018, October). Survey of wearable EEG and ECG acquisition technologies for body area network. In *IECON 2018-44th Annual Conference of the IEEE Industrial Electronics Society* (pp. 5911-5915). IEEE.

[30] Li, B., Cheng, T., & Guo, Z. (2021, May). A review of EEG acquisition, processing and application. In *Journal of Physics: Conference Series* (Vol. 1907, No. 1, p. 012045). IOP Publishing.

[31] Y. Liu et al., "Wrist angle prediction under different loads based on GA-ELM neural network and surface electromyography," *Concurrency and Computation: Practice and Experience, vol. 34, no. 3,* Sep. 2021, doi: 10.1002/cpe.6574.

[32] J. Tryon and A. L. Trejos, "Classification of Task Weight During Dynamic Motion Using EEG–EMG Fusion," *IEEE Sensors Journal, vol. 21, no. 4,* pp. 5012–5021, Feb. 2021, doi: 10.1109/jsen.2020.3033256.

[33] S. Aziz, M. U. Khan, F. Aamir, and M. A. Javid, "Electromyography (EMG) data-driven load classification using empirical mode decomposition and feature analysis," *in 2019 International Conference on Frontiers of Information Technology (FIT),* 2019, pp. 272–2725.

[34] M. Chakraborty and D. Parbat, "Fractals, chaos and entropy analysis to obtain parametric features of surface electromyography signals during dynamic contraction of biceps muscles under varying load," *in 2017 2nd International Conference for Convergence in Technology (I2CT),* 2017, pp. 222–229.

[35] M. Chakraborty and D. Parbat, "Fractal analysis of sEMG signal under varying load conditions," *in 2016 2nd International Conference on Control, Instrumentation, Energy Communication (CIEC),* 2016, pp. 149–152.

[36] Biswas, A., Parbat, D., & Chakraborty, M. (2019, March). Establishment of EMG-Force relationship obtained during Simultaneous Voluntary Contraction of Biceps and Flexor Digitorum Profundus Muscles. In *2019 IEEE 5th International Conference for Convergence in Technology (I2CT)* (pp. 1-6). IEEE.

[37] Schmorrow, D. D., & Fidopiastis, C. M. (Eds.). (2020). *Augmented Cognition. Theoretical and Technological Approaches: 14th International Conference, AC 2020, Held as Part of the 22nd HCI International Conference, HCII 2020, Copenhagen, Denmark, July 19–24, 2020, Proceedings, Part I* (Vol. 12196). Springer Nature.

[38] Pennanen, K., Närväinen, J., Vanhatalo, S., Raisamo, R., & Sozer, N. (2020). Effect of virtual eating environment on consumers' evaluations of healthy and unhealthy snacks. *Food Quality and Preference*, *82*, 103871.

[39] Giezenaar, C., & Hort, J. (2021). A narrative review of the impact of digital immersive technology on affective and sensory responses during product testing in digital eating contexts. *Food Research International*, *150*, 110804.

[40] Mohamed, M., Yoshizawa, M., Sugita, N., Yamaki, S., & Ichiji, K. (2020). Noncontact monitoring of heart rate responses to taste stimuli using a video camera. *Indonesian Journal of Electrical Engineering and Computer Science*, *18*(1), 293-300.

[41] Kappattanavar, A. M., Hecker, P., Moontaha, S., Steckhan, N., & Arnrich, B. (2023). Food Choices after Cognitive Load: An Affective Computing Approach. *Sensors*, *23*(14), 6597.

[42] Gilgen-Ammann, R., Schweizer, T., & Wyss, T. (2019). RR interval signal quality of a heart rate monitor and an ECG Holter at rest and during exercise. *European journal of applied physiology*, *119*(7), 1525-1532.

[43] Nouira, I., Abdallah, A. B., Bedoui, M. H., & Dogui, M. (2013). A Robust R Peak Detection Algorithm Using Wavelet Transform for Heart Rate Variability Studies. *International Journal on Electrical Engineering & Informatics*, *5*(3).

[44] Ameera, A., Saidatul, A., & Ibrahim, Z. (2019, June). Analysis of EEG spectrum bands using power spectral density for pleasure and displeasure state. In *IOP conference series: Materials science and engineering* (Vol. 557, No. 1, p. 012030). IOP Publishing.

[45] Kesić, S., & Spasić, S. Z. (2016). Application of Higuchi's fractal dimension from basic to clinical neurophysiology: A review. *Computer methods and programs in biomedicine*, *133*, 55-70.

[46] Yeh, S. C., Hou, C. L., Peng, W. H., Wei, Z. Z., Huang, S., Kung, E. Y. C., ... & Liu, Y. H. (2018). A multiplayer online car racing virtual-reality game based on internet of brains. *Journal of Systems Architecture*, *89*, 30-40.

[47] Hardstone, R., Poil, S. S., Schiavone, G., Jansen, R., Nikulin, V. V., Mansvelder, H. D., & Linkenkaer-Hansen, K. (2012). Detrended fluctuation analysis: a scale-free view on neuronal oscillations. *Frontiers in physiology*, *3*, 450.

[48] Ghosh, D., Sengupta, R., Sanyal, S., Banerjee, A., Ghosh, D., Sengupta, R., ... & Banerjee, A. (2018). Non linear techniques for studying complex systems. *Musicality of Human Brain through Fractal Analytics*, 21-48.

[49] Das, N., & Chakraborty, M. (2020, February). Fractal Characterization of ECG signals: Indian Classical Music as stimulus. In *2020 Sixth International Conference on Bio Signals, Images, and Instrumentation (ICBSII)* (pp. 1-6). IEEE.

[50] Ihlen, E. A. (2012). Introduction to multifractal detrended fluctuation analysis in Matlab. *Frontiers in physiology*, *3*, 141.

[51] Das, N., & Chakraborty, M. (2019, March). Effects of Indian Classical Music on Heart Rate Variability. In *2019 IEEE 5th International Conference for Convergence in Technology (I2CT)* (pp. 1-4). IEEE.

[52] Parbat, D., Bhattacharjee, U., Paria, S., Das, N., & Chakraborty, M. (2022). Fractal Dimension and lacunarity based microscopic image texture characterization of coated and non-coated metallic substrates. *Advances in Materials and Processing Technologies*, *8*(2), 2244-2258.

[53] Paria, S., Bhattacharjee, U., Das, N., & Chakraborty, M. (2020, February). Fractal Characterization of Auditory Evoked Potentials. In *2020 Sixth International Conference on Bio Signals, Images, and Instrumentation (ICBSII)* (pp. 1-4). IEEE.

Sanjoy Kumar Das

ORIGINALITY REPORT

9%	3%	7%	2%
SIMILARITY INDEX	INTERNET SOURCES	PUBLICATIONS	STUDENT PAPERS

PRIMARY SOURCES

1	Sanjoy Kumar Das, Nilotpal Das, Monisha Chakraborty. "Power Spectral Density, Higuchi's Fractal Dimension and Detrended Fluctuation Analysis of sEMG at Varying Weights", 2023 International Conference on Computer, Electrical & Communication Engineering (ICCECE), 2023 Publication	3%
2	www.ncbi.nlm.nih.gov Internet Source	<1%
3	ir.lib.hiroshima-u.ac.jp Internet Source	<1%
4	Submitted to University of Namibia Student Paper	<1%
5	dspace.vsb.cz Internet Source	<1%
6	Submitted to University of Warwick Student Paper	<1%
7	Submitted to Uxbridge College, Middlesex Student Paper	<1%

8	spree-now.com Internet Source	<1%
9	bura.brunel.ac.uk Internet Source	<1%
10	Submitted to University of Northumbria at Newcastle Student Paper	<1%
11	Submitted to American InterContinental University Student Paper	<1%
12	Koscielny-Bunde, E.. "Long-term persistence and multifractality of river runoff records: Detrended fluctuation studies", Journal of Hydrology, 20060515 Publication	<1%
13	"Handbook of Cardiac Anatomy, Physiology, and Devices", Springer Science and Business Media LLC, 2009 Publication	<1%
14	Dennis L Youchison, Mark T North, James E Lindemuth, Jimmie M McDonald, Thomas J Lutz. "Thermal performance and flow instabilities in a multi-channel, helium-cooled, porous metal divertor module", Fusion Engineering and Design, 2000 Publication	<1%

15	Sidharth Pancholi, Amit M. Joshi. "Portable EMG Data Acquisition Module for Upper Limb Prosthesis Application", IEEE Sensors Journal, 2018 Publication	<1 %
16	ia803406.us.archive.org Internet Source	<1 %
17	myhartono.com Internet Source	<1 %
18	Submitted to SUNY College of Technology at Delhi Student Paper	<1 %
19	www.frontiersin.org Internet Source	<1 %
20	Submitted to Adtalem Global Education, Inc. Student Paper	<1 %
21	Joachim Liepert, Sylvia Kotterba, Martin Tegenthoff, Jean-Pierre Malin. "Central fatigue assessed by transcranial magnetic stimulation", Muscle & Nerve, 1996 Publication	<1 %
22	repository.tudelft.nl Internet Source	<1 %
23	res.mdpi.com Internet Source	<1 %

24	strathprints.strath.ac.uk Internet Source	<1%
25	Adarsh Sankaran, Thomas Plocoste, Vahid Nourani, Shamseena Vahab, Aayisha Salim. "Assessment of Multifractal Fingerprints of Reference Evapotranspiration Based on Multivariate Empirical Mode Decomposition", Atmosphere, 2023 Publication	<1%
26	Li, D.. "Heartbeat dynamics in adrenergic blocker treated conscious beagle dogs", Journal of Pharmacological and Toxicological Methods, 200809/10 Publication	<1%
27	W.R.W. Omar, M.N. Taib, R. Jailani, N. Fuad, R.M. Isa, A.H. Jahidin, Z. Sharif. "Acute Ischemic Stroke Brainwave Classification Using Relative Power Ratio Cluster Analysis", Procedia - Social and Behavioral Sciences, 2013 Publication	<1%
28	Utkarsh Lal, Arjun Vinayak Chikkankod. "Leveraging SVD Entropy and Explainable Machine Learning for Alzheimer's and Frontotemporal Dementia Detection using EEG", Institute of Electrical and Electronics Engineers (IEEE), 2023 Publication	<1%

29	Yashar Sarbaz, Hakimeh Pourakbari. "Exploring the nature of Parkinsonian rest tremor and the effects of common treatments on it: Stochastic process or chaotic behavior?", Biomedical Signal Processing and Control, 2020 Publication	<1 %
30	ieeexplore.ieee.org Internet Source	<1 %
31	repository.essex.ac.uk Internet Source	<1 %
32	www0.health.nsw.gov.au Internet Source	<1 %
33	Akdemir Akar, Saime, Sadık Kara, Sümeyra Agambayev, and Vedat Bilgiç. "Nonlinear analysis of EEGs of patients with major depression during different emotional states", Computers in Biology and Medicine, 2015. Publication	<1 %
34	Hugues Berry. "Chaos in computer performance", Chaos An Interdisciplinary Journal of Nonlinear Science, 2006 Publication	<1 %
35	Nabil Al Ali, Patrick Mardini. "Oil return, fed funds and the dollar from 1987 to 2013 - preliminary; please do not quote or cite without the authors' permission", 2015	<1 %

	International Mediterranean Gas and Oil Conference (MedGO), 2015 Publication	
36	Ricardo Da Silva Viola, Xavier Balandraud, Fabien Poulhaon, Pierre Michaud, Emmanuel Duc. "Complex interaction between CMT equipment and robot controllers during the WAAM process: consequences for toolpath accuracy", The International Journal of Advanced Manufacturing Technology, 2023 Publication	<1 %
37	Springer Handbook of Bio-/Neuroinformatics, 2014. Publication	<1 %
38	opac.ll.chiba-u.jp Internet Source	<1 %
39	www.researchgate.net Internet Source	<1 %
40	Beam, W.. "An efficient and accurate new method for locating the F3 position for prefrontal TMS applications", Brain Stimulation, 200901 Publication	<1 %
41	Cynthia L. Price, Mark A. Chappell, Brad A. Pettway, Beth E. Porter. "Potential Anaerobic Bioremediation of Perchlorate-Contaminated	<1 %

Soils through Biosolids Applications", American Chemical Society (ACS), 2011
Publication

42	T. G. GRACE ELIZABETH RANI, G. JAYALALITHA. "COMPLEX PATTERNS IN FINANCIAL TIME SERIES THROUGH HIGUCHI'S FRACTAL DIMENSION", Fractals, 2016 Publication	<1 %
43	dokumen.pub Internet Source	<1 %
44	encyclopedia2.thefreedictionary.com Internet Source	<1 %
45	fr.scribd.com Internet Source	<1 %
46	www.csulb.edu Internet Source	<1 %
47	Huang, Yong, Yongchao Yang, and Hui Li. "", Health Monitoring of Structural and Biological Systems 2010, 2010. Publication	<1 %
48	Lakhan Dev Sharma, Abhijit Bhattacharyya. "A Computerized Approach for Automatic Human Emotion Recognition Using Sliding Mode Singular Spectrum Analysis", IEEE Sensors Journal, 2021 Publication	<1 %

49	"Signal and Image Processing Techniques for the Development of Intelligent Healthcare Systems", Springer Science and Business Media LLC, 2021 Publication	<1%
50	Kensuke Fukuda, Toshio Hirotsu, Osamu Akashi, Toshiharu Sugawara. "Chapter 23 Time and Space Correlation in BGP Messages", Springer Science and Business Media LLC, 2005 Publication	<1%

Exclude quotes	Off	Exclude matches	Off
Exclude bibliography	Off		